

Dasgupta, S., Novel Gene C17orf37 in Prostate Cancer Progression and Metastasis. Doctor of Philosophy (Biomedical Sciences), May 2010, 167 pp., 2 tables, 30 illustrations, 152 titles.

C17orf37 also known as *MGC14832*, *C35*, *Rdx12*, a novel gene located on human chromosome 17q12 in the *ERBB2* amplicon, is abundantly expressed in different forms of human cancer. *C17orf37* expression has been reported to positively correlate with grade and stage of cancer progression; however the functional significance of *C17orf37* overexpression in cancer biology is not known. Here, we show that *C17orf37* is highly expressed in prostate cancer cell lines and tumors, compared to minimal expression in normal prostate cells and tissues. RNA interference mediated downregulation of *C17orf37* resulted in decreased migration and invasion of DU-145 prostate cancer cells, and suppressed the DNA binding activity of NF- κ B transcription factor resulting in reduced expression of downstream target genes MMP-9, uPA and VEGF. Phosphorylation of PKB/Akt was also reduced upon *C17orf37* downregulation, suggesting *C17orf37* acts as a signaling molecule that increases invasive potential of prostate cancer cells by NF- κ B mediated downstream target genes. Cellular localization studies by confocal and total internal reflection (TIRF) microscopy revealed expression of *C17orf37* protein in the cytosol predominantly surrounding the membrane of prostate cancer cells. We identified that *C17orf37* has a functional prenylation motif and is post-translationally modified by geranylgeranyl transferase-I (GGTase-I) enzyme. Prenylated

proteins (often referred to as CAAX family of proteins) contain a CAAX motif (C denotes cysteine, A represents aliphatic amino acids, and X any amino acid) at the carboxyl terminal which serves as a substrate for a series of post-translational modifications converting otherwise hydrophilic to lipidated proteins with hydrophobic domain, facilitating membrane localization. Geranylgeranylation of C17orf37 at the 'CVIL' motif translocates the protein to the inner leaflet of plasma membrane, enhances migratory phenotype of cells by inducing increased filopodia formation and potentiates directional migration. The prenylation-deficient C17orf37 mutant is functionally inactive and fails to disseminate injected cells in the mouse model of metastasis. This implies that prenylation activates the C17orf37 protein in cancer cells and functionally regulates metastatic progression of the disease. Our data strongly suggest C17orf37 overexpression in prostate cancer functionally enhances migration and invasion facilitating metastatic dissemination of tumor cells, and is an important target for cancer therapy.

NOVEL GENE *C17ORF37* IN PROSTATE
CANCER PROGRESSION AND METASTASIS

DISSERTATION

Presented to the Graduate Council of the
Graduate School of Biomedical Sciences

University of North Texas

Health Science Center at Fort Worth

in Partial Fulfillment of the Requirements

For the Degree of

DOCTOR OF PHILOSOPHY

By

Subhamoy Dasgupta, B.S., M.S.

Fort Worth, Texas

May, 2010

ACKNOWLEDGEMENTS

I am grateful for having this opportunity to pursue my doctorate degree at University of North Texas Health Science Center at Fort Worth, Texas. I would like to dedicate this work to my parents and all my teachers for their help and support in fostering my interest to be a good scientist.

First and foremost, I would like to express my deepest gratitude to my mentor Dr. Jamboor K. Vishwanatha for his support, guidance and encouragement. His passion for science and faith in my abilities has given me perseverance and immense confidence to thrive forward. I further wish to thank my advisory committee members Drs. Karol Gryczynski, Alakananda Basu, Wolfram Siede and Hriday Das, for their constructive criticisms, and suggestions that improved the merit of my work.

I would like to take this opportunity to thank all the present and past members of our laboratory for their support and help. In particular, I would like to thank my friend Mallika with whom I spent the most memorable time in the graduate school. I want to extend my thanks to Drs. S. Das, Art, and Praveen for their technical advices and help.

Finally, I would like to thank my wife Sreejeta for her unconditional love and support which have indisputably been my pillars of strength during this endeavor, to my parents Mr. Susobhan Dasgupta and Mrs. Ruma Dasgupta for their blessings and inspiration, and to all my friends and family in particular to my brother Shiladitya for their well wishes.

This work was supported by Department of Defense (DOD), Prostate Cancer Research Program (PCRP) Predoctoral Training Award W81XWH-09-1-0220.

TABLE OF CONTENTS

ABBREVIATIONS.....	viii
LIST OF TABLES.....	xi
LIST OF ILLUSTRATIONS.....	xii

CHAPTER

I. INTRODUCTION.....	1
Pathobiology of prostate cancer	2
Benign prostatic hyperplasia.....	2
Prostatic intraepithelial neoplasia	3
Grading prostate cancer: Gleason Scores	3
Metastatic prostate cancer.....	4
Molecular basis of prostate cancer migration, invasion and metastasis.....	6
Cell Migration.....	7
Cell Invasion.....	8
Role of proteases in the pathophysiology of metastatic prostate cancer.....	8
Genes and signaling pathways in prostate cancer progression.....	11
17q12-21 amplicon: Genes at <i>ERBB2</i> locus.....	12
Expression of C17orf37 in cancer cells and tissues.....	14
Analysis of C17orf37 protein sequence and putative motifs.....	17

Biochemistry of prenylation.....	19
Importance of prenylated proteins in cancer	
oncogenesis and metastasis.....	20
Prenylated proteins and processing enzymes as novel drug targets....	22
Objectives of the present study.....	23
References.....	26

II. NOVEL GENE *C17ORF37* IN 17q12 AMPLICON

PROMOTES MIGRATION AND INVASION OF

PROSTATE CANCER CELLS.....	38
Abstract.....	38
Introduction.....	40
Results.....	42
Discussion.....	64
Materials and methods.....	70
References.....	75
Supplementary.....	82
Supplementary methods.....	84
Supplementary figures.....	92
Supplementary references.....	102

III. ISOPRENYLATION REGULATES C17ORF37	
MEDIATED CANCER CELL MIGRATION	
AND INVASION.....	103
Abstract.....	103
Introduction.....	105
Results.....	107
Discussion	129
Materials and methods.....	131
Supplementary Figures.....	136
References	150
IV. SUMMARY AND DISCUSSION.....	155
Future Directions.....	163
References.....	164
APPENDIX.....	166

ABBREVIATIONS

AKT	v-akt murine thymoma viral oncogene
AR	Androgen receptor
BPH	benign prostatic hyperplasia
C17orf37	Chromosome 17 open reading frame 37
Cdc42	Cell division control protein 42 homolog
Cys	Cysteine
DNA	Deoxyribonucleic acid
ERBB2 (ErbB-2)	erythroblastic leukemia viral oncogene homolog 2, neuro/glioblastoma derived oncogene homolog (avian), same as Her-2/neu
ECM	Extra-cellular matrix
ELISA	Enzyme linked immunosorbent assay
EMSA	Electrophoresis mobility shift assay
EphB1	Ephrin type-B receptor 1
ERK	Extracellular signal regulated kinase
ESI-FTICR	Electrospray ionization Fourier transform ion cyclotron
FISH	Fluorescence <i>in situ</i> hybridization
GFP	Green fluorescent protein
GRB7	Growth receptor bound protein 7
H&E	Hematoxylin and Eosin Staining
Her-2/neu	Human Epidermal growth factor Receptor 2

HGF	Hepatocyte growth factor
IDC	Infiltrating ductal carcinoma
IκB-α	Inhibitor of nuclear factor kappa-B kinase subunit alpha
IKK	I κ B kinase
ILC	Invasive lobular carcinoma
MGC14832	Mammalian genome collection 14832, also known as C17orf37
MMP	Matrix metalloproteinase
Myc	myelocytomatosis viral oncogene homolog (avian)
NF-κB	Nuclear factor of kappa light polypeptide gene enhancer in B- cells
PBS	Phosphate buffered saline
PCR	Polymerase chain reaction
PI3K	Phosphoinositide Kinase-3
PIN	Prostate intraepithelial neoplasia
PKB	Protein kinase B, also known as Akt
PPP1R1B	Protein phosphatase 1, regulatory (inhibitor) subunit 1B
PSCA	Prostate stem cell antigen
PPi	Pyrophosphate
PTEN	phosphatase and tensin homolog
Rac1	Ras-related C3 botulinum toxin substrate 1
RARA	retinoic acid receptor – alfa
RhoA	Ras homolog gene family, member A

RNA	Ribonucleic acid
SD	Standard deviation
SDS-PAGE	Sodium dodecyl sulfate polyacrylamide gel electrophoresis
Ser	Serine
siRNA	short interference RNA
STARD3	steroidogenic acute regulatory protein (<i>START</i>) domain containing 3
STAT	Signal transducer and activator of transcription
tPA	Tissue-type plasminogen activator
TURP	transurethral resection of the prostate
uPA	urokinase-type plasminogen activator
uPAR	uPA receptor
VEGF	Vascular epidermal growth factor

LIST OF TABLES

CHAPTER II

Table 1	Primer sequences.....	82
Table 2	siRNA sequences.....	83

LIST OF ILLUSTRATIONS

CHAPTER I

Figure

1. An updated version of Dr. Gleason's simplified drawing of the five grades of prostate cancer. From *Urologic Pathology: The Prostate. Lea and Febiger, Philadelphia, 1977, 171-198*..... 5
2. Schematic representation of tumor cell metastasis..... 10
3. 17q12-21 amplicon..... 15
4. C17orf37 protein..... 18
5. Biochemistry of prenylation..... 21

CHAPTER II

Figure

1. C17orf37 mRNA and protein expression in human prostate cancer cells..... 43
2. Expression of C17orf37 in human normal, benign prostatic hyperplasia (BPH) and prostate adenocarcinoma tissue specimens..... 46
3. Subcellular localization of C17orf37 in human prostate cancer cell lines..... 49

4. C17orf37 expression regulates migration and invasion of prostate cancer cells.....	53
5. siRNA mediated silencing of <i>C17orf37</i> results in the downregulation of <i>MMP-9</i> , <i>uPA</i> and <i>VEGF</i> expression.....	57
6. Knockdown of C17orf37 by siRNA reduces the NF- κ B DNA binding activity via suppressing the AKT activation.....	61
7. Expression of <i>C17orf37</i> mRNA in prostate cancer cells.....	92
8. Mass spectrum of recombinant C17orf37 protein.....	94
9. Overexpression of C17orf37 increases invasive potential of DU-145 cells.....	96
10. Graphical representation showing expression ratio of p-Akt/Akt and p-ERK/ERK normalized to housekeeping gene GAPDH.....	98
11. Confocal microscopy showing the expression of C17orf37 preferentially localized to the leading edge of the migrating DU-ORF-9 cells.....	100

CHAPTER III

Figure

1. C17orf37 is geranylgeranylated by GGTase-I enzyme at Cys 112.....	108
2. Post-translational modifications are necessary for membrane association of C17orf37 protein.....	113

3. Expression of prenylation-deficient C17orf37 mutant inhibits	
cell migration.....	118
4. C17orf37 prenylation by GGTase-I stimulates filopodia formation.....	121
5. The Cys112Ser mutation impairs C17orf37 function <i>in vivo</i>	125
6. Cys 112 to Ser mutation of C17orf37 impairs addition of	
geranylgeranyl group by GGTase-I enzyme.....	136
7. C17orf37 is predominantly localized to the cell membrane.....	138
8. Stable expression of GFP-tagged C17orf37	
constructs in NIH3T3 cells.....	140
9. C17orf37 is expressed in the non-raft microdomains	
of plasma membrane.....	142
10. Ectopic stable expression of C17orf37 increases	
migration of DU-145 cells.....	144
11. Expression of GFP-fused constructs injected in the	
tail vein of the mouse.....	146
12. Experimental lung metastasis.....	148

CHAPTER IV

Figure

1. Different states of C17orf37 protein.....	158
2. Schematic representation of the role of C17orf37 in migration	
and invasion of cancer cells.....	161

CHAPTER I

INTRODUCTION

Prostate cancer is the most common type of cancer diagnosed in American men and is the second leading cause of cancer related death in men (Pienta and Loberg, 2005). National Cancer Institute (NCI) estimates about 192,280 American men will be diagnosed with prostate cancer in 2009 and approximately 27,360 will die of the disease. It is the most prevalent tumor in men and despite increasing efforts at early detection, 10-20% of the cases present bone metastasis at diagnosis. Most men diagnosed with prostate cancer can survive the primary localized tumor, but because of the widespread metastasis that are resistant to conventional treatment including improved surgical techniques, mortality rates remain extremely high. Development of prostate cancer is prevalently asymptomatic, and once symptoms are noticed, it usually implies an advanced disease stage. Metastatic dissemination of cancer cells consists of series of sequential interrelated steps that lead to spread of the disease to distant organs like bone, lymph nodes, rectum, urinary bladder and brain, which ultimately lead to death. So it is critical to understand the mechanisms that drive prostate cells to become metastatic. Moreover, it is also important to diagnose the disease at an early stage so that proper therapy can be administered, for which we need a predictable biomarker. Thus understanding the molecular events in the pathogenesis of prostate cancer and detecting a reliable biomarker

will offer improved diagnosis, prognosis and therapy of the disease which will ultimately help us to eliminate prostate cancer.

Pathobiology of Prostate Cancer

Benign Prostatic Hyperplasia

Tumorous growth in prostate can either be benign or malignant. Benign, nodular, paraurethral hyperplasia of the prostate (BPH) is one of the most prevalent disease of elderly American men. BPH can develop due to hormonal imbalance, due to altered testosterone level, or may be stimulated by testosterone or dihydrotestosterone. Several growth factors may play important roles in regulating epithelial and stromal cells in BPH (Aumuller *et al.*, 1993). The most common growth factors include epidermal growth factor (EGF), basic fibroblastic growth factors (bFGF), and transforming growth factors-alpha and beta (TGF- α , and TGF- β) (Harper *et al.*, 1993). These growth factors regulate epithelial and stromal cell growth, proliferation and achieve prostatic homeostasis. In presence of hormonal imbalance, the expression of the growth factor receptors are altered, which leads to increased cellular signaling and stromal cell proliferation. Nodular hyperplasia of the prostate is due to increased proliferation of glandular-epithelial compartment, with simultaneous mesenchymal-stromal cell proliferation. This may lead to the alteration of the stromal unit, with inversion of the proliferation compartment, shift of luminal cells, thereby resulting in development of adenomatous hyperplasia. If this develops in the peripheral part of the prostate gland it is termed as prostatic intraepithelial neoplasia (PIN) (Aumuller *et al.*, 1993).

Prostatic Intraepithelial Neoplasia

Histopathologically PIN is regarded as the precursor of prostatic adenocarcinoma. PIN exists with more than 85% of cancer, and clinically it has a strong association with prostatic carcinoma (Bostwick and Brawer, 1987; Hull *et al.*, 2009). Identification of PIN in biopsy specimens warrants further investigation to detect invasive carcinoma. However, since it is not known whether PIN can progress, regress or remains stable, several classifications of PIN has been defined for correct pathological identification. This includes PIN1 - low grade, and PIN 2 and PIN3 considered as high grade PIN. Although several studies have identified PIN as predictive biomarker for development of aggressive carcinoma, low grade PIN in general is regarded as nonmalignant, and may or may not develop adenocarcinoma of the prostate (Markham, 1989). On the other hand, high grade PIN is characterized by enlarged nuclei, dense chromatin and disruption of basal cell layer, and frequently associated with invasive carcinoma (Bostwick and Brawer, 1987).

Grading Prostate Cancer: Gleason Grades

Majority of prostate malignancies are adenocarcinomas derived from outer zone of prostate gland and it is a daunting task to predict individual patient's tumor. Several grading systems have been implemented to improve pathologist's ability to predict biological behavior of the tumor. The most common and widely accepted method of grading prostate cancer is 'Gleason Grading System' commonly referred to as 'Gleason Scores'. The morphological methods of grading prostate cancer based on Gleason score

is based on prostatic glandular architecture and stromal involvement (Lotan and Epstein, 2010). Gleason grades are scored as integers ranging from 1 through 5 to give the histologic score (Epstein, 2010). Grade 1 (also known as very well differentiated) contains closely packed neoplastic glands of uniform size and shape, and sharply separated glands surrounded by fibrovascular stromal cells. Grade 2 (known as well-differentiated) is characterized by mild separation of tumor glands by stroma and irregularly shaped neoplastic glands. Grade 3 (termed as moderately differentiated carcinoma) is characterized by irregular extension of glands into the surrounding prostatic stroma with prevalent large nuclei. The glands are smaller in size with tiny or no lumina, and lack invasive edges. Grade 4 and 5, known as poorly differentiated are the most aggressive tumors and denotes the advanced stage of the disease. Grade 4 is characterized by tiny glands or loss of glandular differentiation with invasive edges and solid tumor cells. Grade 5 shows no glandular differentiation and carcinomas resemble smooth rounded packed foci, with infiltrating tumor masses. Due to close resemblance between certain grades, the Gleason grading system is currently simplified by compressing the grades into three categories: (1) 2-3-4: well-differentiated, (2) 5-6-7: moderately differentiated and (3) 8-9-10: poorly differentiated (May *et al.*, 2010).

Metastatic Prostate Cancer

Prostate cancer is a remarkably prevalent tumor, possibly representing histologically the most common malignant tumor in the world. Carcinoma of prostate usually develops as a small, well-differentiated lesion and gradually increases in size and de-differentiates into

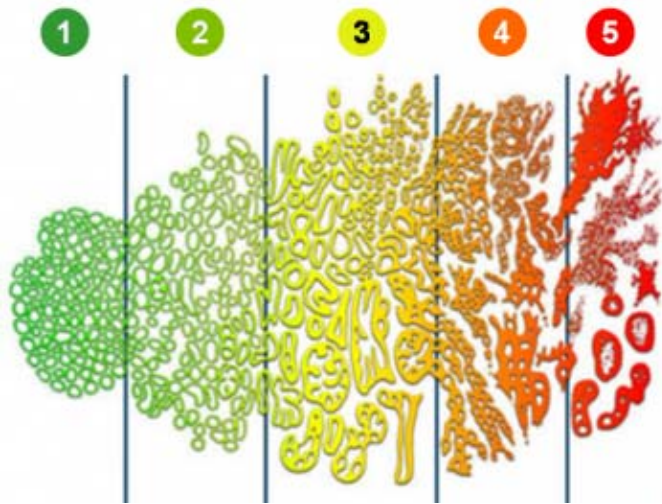


Figure 1: An updated version of Dr. Gleason's simplified drawing of the five Gleason grades of prostate cancer. Grade 1 appears on the far left and grade 5 on the far right.
Adapted from Gleason DF. The Veteran's Administration Cooperative Urologic Research Group: histologic grading and clinical staging of prostatic carcinoma. In Tannenbaum M (ed.) Urologic Pathology: The Prostate. Lea and Febiger, Philadelphia, 1977; 171-198.

moderately or poorly differentiated lesions. Some prostate cancers that remain small and well-differentiated rarely metastasize. The initial metastases of prostate carcinomas are usually moderately differentiated and fewer are well-differentiated. Tumor cells are spread by both the lymphatic route and the bloodstream (Randolph *et al.*, 1997). Metastases are usually found first in the regional lymph nodes or bone, and can subsequently spread to urinary bladder, liver, kidney, rectum, lungs and even to brain. Bone is the most common site for prostate cancer metastasis, as it has a suitable microenvironment for cancer cell growth because of large amounts of cytokines secreted by tissues. Insulin growth factor -II (IGF-II), TGF- β and platelet derived epidermal growth factor (PDGF) are the most abundant cytokines found in the bony tissue (Diener *et al.*, 2010). Prostate cancer cells can pass through the veins and enter the bone marrow, where it can interact with the bone tissues and stem cells. It then invades the trabecular bone and grows inside the cortical bone tissues developing osteoblastic metastasis (Edlund *et al.*, 2004; Lu and Kang, 2010).

Molecular basis of Prostate Cancer Migration, Invasion and Metastasis

The molecular basis of tumor progression depends on local invasion, intravasation, survival in the circulation, extravasation and colonization. Metastasis is thus a multistage process in which the prostate cancer cells spread from localized tumors to distant organs. The temporal course of metastasis particularly for prostate cancer is delayed compared to other adenocarcinomas like lungs (Nguyen *et al.*, 2009).

Cell Migration

Migration and invasion are the hallmarks of cancer cell metastasis, which are very closely interrelated, yet mechanistically distinct physiological steps (Lauffenburger and Horwitz, 1996). This allows the neoplastic cells to enter the lymphatic and blood vascular system for dissemination into the circulation, and then proliferate in distant organs (Fidler, 2003; Gupta and Massague, 2006). Cellular motility allows the tumor cells to move through the extracellular matrix (ECM), coordinated by release of several enzymes, proteases and growth factors (Christofori, 2006; Zamir *et al.*, 2000). Cell migration through the tissues occurs due to continuous cycle of events. First, the cell gets polarized, followed by formation of protrusion known as pseudopod at the leading edge, and subsequently retraction and contraction generates force which allows the cell to glide through the tissues. The cellular protrusions are driven by actin polymerization which assembles filaments to generate projections known as lamellipodia and filopodia. Filopodia are finger-like projections often referred to as ‘antenna’ for sensing the direction of cellular migration. The polymerization of actin is a highly regulated process, mediated by small GTPase like Rac1, Rho and Cdc42 (Kaibuchi *et al.*, 1999). These proteins assemble cortical actin filaments beneath the plasma membrane known as stress fibers. Growing cell protrusions then touch the adjacent ECM and initiate binding to the substratum via adhesion molecules like integrins, and cell adhesion molecules (CAM). Multiple environmental factors regulate cellular motility and contribute to increased invasiveness in prostate cancer cells (Hynes and Zhao, 2000). Motility inducing chemokines and growth factors maintain promigratory signals which activate Rac, Rho, and Cdc42

thereby propelling the cellular migratory process (Nobes and Hall, 1995). Several signaling pathways have been indicated to play important role in cell migration, of which PI3K/AKT and ERK pathways are widely studied (Leopoldt *et al.*, 1998; Ren *et al.*, 1996).

Cell Invasion

Role of proteases in the pathophysiology of the metastatic prostate cancer

Malignancy and metastatic dissemination require both the capacity for deregulated proliferation and local invasion. Invasion and metastasis are interlinked and require common cell processes like cell adhesion, cell migration, and proteolytic cleavage (Figure 2) (Price *et al.*, 1997). Although cellular invasion is a regular physiological process in embryological development, cancer cell invasion is deregulated due to aberrant activation of signaling pathways. Several oncogenes and tumor suppressor genes have been shown to have prominent role in cancer development. Tumor cells growing at the primary site need a vascular structure, which is induced when tumor mass exceeds 1-2 mm in diameter. Vascular endothelial growth factor (VEGF), PDGF and HGF are a prerequisite to the establishment of a capillary network from the surrounding tissue (Grant *et al.*, 1993; Kubota *et al.*, 1997; Leung *et al.*, 1989). Tumor cells released from the primary foci infiltrate the surrounding tissue and basement membrane by degrading the extracellular matrix proteases. Several proteolytic enzymes specifically degrade the extracellular matrix proteins like matrix metalloproteinases (MMPs), cysteine proteases and serine proteases. Plasminogen activators (PA) are serine specific proteases that

convert inactive plasminogen to active plasmin that has broad specificity to degrade ECM proteins. Urokinase type plasminogen activator (uPA) is a glycoprotein primarily involved in degrading ECM proteins by generating active plasmin, thereby regulating invasiveness and metastatic dissemination of cancer cells (Andreasen *et al.*, 1997). uPA has been shown to activate certain growth factors by converting them from latent form to activated form. This implicates the role of uPA both in extracellular modeling as well as in tumor cell migration and invasion (Price *et al.*, 1997). uPA exerts its non-proteolytic activity through its interaction with uPA receptor (uPAR) which forms complex with integrins and controls cell adhesion and migration. Plasmin generated by uPA mediates invasion of prostate tumor cells directly by degrading matrix proteins such as collagen IV, fibronectin, and laminin or indirectly by activating MMPs. MMPs are metalloproteases that depend on zinc ion for their activity and are secreted as inactive proenzymes. Conversion of proenzymes to active MMPs results in proteolytic cleavage of ECM proteins thus facilitating migration and invasion. In normal cells MMPs are regulated at a number of levels, including transcriptional regulation by growth factors, post-transcriptional regulation due to changes in mRNA stability, post-translational by activation of the secreted latent form and inhibition by endogenous inhibitors (Coussens and Werb, 1996). In advanced prostate cancer patients, MMP-2 and MMP-9 are found to be overexpressed and correlate with poor prognosis (Zhang *et al.*, 2005). Both MMP-2 and MMP-9 are broadly classified as gelatinases and their preferred substrate includes gelatin, collagen I and IV, vitronectin and fibronectin (Price *et al.*, 1997). In prostate cancer, MMP-2 and MMP-9 expression is activated transcriptionally by ERK-AP2 and

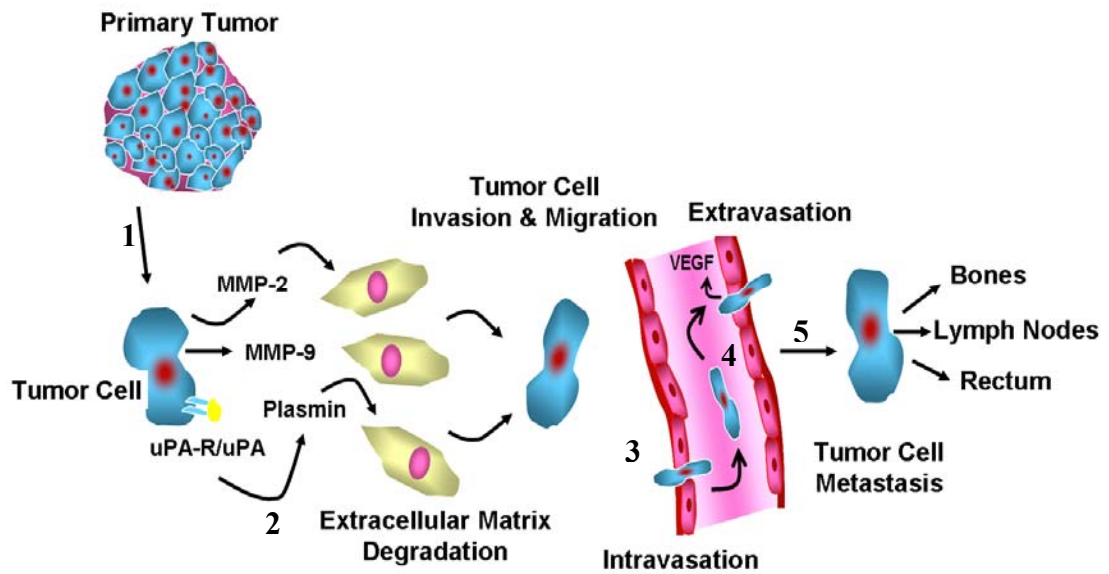


Figure 2: Schematic representation of tumor cell metastasis. (1) Local Invasion, (2) Migration and Invasion, (3) Intravasation, (4) Circulation, and (5) Extravasation.

NF- κ B pathways, as well as by the downregulation of the endogenous inhibitors of MMPs facilitating aggressive invasion and metastasis (Price *et al.*, 1997; Sliva, 2004). Another important regulator of plasmin generation is tissue-type plasminogen activator (tPA). Although the role of tPA in endothelial cell migration is prominent, studies have shown that invasive prostate cancer cells like PC-3 show increased expression of cell surface bound and secreted tPA (Forbes *et al.*, 2003). tPA is an important member of the fibrinolytic system which converts inactive plasminogen to active plasmin. As mentioned above, secreted plasmin has a variety of target molecules which result in ECM degradation. So it is quite evident that deregulated activation of plasmin is an important event that facilitates the prostate tumor cells to gain invasive potential, thereby resulting in metastasis.

Genes and Signaling Pathways in Prostate Cancer Progression

A number of studies have identified differentially regulated genes that are expressed in neoplastic progression of prostate cancer. Differentially expressed genes are predicted to play key roles in prostate cancer development and may also serve as clinically useful biomarkers for early detection and diagnosis. Although large sets of genes have been identified, few have been characterized in the molecular progression of the disease. The most widely studied oncogenes which have been implicated in prostate cancer include *RAS*, *MYC*, *ERBB2*, *PSCA* and *AR* (Baxevanis *et al.*, 2006; Bianco, 2004; Dong, 2006; Kung and Evans, 2009; Pearson *et al.*, 2009). The *RAS* oncogene is activated by point mutation, the *MYC* oncogene by amplification and *ERBB2* is either amplified or modified

through transcriptional and post-transcriptional deregulation. Several prostate cancer susceptibility loci have been identified at 1q24-25, 1q42, 8q24, 10q23, 16q23, 17p21, and 17q12 (Edwards, 2010; Eeles *et al.*, 2008; Sun *et al.*, 2008). Candidate genes in these loci are frequently found to be amplified or lost, which may lead to prostate cancer. Almost 50% of prostate cancer patients have been found to harbor deletions on 10q amplicon, harboring *PTEN* gene, a known tumor suppressor (Dong, 2006). *PTEN* loss results in increased activation of several oncogenes including Akt which activates downstream signaling facilitating metastatic progression of prostate cancer (Assinder *et al.*, 2009). *PTEN* mutations have also been detected in 5-27% of primary prostate tumors and 30-58% in metastatic prostate cancer (Dong, 2006). Mutations in the *ERBB2* gene have been reported in number of tumors including breast and ovarian, although high level amplification does not occur in prostate cancer. Nevertheless, inhibition of *ERBB2* by monoclonal antibody Herceptin (Bianco, 2004) does inhibit growth of prostate cancer cells *in vitro*. In hormone refractory cancer, *ERBB2* is known to enhance androgen receptor signaling, thereby promoting tumor growth and metastasis.

17q12-21 Amplicon: Genes at ERBB2 Locus

17q12 amplicon encodes several genes that have been shown to have profound effect in the development of different types of cancer including prostate cancer. Among the genes that have been shown to be involved in prostate cancer progression include *ERBB2*, *GRB7*, *RARA*, *STARD3* also known as metastatic lymph node 64 (*MLN64*). Overexpression of *ERBB2* by gene amplification and resulting increase in gene copy

number activates the flanking genes that are supposed to impose relevant function in the development of primary breast tumor and subsequently progression to metastasis. Among the genes that are co-amplified with *ERBB2* are topoisomerase II α (*TOP2A*), retinoic acid receptor α (*RARA*) (Keith *et al.*, 1993) and growth factor receptor-bound protein 7 (*GRB7*) (Stein *et al.*, 1994) which are already known to impart crucial function in tumorigenesis. *RARA-ERBB2* ratio analysis by FISH is an important predictor for gene amplification at 17q12 (Troxell *et al.*, 2006). *TOP2A* is frequently amplified with *ERBB2* and confer resistance to *ERBB2* targeted therapy. *TOP2A* inhibitors like anthracyclines have shown good results in *ERBB2* amplified tumors. Grb7 is an adapter-type signaling protein molecule that has been shown to physically interact with *ERBB2* by its SH2 domain (Pero *et al.*, 2007). Grb7 expression has been associated with invasive and metastatic phenotype of tumor cells, regulating cell migration through its association with focal adhesion kinase and ephrin receptor EphB1 (Han *et al.*, 2002). In an effort to identify other novel genes of 17q12-21 chromosomal region that are amplified with *ERBB2*, Kauraniemi *et al.* (Kauraniemi *et al.*, 2003) defined the core region of the amplicon and found 8 flanking genes that show coordinated expression. By cDNA microarray analysis, they found a 280kb core region that map between *PPP1R1B/DARP-32* and *GRB-7* to be frequently amplified with *ERBB2*. Despite the small size of the amplicon, they demonstrated six known genes, two of which are hypothetical proteins MGC9753 (*PERLD1*) and MGC14832 (*C17orf37*) that show statistically significant correlation between amplification and expression (Kauraniemi *et al.*, 2003). Genes that are already linked to tumor development are steroidogenic acute regulatory protein

(*START*) domain containing 3 (*STARD3*) which is overexpressed in breast cancer cells thereby increasing steroid hormone production and promoting growth of hormone-responsive tumors (Alpy *et al.*, 2001). Peroxisome proliferator-activated receptor (*PPAR*) binding protein (*PPARBP*) is a nuclear co-activator which interacts with several receptors that promotes cell growth, differentiation, and neoplastic conversion. *PPARBP* has been shown to regulate p53 dependent apoptosis and its inappropriate activation contributes to tumor progression (Misra *et al.*, 2002). Among the two hypothetical proteins *C17orf37* displayed the tightest correlation between amplification and increased expression, thus making *C17orf37* an attractive amplification target gene (Kauraniemi and Kallioniemi, 2006). *C17orf37* is a novel gene and does not show any sequence similarity with any known gene or protein, leaving its function unknown.

Expression of C17orf37 in cancer cells and tissues

Chromosome 17 open reading frame 37 (C17orf37), also known as *C35/Rdx12/MGCI4832*, is a novel gene located in the 17q12-21 chromosomal region that is frequently amplified with *ERBB2*. The gene is located 505 nucleotides away from 3' end of *ERBB2* oncogene in a tail to tail chromosomal rearrangement and 7402 nucleotides away from *GRB7* (Evans *et al.*, 2006). Several studies have shown amplification and overexpression of *C17orf37* in *ERBB2* amplified tumors. *C17orf37* messenger expression is significantly higher in breast tumor cell lines and primary tumors with *ERBB2* amplification, compared to tumor cells with basal *ERBB2* expression.

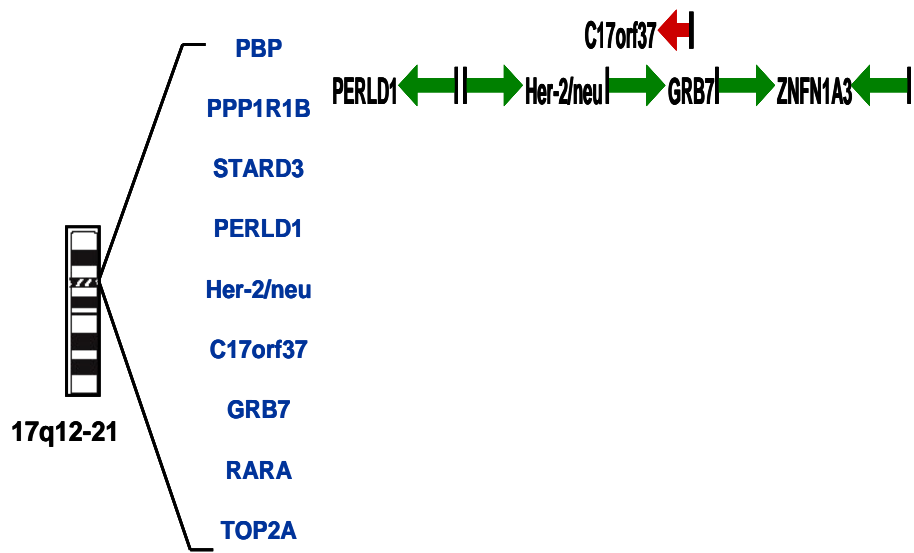


Figure 3: 17q12-21 amplicon. Left - Showing the human chromosome 17q12 amplicon region. Right – Shows the location of C17orf37 gene in a tail to tail rearrangement with Her-2/neu.

Immunohistochemical analysis of breast cancer tissues revealed C17orf37 as a predictive prognostic marker of invasive breast cancer. C17orf37 expression was found to positively correlate with the grade and stage of IDC indicating C17orf37 expression increases with breast tumor progression. Expression of C17orf37 in the breast cancer tissue specimens was found to be uniform throughout the tumor cells. Pathological analysis of the sections revealed C17orf37 positive tumor cells exhibited necrosis and lymphocytic infiltration (Evans *et al.*, 2006). Although C17orf37 is expressed in primary and low grade breast tumors, its expression was found to be intense in metastatic breast tumor cell lines and tissues that have been examined. Metastatic breast tumor lines BT-474, T-47D and SKBR-3 showed increased expression of C17orf37 compared to normal breast epithelial cell line H16N2 (Evans *et al.*, 2006). Analysis of breast cancer tissue sections that metastasized to distant organs revealed robust expression of C17orf37. Patients with breast cancer that metastasized to distant organs showed intense expression of C17orf37 in the transformed malignant cells of liver and lungs (Evans *et al.*, 2006). Even metastasis of breast tumor cells to skin on mid back showed persistent expression of C17orf37, suggesting C17orf37 is associated with invasion and migration of breast tumor cells to distant organs. On the contrary, analysis of normal tissues or adjoining tissues of breast cancer cells showed minimal expression of C17orf37. A broad search of 38 normal tissues of different organs showed none of the tissues to be positive for C17orf37 (Evans *et al.*, 2006) except for Leydig cells of testis, suggesting expression of C17orf37 may be involved in tumorigenesis and progression of the disease to metastatic variant.

Analysis of C17orf37 protein sequence and putative motifs:

The full length C17orf37 transcript is 776 nucleotides with 4 exons and the final spliced product includes an open reading frame encoding a protein of 115 amino acids with a molecular weight of 12kD (Figure 4A). C17orf37 has been found to be highly conserved in higher eukaryotes. Immunohistochemical analysis of breast tumor cells expressing C17orf37 showed intense punctate staining in the cytosol around the membrane (Evans *et al.*, 2006). The punctate staining can argue for the expression of the protein in cytosolic compartments and organelles. Scanning the putative sequence of the protein (Figure 4B) to identify potential motifs revealed a “CaaX” C- terminal prenylation site comprising the last four amino acids “CVIL”. “CaaX” group of proteins are either prenylated or geranylgeranylated by enzymes farnesyltransferase (FTase) and geranylgeranyl transferase type I (GGTase-I) respectively (Fu and Casey, 1999). However, specificity of the enzyme is determined by the carboxyl terminal residue of the CaaX motif. If “X” is leucine, the protein is preferentially modified by GGTase-I enzyme (Fu and Casey, 1999), suggesting C17orf37 translocation to the membrane may be mediated by GGTase-I. Additional search for phosphorylation motifs revealed Ser-97 of C17orf37 to be a predicted kinase substrate for Protein kinase A (PKA). Moreover, it has been reported that C17orf37 has a prototypical immunoreceptor tyrosine-based activation motif (ITAM) of consensus sequence “D/E/N xx Y xx L/I_{x6-8} Y xx L/I” in the N-terminal region “EATYLELASAVKEQYPGIEI” (Figure 4B) (Evans *et al.*, 2006). ITAM is conserved sequence of four amino acids that is repeated twice in the cytoplasmic tails of certain cell

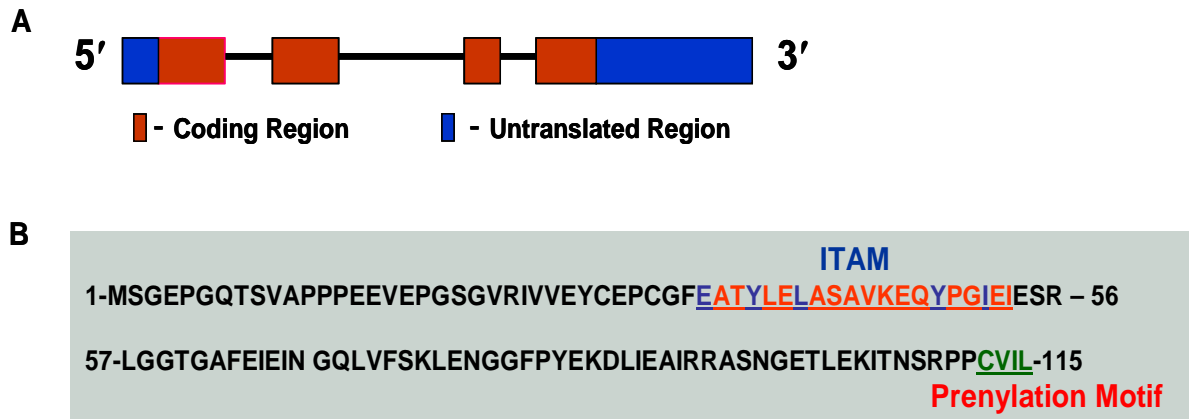


Figure 4: C17orf37 protein. A- C17orf37 has 4 exons and, 5' and 3' untranslated region. B- Potential motifs in C17orf37 sequence. An immunoreceptor tyrosine based activation motif (ITAM) is present near the N-terminal region, marked in red and blue. A prenylation motif 'CaaX' is present at the C-terminal end of the protein marked in green.

surface proteins. The motif contains a tyrosine separated from a leucine by any two other amino acids, giving the signature “YxxL”. ITAMs are important for signal transduction and are found in the tails of important cell signaling molecules such as the CD3 and ζ -chains of the T cell receptor complex, the CD79-alpha and -beta chains of the B cell receptor complex and certain Fc receptors (Abram and Lowell, 2007). The tyrosine residues within these motifs become phosphorylated following interaction of the receptor molecules with their ligands and form docking sites for other proteins involved in the signaling pathways of the cell. These putative motifs of C17orf37 predict it to be prenylated protein bound to the membrane on the cytoplasmic side with the potential ITAM at the N-terminal end acting as docking site for adapter proteins that trigger downstream signaling.

Biochemistry of Prenylation

Post-translational modification of protein by addition of isoprenyl groups to the cysteine residue of the ‘CAAX’ box is a multistep process. Prenylation of proteins involves three specific steps. First, the isoprenyl groups are attached to the cysteine residue by prenyl transferase enzymes (Figure 5, step 2). The ‘X’ amino acid of the ‘CAAX’ box is involved in the recognition and specificity for enzyme substrate binding. If, ‘X’ is leucine, geranylgeranyl transferase enzyme catalyzes the addition of 20 carbon geranylgeranyl group to the cysteine, or if ‘X’ is methionine or serine, farnesyl transferase enzyme (FTase) modifies the protein. Following the attachment of the

isoprenyl groups, the last three amino acids “aaX” are cleaved by specific enzyme called “CaaX proteases or Ras converting enzyme 1 (Rce1) bound to the outer surface of the endoplasmic reticulum membrane (Figure 5, step 3). Finally, the carboxyl group of the prenylcysteine residue is methylated by a ‘CaaX’ methyltransferase, called isoprenylcysteine-O-carboxyl transferase (Icmt) (Figure 5, step 4). These modifications make the C-terminal end substantially hydrophobic thus exhibiting higher affinity for membrane localization (Fu and Casey, 1999; Winter-Vann and Casey, 2005) (Figure 5).

Importance of prenylated proteins in cancer oncogenesis and metastasis

Family of prenylated proteins include Ras adapter proteins and Rho GTPases that act as intracellular signaling molecule. In tumor cell Ras and Rho GTPases occupy central and pivotal role as a molecular switch controlling several aspects of cytoplasmic rearrangement during motility and invasion (van Golen, 2003). Increased signaling by other GTPase like TAP1A has also been shown to play crucial role in myeloproliferation (Aiyagari *et al.*, 2003). G-protein coupled receptors (GPCR) have been implicated in cancer and γ -subunits of the heterotrimeric G proteins are prenylated at the ‘CAAX’ motif as well. The best understood importances of prenylation are for protein-protein interactions that regulate protein activity and function. Addition of isoprenyl groups confers hydrophobicity which allows prenylated proteins to bind to other proteins. This includes interaction of small GTPase like Rho, Rac, Ras with Guanine exchange factor (GEF) proteins, which is an important rate limiting step for their

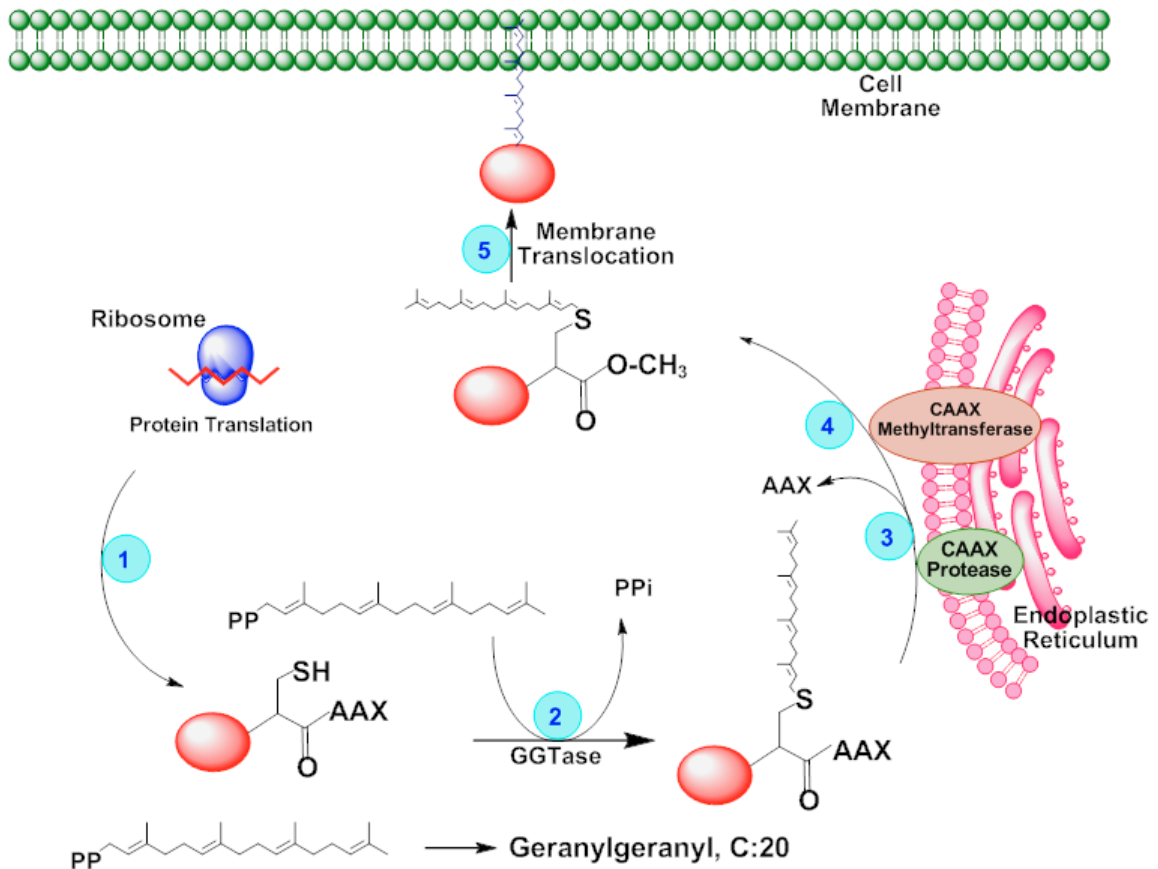


Figure 5: Biochemistry of Prenylation. (1) After translation, CAAX proteins present the cysteine -SH group to the GGTase enzymes, (2) Geranylgeranyl (carbon 20) or farnesyl (carbon 15) are added to the cysteine residue, (3) Last three amino acids “AAX” are cleaved by CAAX protease enzyme present on ER membrane, (4) The free carboxyl group is methylated by CAAX methyltransferase enzyme, and (5) Prenylated protein translocates to the membrane.

activity and function (Allal *et al.*, 2000; Fukada *et al.*, 1990; Hori *et al.*, 1991; Kato *et al.*, 1992). Blocking of prenylation enzymes with FTase and GTase inhibitors have shown substantial reduction in migration, invasion and viability of breast tumor cells (Peterson *et al.*, 2006; Sparano *et al.*, 2006). Even statins that block cholesterol biosynthesis thus reducing the synthesis of isoprenyl molecules have been shown to reduce the invasive behavior of the breast tumor cells (Efuet and Keyomarsi, 2006). This suggests that prenylated form of the proteins is the activated molecule that can control invasive and metastatic behavior in tumor cells and blocking their modification will allow us to regulate the progression of the cancer.

Prenylated proteins and processing enzymes as novel drug targets

Several inhibitors targeting FTase and GGTase enzymes have been developed over the years, and clinical trials of two such compounds have reached Phase III clinical trials (Doll *et al.*, 2004; Mazieres *et al.*, 2004). Although FTase inhibitors showed good *in vitro* efficacy, clinically they were not that potent against solid tumors. However, in hematological cancers, the overall response rate in patients was much better. The reasons for this can be attributed to the possibility, that 'CAAX' proteins sometimes undergo alternate prenylation (James *et al.*, 1995; Sebti and Der, 2003), which allows farnesylated proteins to be isoprenylated by GGTase enzyme in the absence of FTase. After the discovery of Rce1 and Icmt post-prenylation processing enzymes and their importance in correct subcellular localization of prenylated proteins, several studies have projected Icmt and Rce1 as an alternate drug targets. Deletion of *Rce1* and *Icmt* genes in mouse is

embryonically lethal (Bergo *et al.*, 2001; Bergo *et al.*, 2004; Lin *et al.*, 2002), and mouse embryonic fibroblasts (MEF) established from the knockout mice showed mislocalization of exogenously added Ras and Rho GTPases. Currently there are few effective inhibitors against Rce1 and Icm1 enzymes, however drugs that mimics S-adenosyl homocysteine (SAH) can act as competitive inhibitors and substantially block methyltransferase activity (Perez-Sala *et al.*, 1992). Several classes of compounds are currently under study that specifically blocks Icm1 activity of prenylated proteins *in vitro* (Cushman and Casey, 2009).

Objectives of the present study

Prostate cancer is the second leading cause of cancer related death in men (Pienta and Loberg, 2005). Despite the increasing efforts to diagnose the disease at an early stage, around 10-20% of the patients develop bone metastasis at diagnosis. Therefore it is important to discover predictable biomarkers which will allow us to diagnose the disease at an early stage. Chromosome 17q12 -contains multiple genes that play important roles in different forms of cancer. Recent genetic studies have projected 17q12 loci genes as an important risk factor in prostate cancer progression (Eeles *et al.*, 2008; Sun *et al.*, 2008). *ERBB2* located in the same amplicon is known to play a significant role in prostate cancer progression and its expression correlates with poor hormone refractory prostate cancer in patients (Myers *et al.*, 1994). C17orf37 is a novel gene located in the same amplicon just next to *ERBB2* in a tail to tail rearrangement, functional importance of which is presently unknown. C17orf37 has been reported to be frequently amplified with

ERBB2 in breast tumor cells, however independent activation of C17orf37 has been demonstrated in cell lines expressing low levels of *ERBB2* (Evans *et al.*, 2006). C17orf37 expression positively correlates with grade and stage of breast cancer, and increased expression has been shown in patients with breast to liver and lungs metastasis (Evans *et al.*, 2006). This suggests C17orf37 protein may be an important mediator of cancer cell metastasis. Our recent studies have identified novel gene C17orf37 as a predictive biomarker of prostate cancer. C17orf37 is aberrantly overexpressed in prostate cancer patients compared to minimal expression in normal prostate tissues and tends to positively correlate with the disease progression. C17orf37 has a potential prenylation motif at the C-terminal end and post translational modification may be a key event regulating the function of the protein. Based on these observations we hypothesize that ***overexpression of C17orf37 contributes to the development of invasive prostate cancer and facilitate metastatic progression of the disease as a membrane bound prenylated molecule.*** By combining studies on prostate cancer cell lines, *in vivo* xenografts and translating the basic research in clinical prostate specimens, we will evaluate the functional importance of C17orf37 to drive prostate tumorigenesis and metastasis. We will address our hypothesis through the following specific aims:

- 1. To determine the expression of C17orf37 in prostate cancer cells and human clinical specimens, and identify the subcellular localization of the protein.**

- 2. To identify the functional role of C17orf37 in prostate cancer cells and elucidate the molecular pathways that contributes to the development of the disease.**

- 3. To demonstrate that prenylation of C17orf37 at the C-terminal “CVIL” motif is an important regulatory event that regulates the function of the protein.**

- 4. To directly demonstrate the biological consequences of C17orf37 over-expression in promoting prostate tumor metastasis and elucidate the molecular mechanisms regulating the process in vivo.**

REFERENCES

Abram CL, Lowell CA. (2007). The expanding role for ITAM-based signaling pathways in immune cells. *Sci STKE* **2007**: re2.

Aiyagari AL, Taylor BR, Aurora V, Young SG, Shannon KM. (2003). Hematologic effects of inactivating the ras processing enzyme Rce1. *Blood* **101**: 2250-2252.

Allal C, Favre G, Couderc B, Salicio S, Sixou S, Hamilton AD *et al.* (2000). RhoA prenylation is required for promotion of cell growth and transformation and cytoskeleton organization but not for induction of serum response element transcription. *J Biol Chem* **275**: 31001-31008.

Alpy F, Stoeckel ME, Dierich A, *et al.* (2001). The steroidogenic acute regulatory protein homolog MLN64, a late endosomal cholesterol-binding protein. *J Biol Chem* **276**: 4261.

Andreasen PA, Kj oller L, Christensen L, Duffy MJ. (1997). The urokinase-type plasminogen activator system in cancer metastasis: A review. *Int J Cancer* **72**: 1.

Assinder SJ, Dong Q, Kovacevic Z, Richardson DR. (2009). The TGF-beta, PI3K/Akt and PTEN pathways: Established and proposed biochemical integration in prostate

cancer. *Biochem J* **417**: 411-421.

Aumuller G, Goebel HW, Bacher M, Eicheler W, Rausch U. (1993). Current aspects on morphology and functions of the prostate. *Verh Dtsch Ges Pathol* **77**: 1-18.

Baxevanis CN, Sotiriadou NN, Gritzapis AD, Sotiropoulou PA, Perez SA, Cacoullos NT *et al.* (2006). Immunogenic HER-2/neu peptides as tumor vaccines. *Cancer Immunol Immunother* **55**: 85-95.

Bergo MO, Leung GK, Ambroziak P, Otto JC, Casey PJ, Gomes AQ *et al.* (2001). Isoprenylcysteine carboxyl methyltransferase deficiency in mice. *J Biol Chem* **276**: 5841-5845.

Bergo MO, Lieu HD, Gavino BJ, Ambroziak P, Otto JC, Casey PJ *et al.* (2004). On the physiological importance of endoproteolysis of CAAX proteins: Heart-specific RCE1 knockout mice develop a lethal cardiomyopathy. *J Biol Chem* **279**: 4729-4736.

Bianco AR. (2004). Targeting c-erbB2 and other receptors of the c-erbB family: Rationale and clinical applications. *J Chemother* **16 Suppl 4**: 52-54.

Bostwick DG, Brawer MK. (1987). Prostatic intra-epithelial neoplasia and early invasion in prostate cancer. *Cancer* **59**: 788-794.

Christofori G. (2006). New signals from the invasive front. *Nature* **441**: 444-450.

Coussens LM, Werb Z. (1996). Matrix metalloproteinases and the development of cancer. *Chem Biol* **3**: 895.

Cushman I, Casey PJ. (2009). Role of isoprenylcysteine carboxymethyltransferase-catalyzed methylation in rho function and migration. *J Biol Chem* **284**: 27964-27973.

Diener KR, Need EF, Buchanan G, Hayball JD. (2010). TGF-beta signalling and immunity in prostate tumourigenesis. *Expert Opin Ther Targets* **14**: 179-192.

Doll RJ, Kirschmeier P, Bishop WR. (2004). Farnesyltransferase inhibitors as anticancer agents: Critical crossroads. *Curr Opin Drug Discov Devel* **7**: 478-486.

Dong JT. (2006). Prevalent mutations in prostate cancer. *J Cell Biochem* **97**: 433-447.

Edlund M, Sung SY, Chung LW. (2004). Modulation of prostate cancer growth in bone microenvironments. *J Cell Biochem* **91**: 686-705.

Edwards PA. (2010). Fusion genes and chromosome translocations in the common epithelial cancers. *J Pathol* **220**: 244-254.

Eeles RA, Kote-Jarai Z, Giles GG, Olama AA, Guy M, Jugurnauth SK *et al.* (2008). Multiple newly identified loci associated with prostate cancer susceptibility. *Nat Genet* **40**: 316-321.

Efuet ET, Keyomarsi K. (2006). Farnesyl and geranylgeranyl transferase inhibitors induce G1 arrest by targeting the proteasome. *Cancer Res* **66**: 1040.

Epstein JI. (2010). An update of the gleason grading system. *J Urol* **183**: 433-440.

Evans EE, Henn AD, Jonason A, Paris MJ, Schiffhauer LM, *et al.* (2006). C35 (C17orf37) is a novel tumor biomarker abundantly expressed in breast cancer. *Mol Cancer Ther* **5**: 2919.

Fidler IJ. (2003). The pathogenesis of cancer metastasis: The 'seed and soil' hypothesis revisited. *Nat Rev Cancer* **3**: 453-458.

Forbes K, Webb MA, Sehgal I. (2003). Growth factor regulation of secreted matrix metalloproteinase and plasminogen activators in prostate cancer cells, normal prostate

fibroblasts and normal osteoblasts. *Prostate Cancer Prostatic Dis* **6**: 148-153.

Fu HW, Casey PJ. (1999). Enzymology and biology of CaaX protein prenylation. *Recent Prog Horm Res* **54**: 315.

Fukada Y, Takao T, Ohguro H, Yoshizawa T, Akino T, Shimonishi Y. (1990). Farnesylated gamma-subunit of photoreceptor G protein indispensable for GTP-binding. *Nature* **346**: 658-660.

Grant DS, Kleinman HK, Goldberg ID, Bhargava MM, Nickoloff BJ, Kinsella JL *et al.* (1993). Scatter factor induces blood vessel formation in vivo. *Proc Natl Acad Sci U S A* **90**: 1937-1941.

Gupta GP, Massague J. (2006). Cancer metastasis: Building a framework. *Cell* **127**: 679-695.

Han DC, Shen TL, Miao H, Wang B, Guan JL. (2002). EphB1 associates with Grb7 and regulates cell migration. *J Biol Chem* **277**: 45655.

Harper ME, Goddard L, Glynn-Jones E, Wilson DW, Price-Thomas M, Peeling WB *et al.* (1993). An immunocytochemical analysis of TGF alpha expression in benign and

malignant prostatic tumors. *Prostate* **23**: 9-23.

Hori Y, Kikuchi A, Isomura M, Katayama M, Miura Y, Fujioka H *et al.* (1991). Post-translational modifications of the C-terminal region of the rho protein are important for its interaction with membranes and the stimulatory and inhibitory GDP/GTP exchange proteins. *Oncogene* **6**: 515-522.

Hull D, Ma J, Singh H, Hossain D, Qian J, Bostwick DG. (2009). Precursor of prostate-specific antigen expression in prostatic intraepithelial neoplasia and adenocarcinoma: A study of 90 cases. *BJU Int* .

Hynes RO, Zhao Q. (2000). The evolution of cell adhesion. *J Cell Biol* **150**: F89-96.

James GL, Goldstein JL, Brown MS. (1995). Polylysine and CVIM sequences of K-RasB dictate specificity of prenylation and confer resistance to benzodiazepine peptidomimetic in vitro. *J Biol Chem* **270**: 6221-6226.

Kaibuchi K, Kuroda S, Amano M. (1999). Regulation of the cytoskeleton and cell adhesion by the rho family GTPases in mammalian cells. *Annu Rev Biochem* **68**: 459-486.

Kato K, Cox AD, Hisaka MM, Graham SM, Buss JE, Der CJ. (1992). Isoprenoid addition to ras protein is the critical modification for its membrane association and transforming

activity. *Proc Natl Acad Sci U S A* **89**: 6403-6407.

Kauraniemi P, Kallioniemi A. (2006). Activation of multiple cancer-associated genes at the ERBB2 amplicon in breast cancer. *Endocr Relat Cancer* **13**: 39-49.

Kauraniemi P, Kuukasjarvi T, Sauter G, Kallioniemi A. (2003). Amplification of a 280-kilobase core region at the ERBB2 locus leads to activation of two hypothetical proteins in breast cancer. *Am J Pathol* **163**: 1979-1984.

Keith WN, Douglas F, Wishart GC, McCallum HM, George WD, Kaye SB *et al.* (1993). Co-amplification of erbB2, topoisomerase II alpha and retinoic acid receptor alpha genes in breast cancer and allelic loss at topoisomerase I on chromosome 20. *Eur J Cancer* **29A**: 1469.

Kubota Y, Miura T, Moriyama M, Noguchi S, Matsuzaki J, Takebayashi S *et al.* (1997). Thymidine phosphorylase activity in human bladder cancer: Difference between superficial and invasive cancer. *Clin Cancer Res* **3**: 973-976.

Kung HJ, Evans CP. (2009). Oncogenic activation of androgen receptor. *Urol Oncol* **27**: 48-52.

Lauffenburger DA, Horwitz AF. (1996). Cell migration: A physically integrated molecular process. *Cell* **84**: 359-369.

Leopoldt D, Hanck T, Exner T, Maier U, Wetzker R, Nurnberg B. (1998). Gbetagamma stimulates phosphoinositide 3-kinase-gamma by direct interaction with two domains of the catalytic p110 subunit. *J Biol Chem* **273**: 7024-7029.

Leung DW, Cachianes G, Kuang WJ, Goeddel DV, Ferrara N. (1989). Vascular endothelial growth factor is a secreted angiogenic mitogen. *Science* **246**: 1306-1309.

Lin X, Jung J, Kang D, Xu B, Zaret KS, Zoghbi H. (2002). Prenylcysteine carboxylmethyltransferase is essential for the earliest stages of liver development in mice. *Gastroenterology* **123**: 345-351.

Lotan TL, Epstein JI. (2010). Clinical implications of changing definitions within the gleason grading system. *Nat Rev Urol* **7**: 136-142.

Lu X, Kang Y. (2010). Epidermal growth factor signalling and bone metastasis. *Br J Cancer* **102**: 457-461.

Markham CW. (1989). Prostatic intraepithelial neoplasia: Detection and correlation with invasive cancer in fine-needle biopsy. *Urology* **34**: 57-61.

May M, Brookman-May S, Lebentrau S, Gilfrich C, Loy V, Theissig F *et al.* (2010). Concordance of the gleason score in prostate multibiopsy and definitive histology. *Aktuelle Urol* .

Mazieres J, Pradines A, Favre G. (2004). Perspectives on farnesyl transferase inhibitors in cancer therapy. *Cancer Lett* **206**: 159-167.

Misra P, Owuor ED, Li W, Yu S, et al. (2002). Phosphorylation of transcriptional coactivator peroxisome proliferator-activated receptor (PPAR)-binding protein (PBP). stimulation of transcriptional regulation by mitogen-activated protein kinase. *J Biol Chem* **277**: 48745.

Nguyen DX, Bos PD, Massague J. (2009). Metastasis: From dissemination to organ-specific colonization. *Nat Rev Cancer* **9**: 274-284.

Nobes CD, Hall A. (1995). Rho, rac, and cdc42 GTPases regulate the assembly of multimolecular focal complexes associated with actin stress fibers, lamellipodia, and filopodia. *Cell* **81**: 53-62.

Pearson HB, Phesse TJ, Clarke AR. (2009). K-ras and wnt signaling synergize to accelerate prostate tumorigenesis in the mouse. *Cancer Res* **69**: 94-101.

Perez-Sala D, Gilbert BA, Tan EW, Rando RR. (1992). Prenylated protein methyltransferases do not distinguish between farnesylated and geranylgeranylated substrates. *Biochem J* **284 (Pt 3)**: 835-840.

Pero SC, Shukla GS, Cookson MM, Flemer S, Krag DN. (2007). Combination treatment with Grb7 peptide and doxorubicin or trastuzumab (herceptin) results in cooperative cell growth inhibition in breast cancer cells. *Br J Cancer* **96**: 1520.

Peterson YK, Kelly P, Weinbaum CA, Casey PJ. (2006). A novel protein geranylgeranyltransferase-I inhibitor with high potency, selectivity, and cellular activity. *J Biol Chem* **281**: 12445.

Pienta KJ, Loberg R. (2005). The "emigration, migration, and immigration" of prostate cancer. *Clin Prostate Cancer* **4**: 24-30.

Price JT, Bonovich MT, Kohn EC. (1997). The biochemistry of cancer dissemination. *Crit Rev Biochem Mol Biol* **32**: 175.

Randolph TL, Amin MB, Ro JY, Ayala AG. (1997). Histologic variants of adenocarcinoma and other carcinomas of prostate: Pathologic criteria and clinical significance. *Mod Pathol* **10**: 612-629.

Ren XD, Bokoch GM, Traynor-Kaplan A, Jenkins GH, Anderson RA, Schwartz MA. (1996). Physical association of the small GTPase rho with a 68-kDa phosphatidylinositol 4-phosphate 5-kinase in swiss 3T3 cells. *Mol Biol Cell* **7**: 435-442.

Sebti SM, Der CJ. (2003). Opinion: Searching for the elusive targets of farnesyltransferase inhibitors. *Nat Rev Cancer* **3**: 945-951.

Sliva D. (2004). Signaling pathways responsible for cancer cell invasion as targets for cancer therapy. *Curr Cancer Drug Targets* **4**: 327.

Sparano JA, Moulder S, Kazi A, Vahdat L, Li T, Pellegrino C *et al.* (2006). Targeted inhibition of farnesyltransferase in locally advanced breast cancer: A phase I and II trial of tipifarnib plus dose-dense doxorubicin and cyclophosphamide. *J Clin Oncol* **24**: 3013.

Stein D, Wu J, Fuqua SA, Roonprapunt C, Yajnik V, D'Eustachio P *et al.* (1994). The SH2 domain protein GRB-7 is co-amplified, overexpressed and in a tight complex with HER2 in breast cancer. *EMBO J* **13**: 1331.

Sun J, Zheng SL, Wiklund F, Isaacs SD, Purcell LD, Gao Z *et al.* (2008). Evidence for two independent prostate cancer risk-associated loci in the HNF1B gene at 17q12. *Nat Genet*

Troxell ML, Bangs CD, Lawce HJ, Galperin IB, Baiyee D, et al. (2006). Evaluation of her-2/neu status in carcinomas with amplified chromosome 17 centromere locus. *Am J Clin Pathol* **126**: 709.

van Golen KL. (2003). Inflammatory breast cancer: Relationship between growth factor signaling and motility in aggressive cancers. *Breast Cancer Res* **5**: 174.

Winter-Vann AM, Casey PJ. (2005). Post-prenylation-processing enzymes as new targets in oncogenesis. *Nat Rev Cancer* **5**: 405-412.

Zamir E, Katz M, Posen Y, Erez N, Yamada KM, Katz BZ *et al.* (2000). Dynamics and segregation of cell-matrix adhesions in cultured fibroblasts. *Nat Cell Biol* **2**: 191-196.

Zhang XY, Hong BF, Chen GF, Lu YL, Zhong M. (2005). Significance of MMP2 and MMP9 expression in prostate cancer. *Zhonghua Nan Ke Xue* **11**: 359-61, 364.

CHAPTER II

NOVEL GENE C17ORF37 IN 17q12 AMPLICON PROMOTES MIGRATION AND INVASION OF PROSTATE CANCER CELLS

S Dasgupta, L M Wasson, N Rauniyar, L Prokai, J Borejdo and J K Vishwanatha

Oncogene. 2009 Aug 13;28(32):2860-72.

ABSTRACT

C17orf37/MGC14832, a novel gene located on human chromosome 17q12 in the ErbB-2 amplicon, is abundantly expressed in breast cancer. C17orf37 expression has been reported to positively correlate with grade and stage of cancer progression; however the functional significance of C17orf37 overexpression in cancer biology is not known. Here, we show that C17orf37 is highly expressed in prostate cancer cell lines and tumors, compared to minimal expression in normal prostate cells and tissues. Cellular localization studies by confocal and TIRF microscopy revealed predominant expression of C17orf37 in the cytosol with intense staining in the membrane of prostate cancer cells. RNA interference mediated downregulation of C17orf37 resulted in decreased migration and invasion of DU-145 prostate cancer cells, and suppressed the DNA binding activity of NF- κ B transcription factor resulting in reduced expression of downstream target genes MMP-9, uPA and VEGF. Phosphorylation of PKB/Akt was also reduced upon C17orf37 downregulation, suggesting C17orf37 acts as a signaling molecule that increases invasive

potential of prostate cancer cells by NF- κ B mediated downstream target genes. Our data strongly suggest C17orf37 overexpression in prostate cancer functionally enhances migration and invasion of tumor cells, and is an important target for cancer therapy.

INTRODUCTION

Prostate cancer is the most common type of cancer diagnosed in American men and is the second leading cause of cancer related death in men (Pienta and Loberg, 2005). American cancer society estimates about 28,660 men will die of this disease in 2008. Most men diagnosed with prostate cancer can survive the primary localized tumor, but because of the metastasis related disease, mortality rates remain extremely high. Metastasis of prostate cancer is facilitated by migration and invasion of malignant tumor cells from localized neoplastic tumors to distant organs like bone by cleavage of extracellular matrix (ECM) (Arya *et al.*, 2006). Proteases that facilitate malignant cell migration and invasion by cleaving ECM proteins, such as matrix metalloproteinases (MMPs), cysteine proteases and serine proteases have been extensively studied (Sliva, 2004). Although the fundamental role of these proteases in prostate cancer cell migration, invasion and metastasis is clear, the underlying mechanism and regulation of these proteases to promote prostate cancer progression and invasion is vague.

Chromosome 17q12 -contains multiple genes that play important roles in different forms of cancer. Recent genetic studies have projected 17q12 loci genes as an important risk factor in prostate cancer progression in selected individuals (Eeles *et al.*, 2008; Sun *et al.*, 2008). ErbB-2 located in the same amplicon is known to play a significant role in prostate cancer progression and its expression correlates with poor hormone refractory

prostate cancer in patients (Myers *et al.*, 1994). C17orf37 is a novel gene located in the same amplicon just next to ErbB-2 in a tail to tail rearrangement, functional importance of which is presently unknown. C17orf37 has been reported to be frequently amplified with ErbB-2 in breast tumor cells, however independent activation of C17orf37 has been demonstrated in cell lines expressing low levels of ErbB-2 (Evans *et al.*, 2006). C17orf37 protein is abundantly expressed in breast tumor cells and clinical tissues, with reduced or limited expression in 38 different normal tissues (Evans *et al.*, 2006). C17orf37 expression positively correlates with grade and stage of breast cancer, and increased expression has been shown in patients with breast to liver and lungs metastasis (Evans *et al.*, 2006). This suggests C17orf37 protein may be an important mediator of cancer cell metastasis. However, to establish C17orf37 as a biomarker and therapeutic target for cancer treatment, it is utmost important to explore the functional importance of this novel protein.

We demonstrate C17orf37 expression is enhanced in prostate cancer cells and tissues specimens. We also observed the cellular localization of C17orf37 in prostate cells by confocal microscopy and finally by knockdown and overexpression studies, we demonstrate C17orf37 significantly contributes to the migration and invasion of prostate cancer cells. Our results clearly indicate C17orf37 as a critical cancer specific protein promoting tumor cell invasion by enhancing secretion of uPA, MMP-9 and VEGF through NF- κ B pathway.

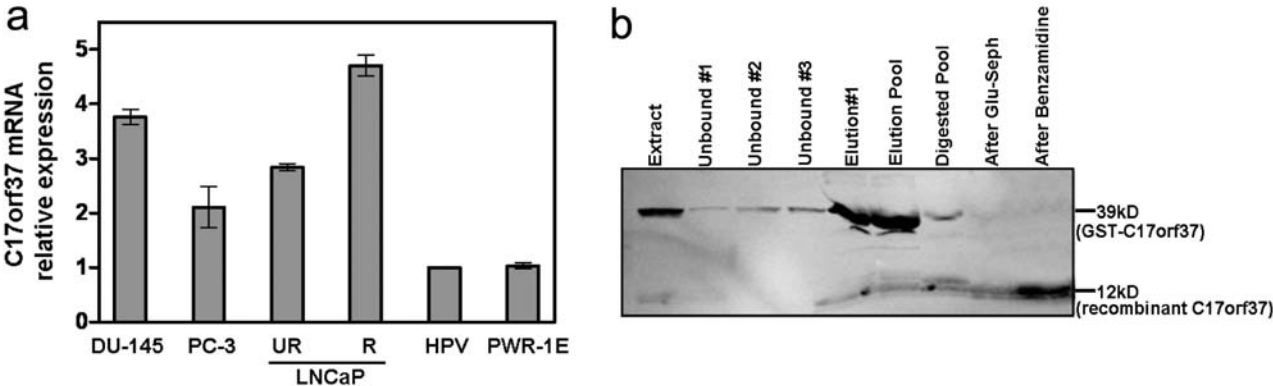
RESULTS

Increased expression of C17orf37 in prostate cancer cells

To investigate C17orf37 expression in prostate cancer, we analyzed mRNA expression of C17orf37 in a panel of prostate cancer cell lines including androgen-independent DU-145 and PC-3, and in a LNCaP cell line prostate cancer progression model consisting of androgen dependent LNCaP-R and androgen independent LNCaP-UR (Wu *et al.*, 1994) by q-RT-PCR (Figure 1a) and RT-PCR (Supplementary Figure 1). We find high levels of C17orf37 mRNA expression in all the prostate cancer cell lines investigated, whereas expression in both the normal prostate epithelial cell lines HPV18 C-1 and PWR-1E are relatively low (Figure 1a). To analyze the protein expression of C17orf37 in prostate carcinoma cells, we first determined the specificity of the anti-C17orf37 antibody (ORF37) using recombinant GST-C17orf37 protein. ORF37 antibody immunoreacts with both GST-C17orf37 (39kD) and GST-tag cleaved purified recombinant C17orf37 protein of 12kD size (Figure 1b). To verify the 12kD band is indeed C17orf37 protein, we analyzed the protein sequence by tandem mass spectrometry. As shown by high-resolution ESI-FTICR analysis (Supplementary Figure 2), the molecular weight of the intact recombinant protein was 11,918 Da and matched 54% amino acid sequence coverage of C17orf37 (Figure 1c).

To find any possible change in C17orf37 protein expression from androgen dependency to independency, we examined two additional prostate cancer cell lines LNCaP-RF, a fast growing androgen responsive LNCaP cell line (Rothermund *et al.*,

Figure 1



c

gi|42822891 hypothetical protein LOC84299 [Homo sapiens], 12403.0 Da
 gi|74732925|sp|Q9BRT3|CQ037_HUMAN Uncharacterized protein C17orf37

```

    M S G E P G O T S V   A P P E E V E P G   S G V R I V V E Y C   E P C G F E A T Y L
    E L A S A V K E Q Y   P G I E I E S R L G   G T G A F E I E I N   G O L V F S K L E N
    G G F P Y E K D L I   E A I R R A S N G E   T L E K I T N S R P   P C V I L
    
```

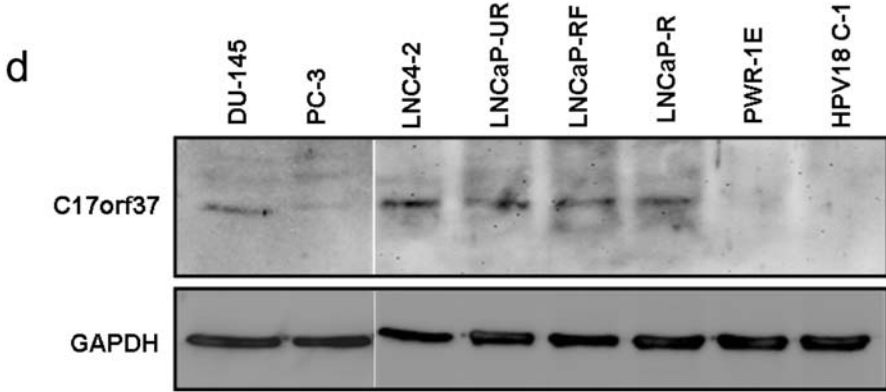


Figure 1 *C17orf37* mRNA and protein expression in human prostate cancer cells and tissues. (a) *C17orf37* mRNA expression was analyzed by real time PCR in prostate cancer cell lines DU-145, PC-3, LNCaP-UR and LNCaP-R, and normal prostate epithelial cell line HPV18 C-1 and prostate derived cell line PWR-1E. Housekeeping gene β -actin was used as an internal control. (b) Western immunoblot showing the expression of GST-C17orf37 protein that was purified and thrombin cleaved to generate recombinant C17orf37 protein. (c) Summary of LC/ESI-MS/MS analysis for the predicted C17orf37 after tryptic digestion (4 unique peptides and 54% sequence coverage, 62 out of 115 amino acid residues shown; the box indicates the amino acid residues covered and grey highlight denotes conversion of E to <E upon proteolytic digestion). (d) C17orf37 protein was analyzed by western immunoblot in a panel of prostate cancer cell lines including - DU-145, PC-3 and LNC4-2 (androgen independent), LNCaP progression model- LNCaP-UR, LNCaP-RF and LNCaP-R (from androgen independent to dependent); and, normal prostate epithelial cell line HPV18 C-1 and PWR-1E. Housekeeping gene GAPDH served as loading control. Expression of C17orf37 protein was higher in prostate cancer cells compared to normal prostate cells.

2002) and LNCaP/C4-2 (LNC4-2), a subline derived from parental LNCaP cells that acquired phenotypes of androgen independence (Thalmann *et al.*, 1994; Wu *et al.*, 1994). Among metastatic prostate cancer cell lines, DU-145 showed higher C17orf37 expression compared to PC-3 (Figure 1d), whereas *in vitro* LNCaP prostate cancer progression model - UR, RF and R along with LNCaP C4-2 showed similar level of protein expression (Figure 1d), suggesting C17orf37 expression persists both in androgen dependent and independent states of prostate cancer. As with our observations made at the mRNA level, normal prostate epithelial cell lines HPV18 C-1 and PWR-1E showed undetectable expression of C17orf37 protein (Figure 1d). These data indicated that expression of C17orf37 persists throughout prostate cancer disease progression, both in early stages of androgen dependency to late stages of androgen independency, with minimal expression in normal prostate cell lines.

C17orf37 is over-expressed in high grade neoplastic glands and stroma of prostate adenocarcinoma

To determine the expression of C17orf37 in normal and cancerous prostate tissue, we examined C17orf37 expression in archival formalin-fixed paraffin embedded prostate specimens by immunohistochemistry. The hematoxylin and eosin (H & E) stained specimens were classified into normal, benign prostatic hyperplasia (BPH), moderately differentiated prostate adenocarcinoma and poorly differentiated prostate adenocarcinoma (Banerjee *et al.*, 2003) (Figure 2a and 2d) by anatomic pathologists.

Figure 2

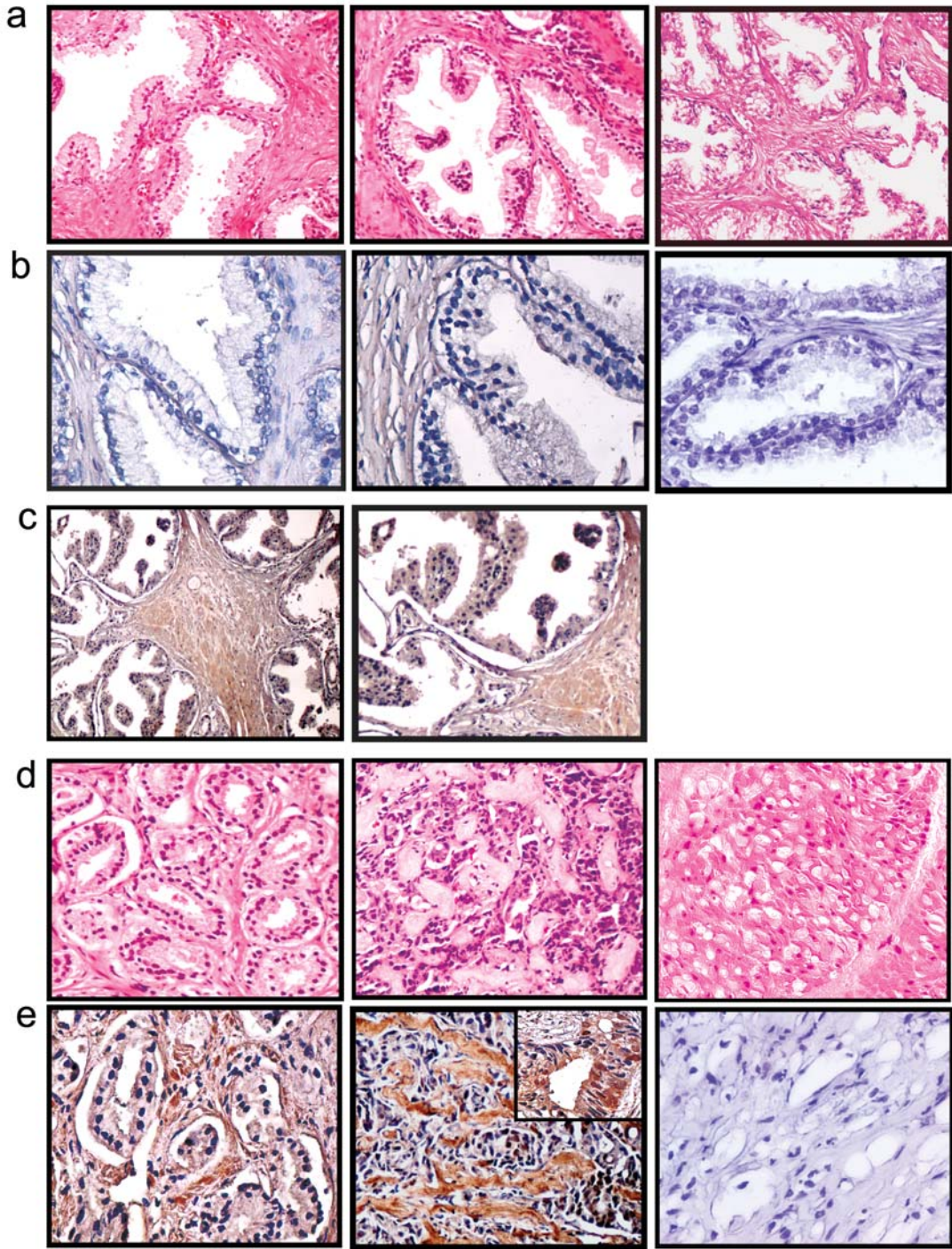


Figure 2 Expression of C17orf37 in human normal, benign prostatic hyperplasia (BPH) and prostate adenocarcinoma tissue specimens. Representative images of normal prostate gland (a, b -left), BPH (a, b -middle), prostate intraepithelial neoplasm (c), moderately differentiated (Gleason Score 6) (d, e - left) and poorly differentiated (Gleason Score 9) (d, e -middle) prostate carcinoma. Sections were stained with H & E (a, d) and ORF37 antibody (b, c, e). (b) Left, C17orf37 expression was found to be minimal in both normal prostate glands ($n=6$), (b) middle, in BPH prostate specimens ($n=6$), and (b) right, negative in IgG control. (c) C17orf37 staining in PIN glands show presence of protein in early stages of cancer progression. (e) Left, Moderately differentiated prostate adenocarcinoma tissue sections show increased expression of C17orf37 in both neoplastic glands and prostatic stroma ($n=15$), (e) middle panel, Poorly differentiated prostate adenocarcinoma tissue sections showed fusion of neoplastic glands with intense diffused C17orf37 immunostain ($n=12$), Inset shows C17orf37 expression in the prostatic glands in poorly differentiated carcinoma, and (e) right panel, shows negative staining in IgG control. All images are *100X* of original magnification except (c) left, which is *40X* of original magnification.

Gleason scores of the prostate carcinoma tissues ranged from 6-10, thus no well differentiated prostate adenocarcinoma specimens (Gleason score 2-4) were available for our study. In both normal prostate glands (Figure 2b left) and transurethral resection of the prostate (TURP) BPH specimens (Figure 2b middle), C17orf37 staining was minimal in prostatic glands and stroma. Prostate intraepithelial neoplasm (PIN) showed moderately increased staining of C17orf37 (Figure 2c) compared to normal or BPH glands in the same section. However, in moderately differentiated specimens C17orf37 expression was found to be intense in the neoplastic glands and stromal cells surrounding the glands (Figure 2e left). Strong C17orf37 expression was found throughout the poorly differentiated prostate cancer sections with intense diffused stain in the stroma around the malignant cell mass and invasive edges (Figure 2e middle). C17orf37 expression was intense in the fused prostatic glands of poorly differentiated prostatic cancer (Figure 2e “inset” middle). The isotype controls (IgG) for each specimen did not show immunoreactivity (Figure 2b, 2e right). Taken together, immunohistochemical detection of C17orf37 protein showed prevalent expression in the higher grades of prostate adenocarcinoma with densely stained malignant cells compared to either low or null expression in both normal and BPH specimens.

Subcellular localization of C17orf37 in prostate cancer cells

We investigated the intracellular localization of C17orf37 protein in prostate cells. In DU-145 and LNCaP cells, western immunoblot of cellular fractions (Figure 3a) and

Figure 3

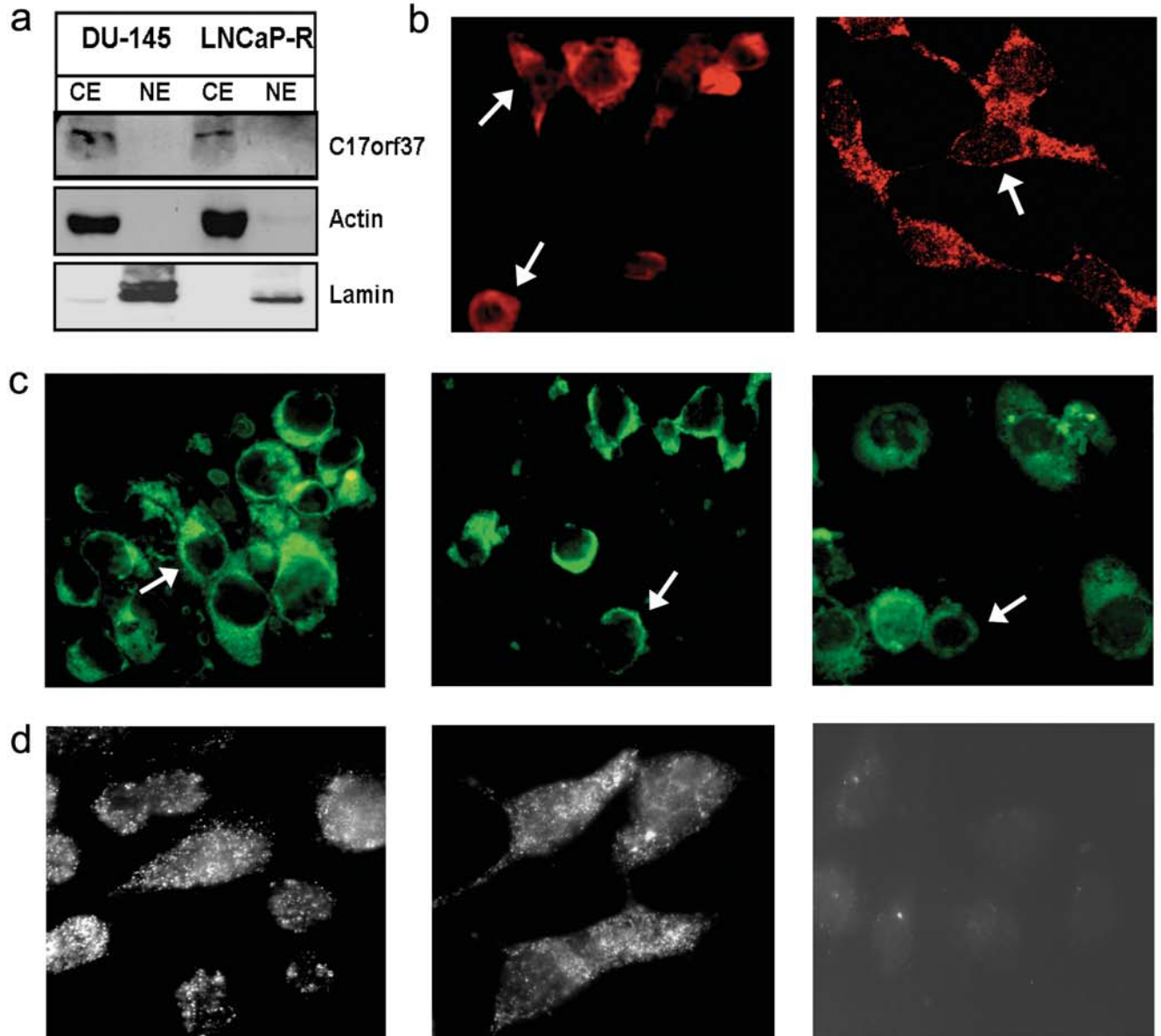


Figure 3 Subcellular localization of C17orf37 in human prostate cancer cell lines. (a) Subcellular fractionation followed by western immunoblot showing endogenous expression of C17orf37 in the cytosolic fractions of DU-145 and LNCaP-R prostate cancer cells. The purity of the cytosolic (CE) and nuclear extracts (NE) were determined using cytosolic marker protein actin and nuclear protein lamin. (b) Immunofluorescent staining of endogenous C17orf37 expression in DU-145 (middle) and LNCaP-R (right) prostate cancer cells. Confocal images show intense C17orf37 staining in the cytosolic compartment with dense spots in the membrane. Original magnification, *X40*. (c) GFP-C17orf37 construct was transiently transfected in DU-145 (left), LNCaP (middle) and HPV18 C-1 cells (right). The cells were then fixed and imaged by confocal microscopy. GFP-C17orf37 was visualized as green fluorescent signals mostly in the cytosolic area predominantly in the membrane. Original magnification, *X40*. (d) DU-145 (left and right) and LNCaP-R cells (middle panel) were grown in coverslips, fixed, unpermeabilized and treated with anti-C17orf37 (left and middle) or anti-tubulin (right) antibody. Coverslips were mounted on special TIRF coverslips as mentioned in the methods section. Slides were visualized by TIRFM. Spots as seen in the images depict the membrane localization of C17orf37 in prostate cancer cells. Original magnification, *X60* oil immersion. White arrows indicate membrane localization of C17orf37 in prostate cancer and non-cancerous cells.

immunocytochemical detection by confocal microscopy (Figure 3b left - DU-145, Figure 3b right - LNCaP) showed endogenous expression of C17orf37 predominantly in the cytosol. Transient transfection of GFP-C17orf37 in DU-145 (Figure 3c left), LNCaP (Figure 3c middle) and HPV18C-1 (Figure 3c right) prostate cells also showed similar pattern of C17orf37 expression. Endogenous C17orf37 and GFP-C17orf37 localized primarily in the cytoplasm of the transfected cells, densely in the perinuclear area around the membrane (white arrows) and less in the nucleus (Figure 3b and 3c). Localization was similar in both C17orf37 positive prostate cancer cells DU-145 and LNCaP, and a null C17orf37 expressing prostate epithelial cell line HPV18 C-1 (Figure 3c). To determine whether C17orf37 is a membrane bound protein, we performed total internal reflection fluorescence microscopy (TIRFM) to monitor membrane localization of C17orf37. In the TIRFM, the evanescent wave produced by the visible light at the cell/substratum interface penetrates only 100-200 nm with decaying intensity with the distance, allowing detection of protein molecules associated with the plasma membrane (Axelrod, 2001). DU-145 (Figure 3d left) and LNCaP (Figure 3d middle) cells labeled with ORF37 antibody tagged to Alexa fluorophore-568 showed numerous dense spots of C17orf37 protein in the membrane region (Figure 3d). We used intracellular cytoskeletal protein tubulin as a control for our experiments, but TIRFM failed to image tubulin protein molecules on the membrane (Figure 3d right). These results indicated that C17orf37 is a cytosolic protein with predominant membrane localization in prostate cancer cells.

Expression of C17orf37 enhances the in vitro invasive and migratory potential of prostate cancer cells

Our results show expression of C17orf37 is higher in advanced prostate adenocarcinomas (Gleason grade: 6 and 9) compared to normal prostate tissues (Figure 2b and 2e). Metastases of malignant cells to distant tissues or organs are mediated by cellular migration, invasion and proteolytic activity that degrade tissue barrier (Sliva, 2004). To investigate the role of C17orf37 in prostate cancer cell migration, we studied the effect of C17orf37 downregulation on the migratory potential of DU-145 cells. Using gene specific siRNA at varying concentrations, we blocked the endogenous expression of C17orf37 in DU-145 cells (Figure 4a). An *in vitro* agarose gel bead assay was performed with C17orf37 knocked down DU-145 cells, to determine the dose dependent effect of siRNA-C17orf37 on DU-145 cell migration. As shown in Figure 4b, siRNA-C17orf37 treatment (Figure 4b, III-V) reduced the number of DU-145 cells that could migrate out of the agarose gel bead into the medium compared to wild type or control-siRNA treated (Figure 4b, I-II). siRNA-C17orf37 treatment at 100nM resulted in ~10 fold decrease in migration of DU-145 cells ($P < 0.0001$) compared to control wild type cells (Figure 4c). *In vitro* tumor invasion assay also showed reduced invasive ability of DU-145 cells treated with siRNA-C17orf37 (Figure 4d). To verify expression of C17orf37 has a dominant effect on tumor cells invasion, we assessed invasiveness of DU-145 and PC-3 cells overexpressed with GFP-C17orf37. C17orf37 positive DU-145 prostate cancer cells showed ~1.8 fold increase, where as PC-3, with low endogenous C17orf37 expression, showed ~1.75 fold increase in invasion compared to respective controls (Figure 4e).

Figure 4

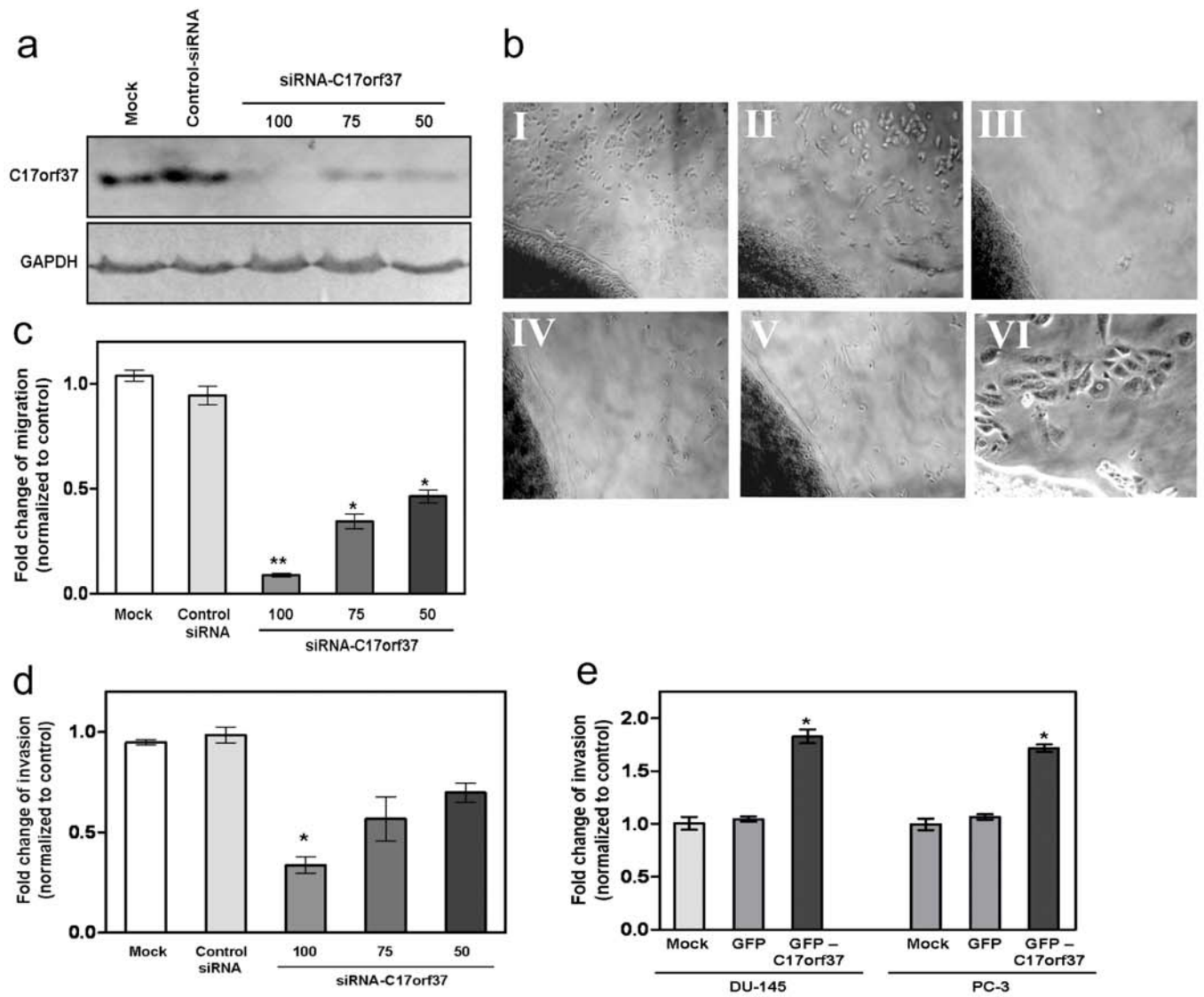


Figure 4 C17orf37 expression regulates migration and invasion of prostate cancer cells. (a) DU-145 cells were transfected with transfection media alone (mock); non-targeting scrambled siRNA (control-siRNA); and 100, 75 and 50 nM doses of C17orf37 specific siRNA. Following 48 hours of transfection, C17orf37 protein knockdown was confirmed by Western immunoblot using ORF37 antibody and compared to GAPDH. Blot is represented image of 4 independent experiments. (b) 48 hours of post-transfection DU-145 cells were mixed in low melting agarose and growth medium, and plated on fibronectin coated plates to form a semisolid gel bead. Representative pictures taken after 36 hours show the number of DU-145 cells that migrate out of the gel beads treated with, *I* - transfection medium only (mock), *II* - nontargeting siRNA (control-siRNA), *III* - 100nM of C17orf37 specific siRNA, *IV* -75 nM of C17orf37 siRNA and *V* - 50nM of C17orf37 specific siRNA. Figure *C-VI* shows the normal morphology of the DU-145 cells that migrate out of the agarose gel beads. (c) Graphical representation of fold change in DU-145 prostate cancer cell migration compared to control (untreated) wild type cells. (d) DU-145 cells transfected with Mock, non-targeting control siRNA, and 100nM, 75nM and 50nM siRNA-C17orf37 were incubated for 48 hours. After the transfection phase, DU-145 cells were seeded onto Matrigel coated BD Biocoat Tumor Invasion system and allowed to migrate towards 10% serum for 24 hours. Fold change of invasion was calculated as described in materials and methods section. (e) DU-145 and PC-3 cells were transiently transfected with transfection media alone (mock), EGFP-C1 vector only (GFP) and EGFP-C17orf37 plasmid (GFP-C17orf37). Twenty four hours later, cells were seeded onto matrigel coated tumor invasion chambers and allowed to migrate toward serum for 24

hours at 37°C. Fold change of invasion and migration was calculated as described in materials and methods section. *Columns* (c, d and e) are mean of three independent experiments; *bars*, SD. **, $P < 0.001$ and *, $P < 0.05$, relative to mock treatment of cells; statistical analysis included Student's *t* test for calculating significant differences within groups.

Stable overexpression of GFP-C17orf37 construct in DU-145 cells (DU-GFP-C17orf37), dramatically increased the invasiveness ~2.0-2.5 fold compared to parental DU-145 cells (Supplementary Figure 3), indicating overexpression of C17orf37 protein leads to increased invasive behavior in prostate cancer cells.

Downregulation of C17orf37 results in reduced expression of MMP-9, uPA and VEGF by lowering NF- κ B DNA binding activity in DU-145 prostate cancer cells

Migration and invasion of malignant cells is facilitated by specific proteases like matrix metalloproteinases (such as MMP-9) and serine proteases (such as uPA) that degrade the ECM (Sliva, 2004). During prostate cancer progression these molecules are found to be predominantly up-regulated to facilitate migration and invasion (Helenius *et al.*, 2006; Li and Cozzi, 2007b; Lokeshwar, 1999; Wilson and Sinha, 1993; Wilson *et al.*, 2004). Prostate cancer cells also secrete high levels of growth factors like VEGF, which is an important mediator of angiogenesis, proliferation and migration (Hicklin and Ellis, 2005). To investigate whether C17orf37 protein has any effect on the metastasis related genes, we knocked down endogenous C17orf37 in DU-145 cells and analyzed expression of several genes that facilitate prostate cancer metastasis and promote ECM cleavage. We observed suppression of endogenous C17orf37, simultaneously reduced MMP-9, uPA and VEGF expression as measured by RT-PCR (Figure 5a) and western immunoblot (Figure 5b) compared to non-targeting siRNA (control-siRNA). To determine if C17orf37 expression increases MMP-9, uPA and VEGF protein in prostate cancer cells,

Figure 5

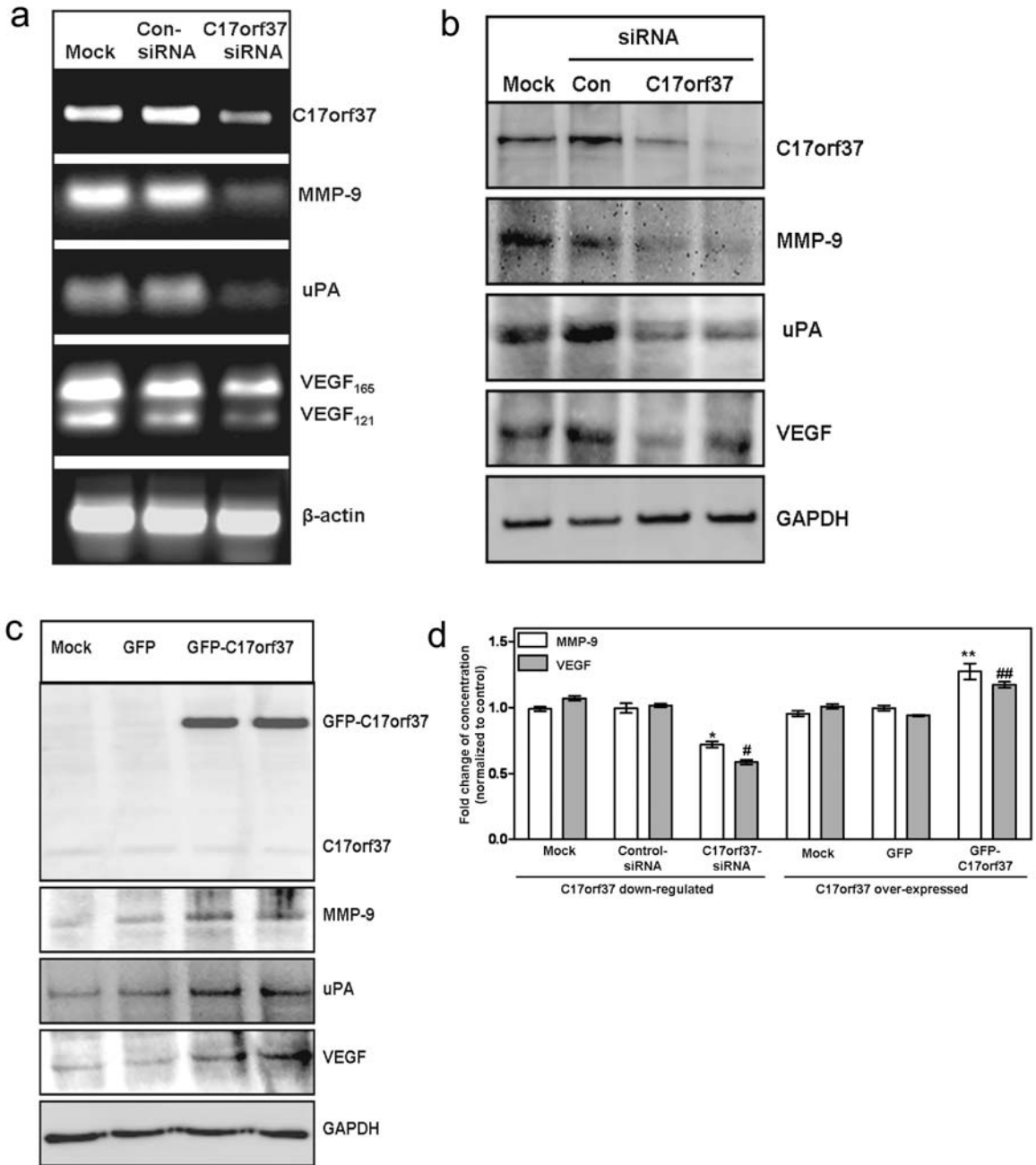


Figure 5 siRNA mediated silencing of *C17orf37* results in the downregulation of *MMP-9*, *uPA* and *VEGF* expression. DU-145 cells were transiently transfected with transfection media-Dharmafect alone (mock), non-targeting siRNA (control siRNA) and SMART pool siRNA specific to *C17orf37* (100nM). (a) Seventy hours later total RNA was isolated and the mRNA expression of *MMP-9*, *uPA* and *VEGF* was analyzed by RT-PCR. House keeping gene β -actin served as internal control. (b) Ninety-six hours of post-transfection total protein was isolated and 30 μ g of protein was used to perform western immunoblot. Expression of *MMP-9*, *uPA* and *VEGF* protein were analyzed in mock, control-siRNA and *C17orf37* specific siRNA - 100nM (in duplicate) treated DU-145 prostate cancer cells. (c) *C17orf37* was over-expressed by transiently transfecting DU-145 cells with GFP-*C17orf37* plasmid. Lipofectamine treated (mock) and GFP vector transfected were used as controls. Twenty-four hours later total protein was isolated and 15 μ g of protein was used to perform western immunoblot. Figures show expression of *MMP-9*, *uPA* and *VEGF* in mock-treated, GFP-vector only and GFP-*C17orf37* treated DU-145 cells (in duplicate). All western blot images are representative of 4 independent experiments. (d) Elisa assay of conditioned media from DU-145 cells treated as in (b) and (c) were used to estimate *MMP-9* and *VEGF*. Fold change of concentration was determined by a ratio of quantitative values of *MMP-9* (ng/mL/ 10^5 cells) and *VEGF* (pg/mL/ 10^5 cells) in experimental group to the control group. Columns mean of four independent experiments; bars, SD. *, $P < 0.005$ relative to mock (Dharmafect) treated (*MMP-9*); #, $P < 0.005$ relative to mock treated (*VEGF*); **, $P < 0.05$ relative to mock (lipofectamine) treated (*MMP-9*) and ###, $P < 0.005$ relative to mock treated (*VEGF*);

statistical analysis included Student's t test for calculating significant differences within groups.

we overexpressed C17orf37 in DU-145 cells by transient transfection of GFP-C17orf37 plasmid. As shown in Figure 5c, western immunoblot confirmed overexpression of C17orf37 increases endogenous MMP-9, uPA and VEGF protein compared to vector treated cells. Interestingly, silencing of C17orf37 in DU-145 prostate cancer cells resulted in reduced mRNA expression of both the isoforms of VEGF (VEGF₁₆₅ and VEGF₁₂₁) (Figure 5a). VEGF₁₂₁ isoform is rapidly secreted and freely diffuses into the tissues, where as VEGF₁₆₅ the potent isoform functionally active in most angiogenic states (Connolly and Rose, 1998; Woolard *et al.*, 2004) was found to be regulated by C17orf37 (Figure 5b,c). To quantitate the relative amount of secreted VEGF (both the isoforms) and MMP-9 we performed ELISA of conditioned media from DU-145 cells overexpressed or depleted C17orf37 protein. Our results show that secreted MMP-9 and VEGF protein is significantly altered due to C17orf37 expression compared to respective controls (Figure 5d).

MMP-9, *uPA* and *VEGF* genes are transcriptionally up-regulated by NF- κ B, which is constitutively active in prostate cancer cells (Suh and Rabson, 2004). We performed EMSA to evaluate the DNA binding activity of NF- κ B in C17orf37 silenced DU-145 cells. Our results indicate increasing concentration of C17orf37 specific siRNA effectively inhibited NF- κ B DNA binding activity in a dose-dependent manner (Figure 6a). These results show that C17orf37 increases migration and invasion in prostate cancer by NF- κ B mediated genes MMP-9, uPA and VEGF. In prostate cancer cells, constitutive activation of NF- κ B is mediated by upstream protein kinase B (PKB/Akt) (Fresno Vara *et al.*, 2004), we performed western immunoblot to detect the levels of phosphorylated Akt

Figure 6

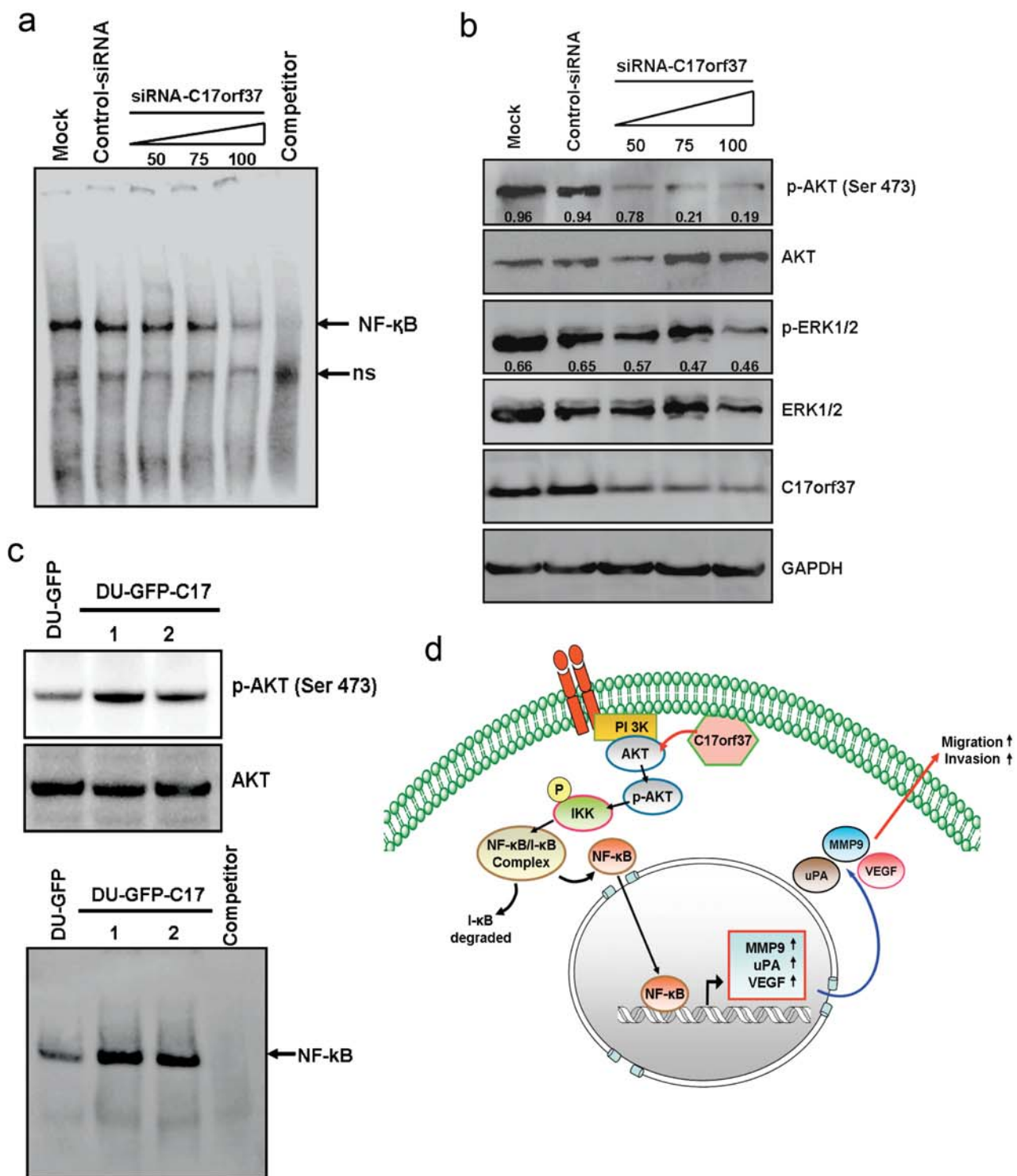


Figure 6 Knockdown of C17orf37 by siRNA reduces the NF- κ B DNA binding activity via suppressing the AKT activation. (a) EMSA was done by incubating 5 μ g of nuclear protein extracts from DU-145 cells treated with non-targeting siRNA (control siRNA) and 50, 75 and 100nM siRNA specific to C17orf37. DU-145 prostate cancer cells without any treatment (untreated) and in presence of competitive oligonucleotides to the probe (competitor) were used as controls. The non significant band (NS) present in all the lanes did not have any effect even in presence of competitor. (b) DU-145 prostate cancer cells were transiently transfected with non-targeting siRNA (Control-siRNA), and increasing concentration of C17orf37 specific siRNA at 50nM, 75nM and 100nM dose for 48 hours. The expression of C17orf37, phospho-AKT (Ser 473), total AKT, phospho-ERK1/2 and total ERK1/2 were detected by western immunoblotting. Housekeeping gene GAPDH was used as loading control to normalize the total AKT and ERK1/2 protein levels, and then used to determine the ratio of the phosphorylated/total AKT and ERK, respectively. Numbers indicate the normalized expression ratio expressed as mean of three independent experiments. (c) Western immunoblotting showing phospho-AKT and total AKT (top panel), and EMSA showing NF- κ B DNA binding activity (bottom panel) in polyclonal populations overexpressing either DU-GFP (DU-145 stably expressing GFP vector) or DU-GFP-C17 (DU-145 stably expressing GFP-C17orf37) in two independent pools #1 and #2. Western blot and EMSA images are representative of three independent experiments. (d) Proposed working model for C17orf37 signaling in prostate cancer cells.

(p-Akt) and total Akt. p-Akt is the active form of the protein that cascades the intracellular signaling and our results show blocking of C17orf37 by siRNA dramatically reduced p-Akt level in DU-145 cells (Supplementary Figure 4). C17orf37 specific siRNA (100nM) treatment abolished 80% phosphorylation of Akt in DU-145 cells (Figure 6b) where as the total Akt expression was constant when normalized to loading control GAPDH. We also observed reduction in the phosphorylated form of ERK1/2 compared to total ERK1/2 (Figure 6b), however the extent of reduction was not significant when compared to Akt activation (Supplementary Figure 4). To validate our observation, we measured p-Akt/Akt level and NF- κ B DNA binding activity in DU-145 cells stably overexpressing GFP-C17orf37 (DU-GFP-C17), and as expected phosphorylation of Akt and NF- κ B activity was significantly higher in the stable clones compared to vector control cells (DU-GFP) (Figure 6c). These results demonstrate that C17orf37 mediates prostate cancer cell migration and invasion through NF- κ B downstream target genes MMP-9, UPA and VEGF.

DISCUSSION

C17orf37 is a novel gene located on human chromosome 17q12, in the 'hot spot locus of cancer' which contains multiple genes that have been shown to be involved in the progression of cancer. C17orf37 gene is 505 nucleotides from ErbB-2 oncogene, which has been demonstrated as an important factor for development of hormone refractory prostate cancer (Berger *et al.*, 2006). Although C17orf37 overexpression in breast cancer has been linked with genomic amplification of Her-2/neu locus, recent report has confirmed overexpression of C17orf37 in Her-2/neu negative breast cancer patients and breast tumor cell lines, suggesting independent transcriptional control mechanisms for C17orf37 (Evans *et al.*, 2006). In the present study, we show that C17orf37 expression is consistently higher in both androgen dependent and independent prostate cancer cell lines and clinical prostate cancer tissues examined, compared to either low or null expression in normal and BPH prostate cells and tissues (Figure 1, 2). In clinical prostate cancer specimens, higher Gleason scored tumors showed increased C17orf37 expression compared to lower scores, suggesting C17orf37 expression may increase with grade and stage of cancer. However, the small number of established prostate cancer cell lines does not show significant changes in C17orf37. A larger study with more patient population will be necessary to establish C17orf37 as a biomarker for prostate cancer progression. Our data provide the first evidence that C17orf37 expression positively correlates with the migratory and invasive potential of metastatic prostate cancer cells and thereby can be regarded as a potential biomarker for the disease progression. This is the first report

delineating the role, functional significance and a proposed mechanism through which this novel gene C17orf37 governs prostate cancer progression.

C17orf37 gene encodes a protein (Accession no. NP_115715) of 115 amino acids with a molecular weight of ~12 KD (Fig. 1C and Supplementary Fig. S2) that has no sequence similarity with any known genes or proteins (Evans *et al.*, 2006; Kauraniemi and Kallioniemi, 2006). By immunoconfocal microscopy, TIRFM and cellular fractionation studies we show that C17orf37 is predominantly a cytosolic protein, densely located in the cell membrane (Figure 3). In migrating prostate cancer cell, C17orf37 protein primarily localizes to the leading edge of cell (Supplementary Figure 5). Careful analysis of the C17orf37 protein sequence (Figure 1c) revealed a “CaaX” prenylation motif comprising of last four amino acids “CVIL” at the C-terminal end. “CaaX” group of proteins are either prenylated or geranylgeranylated by enzymes farnesyltransferase (FTase) and geranylgeranyl transferase type I (GGTase-I), respectively. If “X” is leucine, protein is preferentially modified by GGTase-I enzyme (Fu and Casey, 1999), suggesting C17orf37 translocation to the membrane may be mediated by GGTase-I. Pre-PS (prenylation prediction suite) predicted C17orf37 to be prenylated preferentially by the enzyme GGTase-I with a P-value=0.00049 (Maurer-Stroh and Eisenhaber, 2005) and this idea was also supported by a recent report (Evans *et al.*, 2006).

“CaaX”-type prenylated proteins are primarily located at the cytoplasmic face of cellular membranes and in cancer cells these proteins are found to have significant role in oncogenic transformation, cytoskeletal organization, cellular proliferation, migration, invasion and metastasis (Kelly *et al.*, 2006; Virtanen *et al.*, 2002; Winter-Vann and

Casey, 2005). By RNAi mediated C17orf37 gene silencing and also by overexpressing C17orf37 in prostate cancer cells, we successfully established that C17orf37 regulates migration and invasion (Figure 4). Even in patients with metastasis of breast cancer to liver and lungs, abundant expression of C17orf37 protein has been reported (Evans *et al.*, 2006). Migration and invasion of cancer cells are the hallmark of malignant neoplastic proliferation beyond the vascular boundaries facilitated by ECM cleavage by proteolytic enzymes. siRNA mediated knockdown of C17orf37 in DU-145 cells reduced mRNA and protein expression of important proteolytic enzymes MMP-9 and uPA, and potent angiogenic molecule VEGF (Fig.5), suggesting C17orf37 may act as an important upstream signaling molecule enhancing the transcription of these genes. uPA binding to its receptor uPA-R at the cell surface converts inactive plasminogen to active plasmin, and thereby cleaves ECM proteins inducing migration and invasion of malignant cells (Li and Cozzi, 2007). MMP-9 specifically cleaves ECM proteins like gelatin, collagen I and IV, vitronectin and fibronectin resulting in metastatic dissemination of malignant cells (Price *et al.*, 1997). In prostate cancer development, angiogenic growth factor VEGF plays key role in promoting tumor growth and metastatic progression of the disease. MMP-9, uPA and VEGF have been reported to be overexpressed in invasive prostate cancer (Wilson and Sinha, 1993) and are positively correlated with poor prognosis (Sheng, 2001). We show here that by modulating C17orf37 expression in DU-145 metastatic prostate cancer cells, expression of these key molecules is significantly reduced, thereby inhibiting prostate cancer cell migration and invasion.

In invasive prostate cancer cells, increased expression of *MMP-9*, *uPA* and *VEGF* genes are regulated by transcriptional activation of NF- κ B (Huang *et al.*, 2001). Activation of NF- κ B is due to increased activity of upstream kinase IKK complex which greatly reduces the half-life of the inhibitory I κ B α , there by inducing nuclear localization of NF- κ B (Suh and Rabson, 2004). Knockdown of C17orf37 by gene specific siRNA simultaneously reduced the DNA binding activity of NF- κ B, indicating C17orf37 mediated signaling may modulate *MMP-9*, *uPA* and *VEGF* genes through NF- κ B pathway. This also justifies C17orf37 as an upstream signaling molecule of NF- κ B. PI3K-Akt and MAPK are the two upstream signaling pathways that have been shown to be responsible for constitutive activation of IKK complex and NF- κ B (Suh and Rabson, 2004). In prostate cancer cells, PI3K-Akt works like a signaling hub mainly as a downstream effector of tyrosine kinase growth factor receptors. Modulation of C17orf37 dramatically altered the phosphorylation of Akt at Ser-473 (Figure 6) which indicates C17orf37 may act as an inducer of Akt phosphorylation. The ratio of phosphorylated ERK1/2 to the total ERK1/2 also decreased, albeit minimally, when compared to the control-siRNA treated DU-145 cells. This decrease in ERK1/2 phosphorylation may be due to the reduced expression of uPA protein upon C17orf37 silencing. In prostate cancer cells, uPA binds to its cell surface receptor uPA-R there by activating ERK1/2 signaling (Jo *et al.*, 2005). Several studies have shown that knockdown of uPA abolishes the ERK1/2 phosphorylation (Aguirre Ghiso *et al.*, 1999), indicating decrease in ERK1/2 phosphorylation in C17orf37 knockdown cells may be due to the downstream target molecule uPA.

Thus, based on our data we propose a mechanistic model for C17orf37 mediated signaling in prostate cancer invasion and signaling (Figure 6d). In response to extracellular stimuli, growth receptors (tyrosine kinase) present on the prostate cancer cells cascade down the signal activating PI3K. This results in the activation of AKT which translocates to the membrane where it is phosphorylated at Ser-473 (Chan *et al.*, 1999). Prenylated protein C17orf37 also remains localized to the cytosolic face of the membrane (may be as an adapter protein) and in turn controls the downstream signaling of activated p-AKT. Whether this effect is direct or mediated through other adapter proteins that physically interact with C17orf37 on the membrane needs further investigation. Activated AKT phosphorylates IKK complex which then results in the translocation of NF- κ B to the nucleus by reducing the half life of I κ B α (Suh and Rabson, 2004). In the nucleus NF- κ B acts as transcription factor resulting in the enhanced expression of downstream target genes MMP-9, uPA and VEGF. These molecules are then secreted by prostate cancer cells and there by increases the invasiveness of prostate cancer cells (Sliva, 2004).

In summary, we find that C17orf37 is highly expressed in prostate cancer cells and tissues, compared to minimal expression in normal prostate cells. C17orf37 is predominantly expressed as a membrane bound cytosolic protein and actively regulates prostate cancer cell migration and invasion by upregulating the expression of MMP-9, uPA and VEGF. Additionally, downregulation of C17orf37 by specific siRNA reduced the DNA binding activity of NF- κ B, substantiating the fact that C17orf37 expression contributes to the development of invasive prostate cancer through NF- κ B mediated

downstream target genes. Interestingly, AKT activity was reduced due to C17orf37 gene silencing suggesting membrane bound C17orf37 may be a potential regulator of AKT phosphorylation. We believe our results are the first report to deduce the functional importance of so called 'hypothetical protein' C17orf37 that may be considered as a potential therapeutic target for cancer therapy.

MATERIALS AND METHODS

Cell lines and culture conditions

Details describing cell culture and reagents are provided in the Supplementary information.

Cloning, expression and purification of recombinant C17orf37

Information about the plasmids constructed for the study and details about the protein expression and purification is included in Supplementary Materials and Method.

Transfection procedures and siRNA mediated gene silencing of C17orf37

Stable and transient transfection of DU-145, LNCaP and HPV18 C-1 cells were performed using Lipofectamine 2000 (Invitrogen, Carlsbad, CA) with plasmid DNA (GFP-C17orf37 vector or empty vector-GFP). For C17orf37 knockdown experiments, human C17orf37 (NM_032339) smart pool siRNA (siRNA-C17orf37) and human non-targeting scrambled siRNA duplex (Control-siRNA) were purchased from Dharmacon (Lafayette, CO) and transfected in DU-145 cells according to manufacturer's instructions. Details provided in supplementary information.

Isolation of total RNA and quantitative reverse transcription-PCR

Information about the RNA extraction and q-RT-PCR is included in the Supplementary Materials and Method.

Cell fractionation and immunoblotting

Whole cell protein extracts were prepared from prostate cell lines as described previously (Das *et al.*, 2007). Cytosolic and nuclear fractions of DU-145 and LNCaP cells were prepared using the NE-PER nuclear and cytoplasmic extraction kit (Pierce, Rockford, IL) according to manufacturer's instructions. Bacterial cell lysates were prepared using B-PER extraction kit (Pierce, Rockford, IL). Western immunoblot was performed using a 15% gel for C17orf37 protein analysis and 10% for other proteins, as described previously (Das *et al.*, 2007). List of antibodies purchased for the study are included in the supplementary.

Mass spectrometry and liquid chromatography–tandem mass spectrometry

Mass spectrometry performed using FTICR instrument (LTQ-FT, Thermo Fisher, San Jose, CA) as described in Supplementary Materials and Methods section.

Confocal microscopy, immunofluorescence and total internal reflection fluorescence microscopy

DU-145 and LNCaP cells were grown on glass cover slips and treated with C17orf37 antibody (Affinity Bioreagents, Golden, CO) at a dilution of 1:500, as described

previously (Das *et al.*, 2007). For confocal images, cells were visualized on a Zeiss LSM 410 confocal microscope and images were captured using LSM 4 software (Carl Zeiss Microimaging). For, total internal reflection fluorescence microscopy (TIRFM), cells were grown on coverslips and then fixed by 2% paraformaldehyde. Cells were then washed with PBS and treated with C17orf37 or tubulin antibody (Calbiochem) followed by Alexa 568 conjugated secondary antibody. Coverslips were then mounted on specialized cover glass #1 (Corning) of 22X50 mm size. For TIRF images, cells were visualized on an Olympus IX71 microscope with commercial TIRF attachment as described previously (Burghardt *et al.*, 2006) by 60X oil immersion objective.

Immunohistochemistry

Frozen prostate tumors from patients were provided by the UNMC/Eppley Cancer Center Tumor Bank (Omaha, NE). Two anatomic pathologists independently graded the Hematoxylin & Eosin (H & E) stained sections and Gleason scores for these tissues varied between 6 and 10. Immunohistochemistry was performed as described previously (Das *et al.*, 2007). C17orf37 antibody (Zymed, Carlsbad, CA) (1:200) and rabbit IgG (Sigma, St.Louis, MO) were used for the immunohistochemistry study. Representative images of the clinical prostate sections were captured and analyzed by the pathologist.

Cell migration assays

Forty eight hours post-transfection with siRNA-C17orf37 or control-siRNA, 1×10^6 number of DU-145 cells were mixed with low melting agarose and growth medium to

form a semi-solid gel and migration assay performed as described before (Das *et al.*, 2007). The cells were allowed to migrate out of the semi-solid beads for 36 hours and then visualized on an Olympus Microscope (Carl Zeiss). Representative images of the cells were captured and number of cells that migrate out of the beads were counted from three independent experiments. Fold change of migration was determined by a ratio of migrated cells in experimental group to the control group.

In vitro tumor invasion assay

Tumor invasion assay was performed using BD Biocoat Tumor Invasion System (BD Biosciences, Bedford, MA) according to manufacturer's recommendations. Details about the procedure are included in the supplementary information.

Reverse Transcription-PCR (RT-PCR)

One-step RT-PCR (Invitrogen, Carlsbad, CA) was performed using 1 µg of total RNA as described before (Das *et al.*, 2007). Custom primers were synthesized as mentioned in Supplementary Table. 1.

ELISA assay for MMP-9 and VEGF

Elisa assay performed from the conditioned media as described in Supplementary Materials and Methods section.

Electrophoretic mobility shift assay (EMSA)

NF- κ B DNA binding activity was determined by gel shift assay in C17orf37 knockdown DU-145 prostate cancer cells and stably overexpressed DU-ORF cells using NF- κ B specific EMSA gel-shift assay kit (Panomics Inc., Redwood, CA).

Statistical analyses

Results were expressed as mean and statistical analysis performed using GraphPad Prism 4.02 software. One sample t-test was performed and $P < 0.05$ was considered to be significant.

References

Aguirre Ghiso JA, Kovalski K, Ossowski L. (1999). Tumor dormancy induced by downregulation of urokinase receptor in human carcinoma involves integrin and MAPK signaling. *J. Cell Biol.* **147**:89-104.

Arya M, Bott SR, Shergill IS, Ahmed HU, Williamson M, Patel HR. (2006). The metastatic cascade in prostate cancer. *Surg. Oncol.* **15**:117-128.

Axelrod D. (2001). Selective imaging of surface fluorescence with very high aperture microscope objectives. *J. Biomed. Opt.* **6**:6-13.

Banerjee AG, Liu J, Yuan Y, Gopalakrishnan VK, Johansson SL, Dinda AK *et al.* (2003). Expression of biomarkers modulating prostate cancer angiogenesis: Differential expression of annexin II in prostate carcinomas from india and USA. *Mol Cancer.* **8**:34.

Berger R, Lin DI, Nieto M, Sicinska E, Garraway LA, Adams H *et al.* (2006). Androgen-dependent regulation of her-2/neu in prostate cancer cells. *Cancer Res.* **66**:5723-5728.

Burghardt TP, Ajtai K, Borejdo J. (2006). In situ single-molecule imaging with attoliter detection using objective total internal reflection confocal microscopy. *Biochemistry* **45**:4058.

Chan TO, Rittenhouse SE, Tschlis PN. (1999). AKT/PKB and other D3 phosphoinositide-regulated kinases: Kinase activation by phosphoinositide-dependent phosphorylation. *Annu. Rev. Biochem.* **68**:965-1014.

Connolly JM, Rose DP. (1998). Angiogenesis in two human prostate cancer cell lines with differing metastatic potential when growing as solid tumors in nude mice. *J. Urol.* **160**:932-936.

Das S, Roth CP, Wasson LM, Vishwanatha JK. (2007). Signal transducer and activator of transcription-6 (STAT6) is a constitutively expressed survival factor in human prostate cancer. *Prostate* **67**:1550-1564.

Eeles RA, Kote-Jarai Z, Giles GG, Olama AA, Guy M, Jugurnauth SK *et al.* (2008). Multiple newly identified loci associated with prostate cancer susceptibility. *Nat. Genet.* **40**:316-321.

Evans EE, Henn AD, Jonason A, Paris MJ, Schiffhauer LM, et al. (2006). C35 (C17orf37) is a novel tumor biomarker abundantly expressed in breast cancer. *Mol Cancer Ther* **5**:2919.

Fresno Vara JA, Casado E, de Castro J, Cejas P, Belda-Iniesta C, Gonzalez-Baron M. (2004). PI3K/Akt signalling pathway and cancer. *Cancer Treat. Rev.* **30**:193-204.

Fu HW, Casey PJ. (1999). Enzymology and biology of CaaX protein prenylation. *Recent Prog Horm Res* **54**:315.

Helenius MA, Savinainen KJ, Bova GS, Visakorpi T. (2006). Amplification of the urokinase gene and the sensitivity of prostate cancer cells to urokinase inhibitors. *BJU Int.* **97**:404-409.

Hicklin DJ, Ellis LM. (2005). Role of the vascular endothelial growth factor pathway in tumor growth and angiogenesis. *J. Clin. Oncol.* **23**:1011-1027.

Huang S, Pettaway CA, Uehara H, Bucana CD, Fidler IJ. (2001). Blockade of NF-kappaB activity in human prostate cancer cells is associated with suppression of

angiogenesis, invasion, and metastasis. *Oncogene* **20**:4188-4197.

Jo M, Thomas KS, Marozkina N, Amin TJ, Silva CM, Parsons SJ *et al.* (2005). Dynamic assembly of the urokinase-type plasminogen activator signaling receptor complex determines the mitogenic activity of urokinase-type plasminogen activator. *J. Biol. Chem.* **280**:17449-17457.

Kauraniemi P, Kallioniemi A. (2006). Activation of multiple cancer-associated genes at the ERBB2 amplicon in breast cancer. *Endocr Relat Cancer* **13**:39.

Kelly P, Stemmler LN, Madden JF, Fields TA, Daaka Y, Casey PJ. (2006). A role for the G12 family of heterotrimeric G proteins in prostate cancer invasion. *J. Biol. Chem.* **281**:26483-26490.

Li Y, Cozzi PJ. (2007). Targeting uPA/uPAR in prostate cancer. *Cancer Treat. Rev.* **33**:521-527.

Lokeshwar BL. (1999). MMP inhibition in prostate cancer. *Ann. N. Y. Acad. Sci.* **878**:271-289.

Maurer-Stroh S, Eisenhaber F. (2005). Refinement and prediction of protein prenylation motifs. *Genome Biology* **6**:R55.

Myers RB, Srivastava S, Oelschläger DK, Grizzle WE. (1994). Expression of p160erbB-3 and p185erbB-2 in prostatic intraepithelial neoplasia and prostatic adenocarcinoma. *J. Natl. Cancer Inst.* **86**:1140-1145.

Pienta KJ, Loberg R. (2005). The "emigration, migration, and immigration" of prostate cancer. *Clin. Prostate Cancer.* **4**:24-30.

Price JT, Bonovich MT, Kohn EC. (1997). The biochemistry of cancer dissemination. *Crit Rev Biochem Mol Biol* **32**:175.

Rothermund CA, Kondrikov D, Lin MF, Vishwanatha JK. (2002). Regulation of bcl-2 during androgen-unresponsive progression of prostate cancer. *Prostate Cancer Prostatic Dis* **5**:236.

Sheng S. (2001). The urokinase-type plasminogen activator system in prostate cancer metastasis. *Cancer Metastasis Rev.* **20**:287-296.

Sliva D. (2004). Signaling pathways responsible for cancer cell invasion as targets for cancer therapy. *Curr Cancer Drug Targets* **4**:327.

Suh J, Rabson AB. (2004). NF-kappaB activation in human prostate cancer: Important mediator or epiphenomenon? *J. Cell. Biochem.* **91**:100-117.

Sun J, Zheng SL, Wiklund F, Isaacs SD, Purcell LD, Gao Z *et al.* (2008). Evidence for two independent prostate cancer risk-associated loci in the HNF1B gene at 17q12. *Nat. Genet.* 10.1038/ng.214 .

Thalmann GN, Anezinis PE, Chang SM, Zhau HE, Kim EE, Hopwood VL *et al.* (1994). Androgen-independent cancer progression and bone metastasis in the LNCaP model of human prostate cancer. *Cancer Res* **54**:2577.

Virtanen SS, Vaananen HK, Harkonen PL, Lakkakorpi PT. (2002). Alendronate inhibits invasion of PC-3 prostate cancer cells by affecting the mevalonate pathway. *Cancer Res.* **62**:2708-2714.

Wilson MJ, Sinha AA. (1993). Plasminogen activator and metalloprotease activities of du-145, PC-3, and 1-LN-PC-3-1A human prostate tumors grown in nude mice: Correlation with tumor invasive behavior. *Cell. Mol. Biol. Res.* **39**:751-760.

Wu HC, Hsieh JT, Gleave ME, Brown NM, Pathak S, Chung LW. (1994). Derivation of androgen-independent human LNCaP prostatic cancer cell sublines: Role of bone stromal cells. *Int J Cancer.* 1994 May 1;57(3):406-12 **57**:406.

Wilson SR, Gallagher S, Warpeha K, Hawthorne SJ. (2004). Amplification of MMP-2 and MMP-9 production by prostate cancer cell lines via activation of protease-activated receptors. *Prostate* **60**:168-174.

Winter-Vann AM, Casey PJ. (2005). Post-prenylation-processing enzymes as new targets in oncogenesis. *Nat. Rev. Cancer.* **5**:405-412.

Woolard J, Wang WY, Bevan HS, Qiu Y, Morbidelli L, Pritchard-Jones RO *et al.* (2004). VEGF165b, an inhibitory vascular endothelial growth factor splice variant: Mechanism of action, in vivo effect on angiogenesis and endogenous protein expression. *Cancer Res.* **64**:7822-7835.

Supplementary Table 1

Primer Sequences

Gene	Sequence (5'-3')	Amplified Size(bp)
C17orf37 Forward	CAGTGCTGTGAAGGAGCAGT	202
C17orf37 Reverse	GACGGCTGTTGGTGATCTTT	
VEGF Forward (Munaut <i>et al.</i> , 2003)	CCTGGTGGACATCTTCCAGGAGTA	407 -VEGF ₁₆₅
VEGF Reverse	CTCACCGCCTCGGCTTGTCACA	275 -VEGF ₁₂₁
MMP-9 Forward	TTGACAGCGACAAGAAGTGG	185
MMP-9 Reverse	GCCATTCACGTCGTCCTTAT	
uPA Forward	TTGACAGCGACAAGAAGTGG	781
uPA Reverse	CTACAGCGCTGACACGCTTG	
β -actin Forward	GAGGCTCTCTTCCAGCCTTCCTTCCT	308
β -actin Reverse	CCTGCTTGCTGATCCACATCTGCTGG	

Supplementary Table 2

SMART Pool Duplex for C17orf37 (Dharmacon) Sequences were BLAST searched in NCBI database to determine the specificity with C17orf37 sequence. All the sequences were confirmed to be 100 percent homology with only C17orf37 sequence.

1	Sense Sequence	C.C.G.A.A.G.A.G.C.C.A.G.U.A.A.U.G.G.A.U.U
	Antisense Sequence	5'-p.U.C.C.A.U.U.A.C.U.G.G.C.U.C.U.U.C.G.G.U.U
2	Sense Sequence	U.A.A.A.U.G.G.A.C.A.G.C.U.G.G.U.G.U.U.U.U
	Antisense Sequence	5'-p.A.A.C.A.C.C.A.G.C.U.G.U.C.C.A.U.U.U.A.U.U
3	Sense Sequence	U.A.G.A.A.A.A.G.A.U.C.A.C.C.A.A.C.A.G.U.U
	Antisense Sequence	5'-p.C.U.G.U.U.G.G.U.G.A.U.C.U.U.U.U.C.U.A.U.U
4	Sense Sequence	G.G.A.G.C.A.G.U.A.U.C.C.G.G.G.C.A.U.C.U.U
	Antisense Sequence	5'-p.G.A.U.G.C.C.C.G.G.A.U.A.C.U.G.C.U.C.C.U.U

Supplementary Methods

Cloning, expression and purification of recombinant C17orf37

Full length human C17orf37 cDNA of 347 bp was amplified using a forward primer 5'-CTAGAATTCCACATGAGCGGGGAGCC-3' containing an *EcoRI* restriction site and a reverse primer 5'-AGACTCGAGTGCAGTCACAGGATGA-3' containing a *XhoI* restriction site, and cloned into pGEX-4T-1 vector (GE Healthcare, Piscataway, NJ) in proper reading frame. GST-C17orf37 fused protein was expressed in E.coli BL-21 strain and purified using Glutathione Sepharose 4B column (GE Healthcare, Piscataway, NJ) according to manufacturer's instructions. Purified GST-C17orf37 was cleaved with 20 units/mg thrombin enzyme (Sigma, St.Louis, MO) overnight at room temperature to remove the GST tag. Recombinant C17orf37 is finally eluted from HiTrap Benzamide FF columns (GE Healthcare, Piscataway, NJ) to remove the residual thrombin enzyme.

Full length human C17orf37 cDNA of 347bp was amplified using a forward primer 5'-CAAGCTTCGAATTCATGAGCGGG-3' containing an *EcoRI* restriction site and a reverse primer 5'-ATCCGGTGGATCCAGTCACAG-3' containing a *BamHI* restriction site. PCR products were cloned into the pEGFP-C1 vector and the resulting vector was named GFP-C17orf37.

Cell lines and culture conditions

DU-145, PC-3, LNCaP C4-2, LNCaP-R, RF and UR prostate cancer cells were maintained in RPMI1640 supplemented with 10% fetal bovine serum (FBS) and 1%

penicillin-streptomycin (PS). Prostate epithelial cell lines HPV18 C-1 and PWR-1E were maintained in keratinocyte-SFM (Invitrogen, Carlsbad, CA) supplemented with bovine pituitary extract (25 μ g/ml) and recombinant epidermal growth factor (0.15ng/ml).

Mass spectrometry and liquid chromatography–tandem mass spectrometry

A hybrid linear ion trap–Fourier transform ion cyclotron resonance (7-Tesla) instrument (LTQ-FT, Thermo Fisher, San Jose, CA) equipped with an electrospray ionization (ESI) source and operated with the Xcalibur (version 2.2) data acquisition software was used for all mass spectrometric (MS) analyses (Branca *et al.*, 2007).

The molecular weight of the recombinant protein was determined by direct infusion (protein solution in aqueous solution containing 50% methanol and 1% acetic acid) using FTICR prior to reduction and carbamidomethylation of cysteines. Mass resolution ($M/\Delta M$) was set to 200,000 at m/z 400 and defined as full width at half maximum (FWHM) of the peak.

About 20-fold excess of dithiothreitol (in mass) was added to reduce the protein at 50 °C for 20 min, followed by alkylation with iodoacetamide (about 50:1 weight ratio iodoacetamide to protein) at room temperature for 30 min in the dark. The resulting carbamidomethylated protein solution was then desalted by repeated centrifugation in microcon filters (Millipore, Billerica, MA) at 8000g. Typtic peptides were obtained by incubation of the protein with trypsin (Promega, Madison, WI; ~50:1 protein to trypsin molar ratio) for 24 h at 37 °C in 50 mM ammonium bicarbonate (pH 7.8).

For online RP-HPLC-tandem mass spectrometric analysis of the tryptic digest (Stevens *et al.*, 2008), 5 μ l of the sample was loaded onto a PepMap C18 capillary trap (LCPackings, Sunnyvale, CA) and desalted with 3% acetonitrile, 1% acetic acid for 5 min prior to injection onto a 75 μ m i.d. x 10 cm PicoFrit C18 analytical column (New Objective, Woburn, MA). Following peptide desalting and injection onto the analytical column, a linear gradient provided by a Surveyor MS pump (Thermo) was carried out to 40% acetonitrile in 60 min at 250 nL/min. Spray voltage and capillary temperature during the gradient run were maintained at 2.0 kV and 250 $^{\circ}$ C, respectively. The conventional data-dependent mode of acquisition was utilized in which an accurate m/z survey scan was performed in the FTICR cell followed by parallel recording of tandem mass spectra (MS/MS) in the linear ion trap of the top 10 most intense precursor ions. FTICR full-scan mass spectra were acquired at 100,000 mass resolving power (m/z 400) from m/z 350 to 1500 using the automatic gain control mode of ion trapping (500000 target ion count). Collision-induced dissociation (CID) was performed in the linear ion trap using a 2.0-u isolation width and 35% normalized collision energy with helium as the target gas.

MS/MS data generated by data dependent acquisition via the LTQ-FT were extracted by the manufacturer's BioWorks version 3.3 software and searched against a composite IPI human protein database containing both forward and randomized sequences using the Mascot (version 2.2.1; Matrix Science, Boston, MA) search algorithm. Mascot was searched with a fragment ion mass tolerance of 0.80 Da and a parent ion tolerance of 10 ppm assuming the digestion enzyme trypsin with the possibility of one missed cleavage. Carbamidomethylation of cysteine was specified as a

static modification, while oxidation of methionine, conversion of N-terminal Glu/Gln (E/Q) to pyroglutamyl (<E) in tryptic peptides and N-terminal protein acetylation were specified as variable modifications in the database search. The software program Scaffold (version Scaffold-01_06_13, Proteome Software Inc., Portland, OR) was then employed to compile and validate tandem MS-based peptide and protein identifications. Peptide identifications were accepted at greater than 95.0% probability as determined by the Peptide Prophet algorithm (Keller *et al.*, 2002).

Isolation of total RNA and quantitative reverse transcription-PCR

Total RNA was isolated from prostate cells by Trizol reagent (Invitrogen, Carlsbad, CA) according to manufacturer's instructions. For quantitative reverse transcription-PCR (qRT-PCR) analysis, a two step process was performed using the SuperScript III platinum Two-step qRT-PCR kit with SYBR Green (Invitrogen, Carlsbad, CA). One μ g of isolated RNA was used for conversion to cDNA followed by amplification using a Cepheid Smart Cycler system (Cepheid, Sunnyvale, CA). Ct values were determined at a threshold value of 30 fluorescence units. Samples were run in triplicate and housekeeping gene actin was used as an internal control. The fold change of C17orf37 mRNA expression was calculated according to the formula of Livak and Schmittgen (Livak and Schmittgen, 2001) with respect to HPV18 C-1 cell line which was fixed to base line as 1.

Transfection procedures

Cells were transfected using Lipofectamine 2000 (Invitrogen, Carlsbad, CA) with plasmid DNA (GFP-C17orf37 vector or empty vector-GFP) for a period of 6 hours in OPTI-MEM (Invitrogen, Carlsbad, CA). After transfections, cells were grown in complete media overnight before mounting on slides using Vectashield (Vector Laboratories, Burlingame, CA) for confocal microscopy.

For generation of stable cells, DU-145 cells were transfected using Lipofectamine 2000, with either GFP (empty-vector) or GFP-C17orf37 plasmid DNA for 24hours. Stable transfected cell populations were challenged in complete medium supplemented with 500µg/ml G418 (Invitrogen, Carlsbad, CA) for about 2 weeks. For subsequent experiments, randomly picked single clones were isolated from DU-145 cells transfected with GFP-C17orf37 (DU-ORF-9) and, polyclonal populations were obtained from DU-145 cells transfected with GFP vector (DU-GFP) and DU-145 cells transfected with GFP-C17orf37 plasmid (DU-GFP-C17orf37-1 and 2).

Smart pool siRNA sequences for C17orf37 are listed in Supplementary Table 2.

ELISA assay for MMP-9 and VEGF

DU-145 cells were seeded in 6 well plates and transiently transfected with mock (Dharmafect), non-targeting control siRNA and C17orf37 siRNA; and lipofectamine (mock), GFP vector only, GFP-C17orf37 as mentioned in the transfection procedure section in the Material and methods. After transfections, cells were incubated in serum free RPMI (Invitrogen) for 24 hours. The culture medium was collected, centrifuged to

remove cell debris and stored at -80°C until assay. The number of cells per well was counted using hemocytometer. Quantikine Human MMP-9 and VEGF Elisa assay kit (R & D Systems, Minneapolis, MN) was used to determine the concentration of secreted MMP-9 and VEGF, according to the manufacturer's instructions. MMP-9 concentration (ng/mL) was calculated and normalized to the number of cells (ng/mL/ 10^5 cells). Quantikine VEGF elisa kit determines both VEGF₁₂₁ and VEGF₁₆₅ secreted isoform concentration (pg/mL) and normalized to the total number of cells (pg/mL/ 10^5 cells). The concentration values are graphically represented as ratio of control to the untreated cells.

Antibodies

Antibodies used for the study are as follows: C17orf37 (Abnova, Taiwan; 1:500) and C17orf37 (anti-C35) (Zymed, Carlsbad, CA); Glyceraldehyde 3-phosphate dehydrogenase (GAPDH) (Santa Cruz Biotechnology, Santa Cruz, CA, 1:1250 dilution); actin (Calbiochem, San Diego, CA; 1:2000 dilution); Lamin (1:1000), MMP-9 (1:1000), Akt (1: 1000) and phospho-Akt Ser-473 (1:500) dilutions from Cell Signaling, Danvers, MA; uPA (1:500) and VEGF (1:250) dilutions from R & D Systems, Minneapolis, MN; and ERK1/2 (1:1000) and phospho-ERK1/2 Thr-202/Tyr-204 (1:500) dilutions BD Biosciences, San Jose, CA.

In vitro Tumor Invasion Assay

DU-145 and PC-3 cells either transiently transfected with GFP-vector or GFP-C17orf37; DU-145 cells treated with siRNA-C17orf37 or control-siRNA (as described before), and

stable DU-GFP, DU-ORF-9, DU-GFP-C17orf37-1 and DU-GFP-C17-2 cell suspensions were prepared in growth medium without serum and 2.5×10^4 cells/well were added to the top chamber of the tumor invasion system. 10% FBS was added to the bottom chambers as chemoattractant. Cells were allowed to invade through the Matrigel for 24 hours at 37°C. Following incubation, nonmigratory cells were removed from the top chamber and the cells that successfully invade the Matrigel matrix and migrate to the bottom side of the membrane were stained with 4µg/ml of Calcein AM (Molecular Probes, Carlsbad, CA) and fluorescent reading was taken at excitation/emission wavelengths of 485/530 nm. Growth medium incubated without any cells in the invasion system was used as blank reading and three independent experimental readings were used to calculate the mean fold change of invasion by determining the ratio of fluorescent reading-experimental group to fluorescence reading-control group.

Electrophoretic Mobility Shift Assay (EMSA)

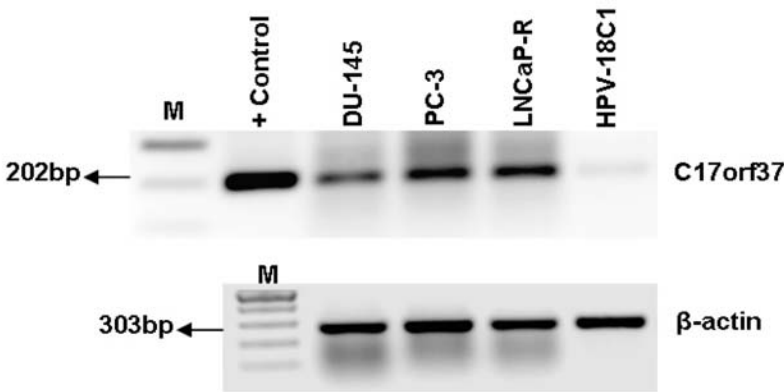
Nuclear extract was prepared using NE-PER (Pierce, Rockford, IL) cytosolic-nuclear extraction kit. 5 µg of nuclear protein extracts were used to incubate with the biotin conjugated probe and gel shift assay performed according to manufacturer's instructions (Panomics Inc., Redwood, CA).

Scratch Wound Healing Migrating Assay

DU-ORF-9 cells were grown on coverslip in a monolayer and scratch was created using pipet tip. Floating cells were removed by changing the medium and cells were imaged at

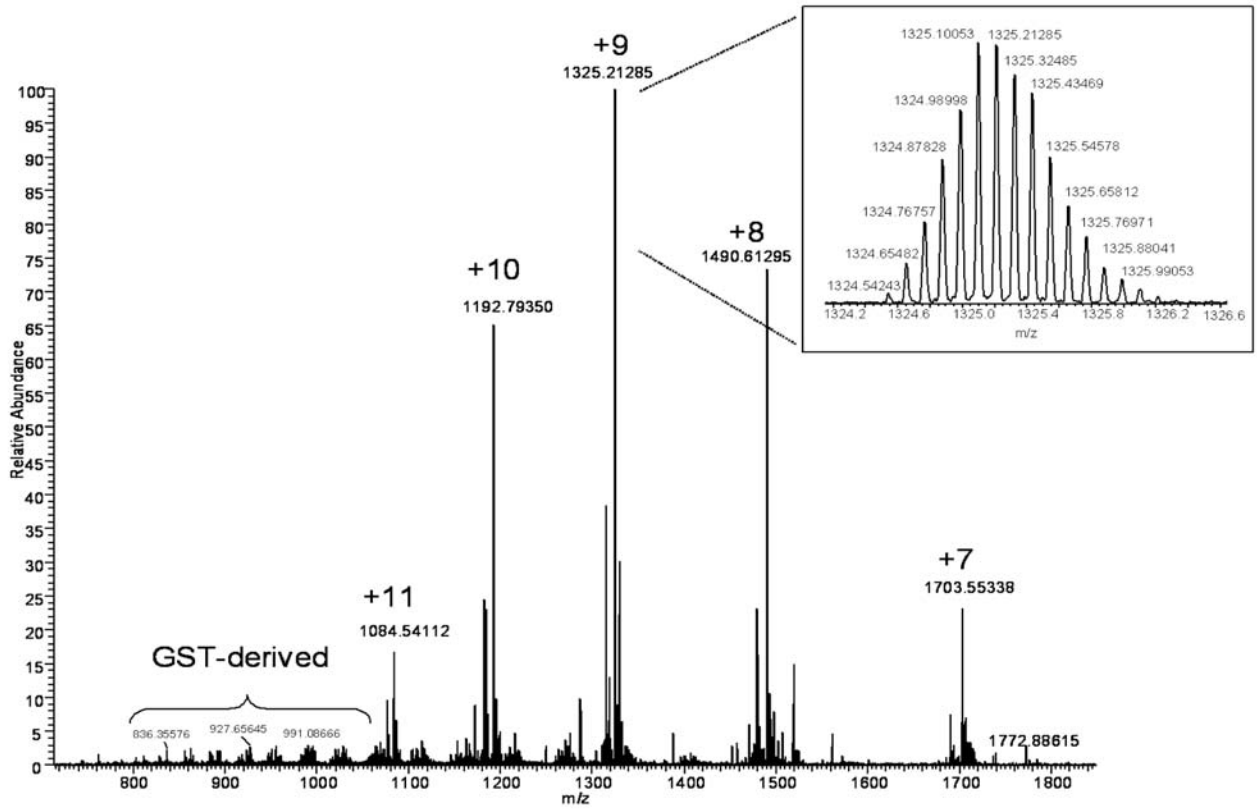
different time points 0, 3, 6 and 9 hours after the creating of the wound. Cells were then washed, fixed, permeabilized and imaged using confocal microscopy.

Supplementary Figure 1



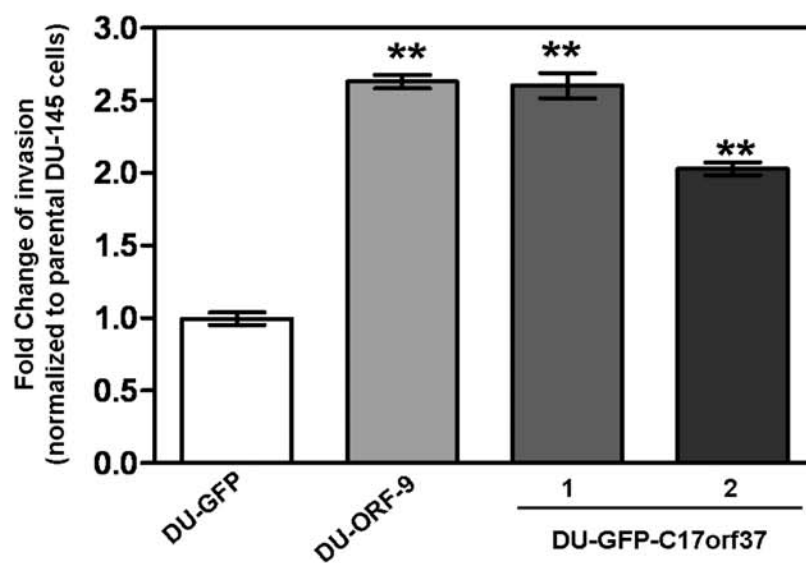
Supplementary Figure 1 Expression of *C17orf37* mRNA in prostate cancer cells. Total RNA was isolated from DU-145, PC-3, LNCaP-R and HPV-18 C-1. *C17orf37* gene was amplified by RT-PCR as described in materials and methods section. GST-C17orf37 vector (as described in Materials and Methods section) was used as positive control. β -*Actin* was used as loading control. *C17orf37* mRNA was found to be highly expressed in DU-145, PC-3 and LNCaP-R prostate cancer cells compared to minimal expression in HPV-18C1 prostate epithelial cells.

Supplementary Figure 2



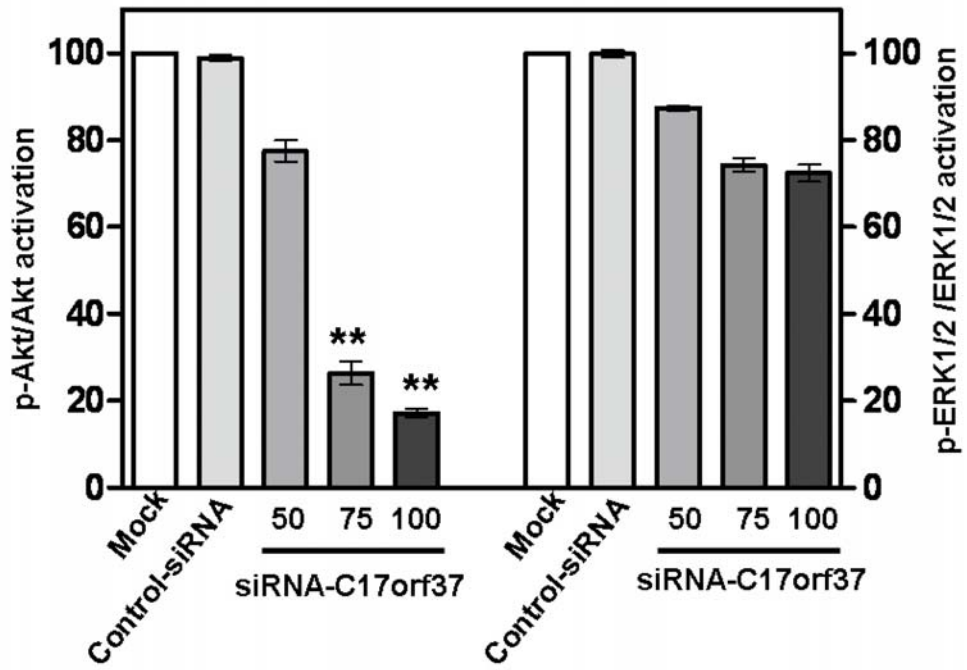
Supplementary Figure 2 Mass spectrum of recombinant C17orf37 protein. Full-scan FTICR mass spectrum acquired of the purified recombinant protein at 200,000 mass resolving power at m/z 400. The resolving power obtained for the +9 charge state isotope cluster ($[M+9H]^{9+}$, inset) was $\sim 55,000$ (FWHM).

Supplementary Figure 3



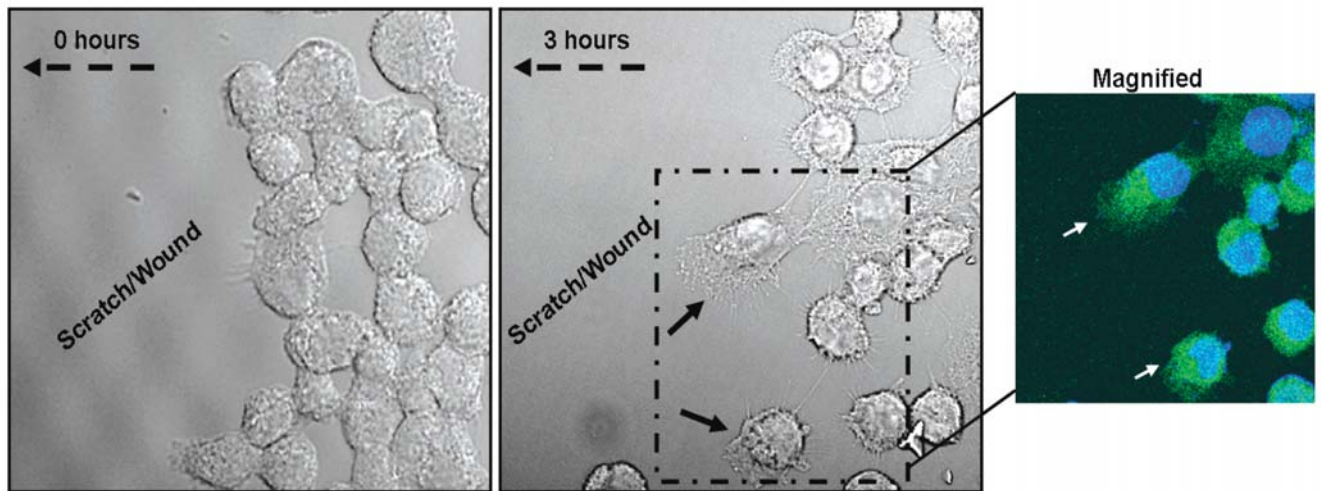
Supplementary Figure 3 Overexpression of C17orf37 increases invasive potential of DU-145 cells. Stable polyclonal population of DU-GFP (vector) and DU-GFP-C17orf37 (pool#1 and #2); stable randomly picked DU-ORF-9 (overexpressing GFP-C17orf37), and parental DU-145 cells were seeded onto matrigel coated tumor invasion chambers and allowed to migrate toward serum for 24 hours at 37°C. Fold change of invasion was calculated as described in supplementary materials and methods section. *Columns* are mean of three independent experiments; *bars*, SD. **, $P < 0.001$, relative to DU-GFP cells; statistical analysis included Student's *t* test for calculating significant differences within groups.

Supplementary Figure 4



Supplementary Figure 4 Graphical representation showing expression ratio of p-Akt/Akt and p-ERK/ERK normalized to housekeeping gene GAPDH as shown in Figure 6b. *Columns* mean of three independent experiments; *bars*, SD. **, $P < 0.005$ relative to mock treated.

Supplementary Figure 5



Supplementary Figure 5 Confocal microscopy showing the expression of C17orf37 preferentially localized to the leading edge of the migrating DU-ORF-9 cells. Cells were grown on coverslip in a monolayer and scratch was created as described in the Supplementary information. After 3 hours, cells were fixed in a slide and imaged using LSM510 confocal microscopy (phase contrast and fluorescence at 488 nm wavelength). Inset shows the magnified image of the area marked with dotted box. Dotted arrow at the top indicates the direction of migration and solid arrows indicate the migrating cells with protruding edge. Original magnification, *X100*.

Supplementary References

Branca RM, Bodo G, Bagyinka C, Prokai L. (2007). De novo sequencing of a 21-kDa cytochrome c4 from *thiocapsa roseopersicina* by nanoelectrospray ionization ion-trap and fourier-transform ion-cyclotron resonance mass spectrometry. *J. Mass Spectrom.*

42:1569-1582.

Keller A, Nesvizhskii AI, Kolker E, Aebersold R. (2002). Empirical statistical model to estimate the accuracy of peptide identifications made by MS/MS and database search.

Anal. Chem. **74**:5383-5392.

Livak KJ, Schmittgen TD. (2001). Analysis of relative gene expression data using real-time quantitative PCR and the 2(-delta delta C(T)) method. *Methods* **25**:402-408.

Munaut C, Noel A, Hougrand O, Foidart JM, Boniver J, Deprez M. (2003). Vascular endothelial growth factor expression correlates with matrix metalloproteinases MT1-MMP, MMP-2 and MMP-9 in human glioblastomas. *Int. J. Cancer* **106**:848-855.

Stevens SM,Jr, Duncan RS, Koulen P, Prokai L. (2008). Proteomic analysis of mouse brain microsomes: Identification and bioinformatic characterization of endoplasmic reticulum proteins in the mammalian central nervous system. *J. Proteome Res.*

CHAPTER III

ISOPRENYLATION REGULATES C17ORF37 MEDIATED CANCER CELL MIGRATION AND METASTASIS

Subhamoy Dasgupta, Ian Cushman, Patrick J. Casey, and Jamboor K. Vishwanatha

ABSTRACT

Post-translational modification by covalent attachment of isoprenoid lipids (prenylation) regulates the functions and biological activities of several proteins implicated in the oncogenic transformation and metastatic progression of cancer. Prenylated proteins (often referred to as CAAX family of proteins) contain a CAAX motif (C denotes cysteine, A represents aliphatic amino acids, and X any amino acid) at the carboxyl terminal which serves as a substrate for a series of post-translational modifications converting otherwise hydrophilic to lipidated proteins with hydrophobic domain, facilitating membrane localization (Der and Cox, 1991; Glomset and Farnsworth, 1994; Zhang and Casey, 1996). A novel gene named Chromosome 17 open reading frame 37 (C17orf37) located in the 17q12 amplicon is overexpressed in different forms of human cancer and its expression correlates with migratory and invasive phenotype of cancer cells. Here we show that C17orf37 has a functional prenylation motif and is post-translationally modified by geranylgeranyl transferase-I (GGTase-I) enzyme. Geranylgeranylation of C17orf37 at the 'CVIL'

motif translocates the protein to the inner leaflet of plasma membrane, enhances migratory phenotype of cells by inducing increased filopodia formation and potentiates directional migration. The prenylation-deficient C17orf37 mutant is functionally inactive and fails to disseminate injected cells in the mouse model of metastasis. This implies that prenylation activates the C17orf37 protein in cancer cells and functionally regulates metastatic progression of the disease.

INTRODUCTION

C17orf37 gene is located in the minus strand of human chromosome 17q12 bounded by *ERBB2* and *Grb7* on both sides. Several studies have reported a 280kB common minimal region of 17q12, containing *ERBB2* and its neighboring genes including *C17orf37*, to be frequently amplified in breast and colon cancer. Although *C17orf37* overexpression is linked with genomic amplification of *ERBB2* locus (Kauraniemi *et al.*, 2003; Kauraniemi and Kallioniemi, 2006), abundant expression of *C17orf37* protein in *ERBB2* non-amplified breast (Evans *et al.*, 2006) and prostate (Dasgupta *et al.*, 2009) tumors suggest *C17orf37* has an independent functional promoter. The gene encodes a 12kD protein which enhances migratory and invasive phenotype of cancer cells (Dasgupta *et al.*, 2009). This function of *C17orf37* is due to its ability to act as a membrane bound signaling molecule modulating the PI-3K/Akt pathway, there by transcriptionally upregulating NF-kB downstream target genes MMP-9, uPA and VEGF (Dasgupta *et al.*, 2009). Thus, *C17orf37* overexpression in tumors contributes to the migratory and invasive phenotype, facilitating the malignant progression of the disease.

C17orf37 is expressed as a cytosolic protein with predominant membrane localization. Like other membrane anchor proteins, *C17orf37* does not have N-terminal hydrophobic domain responsible for its binding to the plasma membrane. In a survey of several computational algorithms, including Pre-PS, PSORT and TargetP,

we identified a prenylation motif 'CVIL' at the C-terminal end of the protein and predicted the protein to be geranylgeranylated by GGTase-I enzyme. We hypothesized that prenylation of C17orf37 may be crucial for its membrane association, and in turn, could regulate its functional activity.

RESULTS

C17orf37 is geranylgeranylated by GGTase-I enzyme at Cys 112

Prenylated proteins are either farnesylated (addition of 15 carbon chain) by farnesyl transferase enzyme (FTase) (Zhang and Casey, 1996), or geranylgeranylated (20 carbon chain) by GGTase enzyme at the cysteine residue (Casey and Seabra, 1996). The carboxyl terminal amino acid (“X”) of the CAAX motif determines which isoprenoid group is to be added to the candidate protein. If the amino acid “X” is leucine, the protein is predicted to be geranylgeranylated, and if not farnesylated (Zhang and Casey, 1996). Based on this understanding, C17orf37 is predicted to be geranylgeranylated by GGTase-I enzyme at the cysteine 112 amino acid. In addition to the ‘CAAX’ motif, certain upstream clusters of polybasic amino acids are also required for efficient membrane association of the prenylated proteins (Der and Cox, 1991; Roberts *et al.*, 2008). Aligning the last 30 amino acids of C17orf37 preceding the ‘CAAX’ motif with the known geranylgeranylated proteins RhoA, RhoB, RhoC, Rac1, and Cdc42, reveals the presence of tandem repeats of polybasic amino acids in C17orf37 protein as well (Fig. 1a). Presence of these polybasic amino acids imparts positive charge to the prenylated C17orf37 protein, which signifies stable association with acidic membrane associated lipids. To directly confirm that GGTase-I enzyme catalyzes the addition of geranylgeranyl isoprene to the Cys 112 of the C17orf37 ‘CAAX’ motif, we performed an *in vitro* prenylation assay using GST-fused C17orf37 (C17-WT) and mutant form of C17orf37, where Cys 112 was substituted

Figure 1

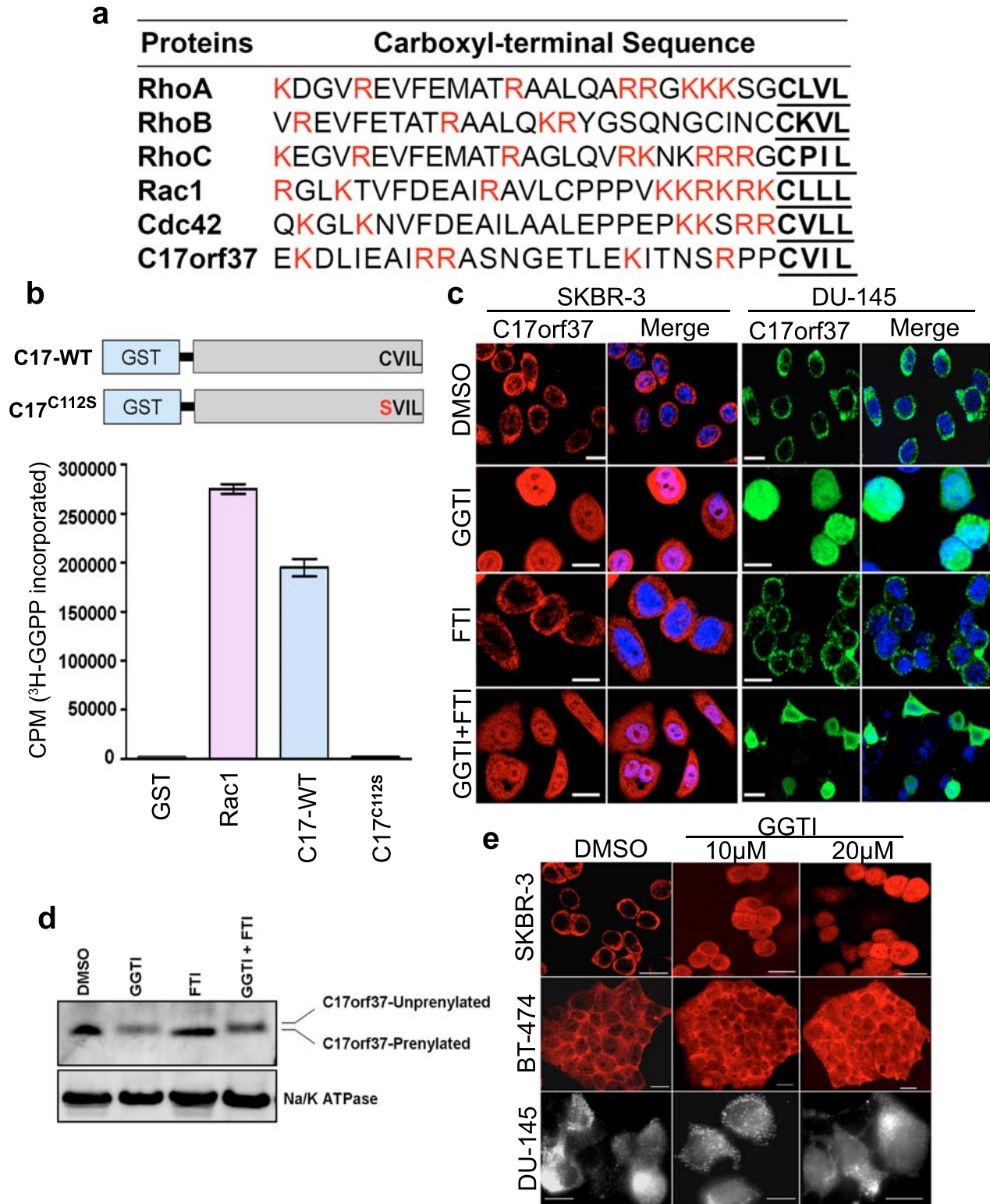


Figure 1. C17orf37 is geranylgeranylated by GGTase-I enzyme at Cys 112. (a) Sequence alignment of last 30 amino acids from the carboxyl-terminal end denoting the membrane binding sequence of known geranylgeranylated proteins. Polybasic amino acids are shown in red, and 'CAAX' motif is boldfaced and underlined. (b) Schematic diagram showing the 'CAAX' box located at the C-terminal end of C17orf37 was mutated to serine (C112S), and Glutathione sepharose transferase (GST) fused recombinant protein C17orf37 wild type (C17-WT) and C17orf37-C112S (C17^{C112S}) was used for *in vitro* prenylation assay. Direct geranylgeranylation of C17-WT (2.5 μ M) was achieved in the presence of recombinant GGTase-I enzyme containing ³H-GGPP (geranylgeranyl pyrophosphate). Rac1 (5 μ M) was used as a positive control and GST protein as a negative control. (c) Immunofluorescence staining of C17orf37 in SKBR-3 (Left, C17orf37 stained red) and DU-145 cells (Right, C17orf37 stained green), and overlay with nuclear 4,6-diamidino-2-phenylindole (DAPI; blue) staining of the same field (merge). SKBR-3 and DU-145 cells were treated with dimethyl sulfoxide (DMSO), geranylgeranyl transferase-I (GGTase-I) inhibitor- DU-40 (GGTI) at a dose of 10 μ M, farnesyl transferase (FTase) inhibitor- FTI-2148 (FTI) at a dose of 10 μ M, or a combination of both GGTI and FTI for 24 hours followed by confocal microscopy to image subcellular localization of C17orf37. Scale bars, 20 μ m. (d) Immunoblotting of C17orf37 in SKBR-3 cell membrane fractions with treatments as indicated in (c). Sodium potassium ATPase (Na/K ATPase) was used as a loading control. (e) SKBR-3, BT-474 and DU-145 cells treated with Left: DMSO, Middle: GGTI-10 μ M dose, Right: GGTI-20 μ M dose for

24 hours and immunofluorescence staining performed to image subcellular localization of C17orf37 (red). DU-145 cells were imaged using total internal reflection (TIRF) microscopy to determine the membrane association of C17orf37 protein, scale bar 20 μ m.

with Ser (C17^{C112S}) (Supplementary Information, Fig. S1). C17-WT protein (at 2.5 μ m concentration) with functional ‘CVIL’ motif efficiently incorporated geranylgeranyl [³H]GG in presence of GGTase-I enzyme, comparable to known geranylgeranylated protein Rac1 (Fig. 1b). However, mutation of Cys112 to Ser (C17orf37^{C112S}) in the ‘CAAX’ box of C17orf37, abolished the prenylation by GGTase-I enzyme (Fig. 1b). C17orf37 protein is expressed subcellularly as a cytosolic protein with predominant membrane association (Supplementary Information, Fig. S2). We sought to identify whether prenylation of C17orf37 by GGTase-I enzyme is required for its membrane association. To determine this, we treated SKBR-3 and DU-145 cells with selective GGTase-I inhibitor DU-40 (GGTI) (Peterson *et al.*, 2006) or FTase inhibitor-2148 (FTI)(Carrico *et al.*, 2004). Inhibition of GGTase-I enzyme, but not FTase, reduced C17orf37 membrane localization both in SKBR-3 (Fig. 1c, left) and DU-145 cells (Fig. 1c, right). Further, combinatorial treatment of GGTI and FTI did not show any synergism and was much similar to the effect observed with GGTI treatment. As expected, membrane fractions of SKBR-3 cells treated with GGTI showed reduced C17orf37 association, and non-prenylated C17orf37 protein migrated with a slower mobility in SDS-PAGE compared to prenylated C17orf37 (Fig. 1d). Dose dependent treatment of GGTI (10 μ M and 20 μ M) resulted in decreased membrane association, and prompted mislocalization of C17orf37 protein to the cytosol and nucleus (Fig. 1e), a prevalent phenomenon observed with other prenylated proteins. These results demonstrate that C17orf37 is indeed a substrate of GGTase-I enzyme, which

catalyzes the addition of geranylgeranyl isoprenyl group to the Cys residue in the 'CVIL' motif required for membrane association.

Post-translational modifications are necessary for membrane association of C17orf37 protein

Prenylation of the CAAX motif is followed by two additional important biochemical processes (Ashby, 1998). Proteolytic cleavage of the last three amino acids ("AAX") by ras converting enzyme 1 (Rce1) and carboxyl methylation of the prenylated cysteine by isoprenylcysteine-*O*-carboxyl methyltransferase (Icmt) are important post-prenylation events required for correct localization and biological functions of "CAAX" proteins (Kim *et al.*, 1999; Roberts *et al.*, 2008). Gene disruption studies in mice have that confirmed *Icmt* and *Rce1* enzymes are essential for mouse development and *Rce1*^{-/-} and *Icmt*^{-/-} mice are embryonically lethal (Bergo *et al.*, 2001; Bergo *et al.*, 2004; Lin *et al.*, 2002). To determine if geranylgeranyl modification of C17orf37 imposes a dependence on Rce1 mediated cleavage of "AAX" tripeptide and carboxymethylation by Icmt enzyme, we evaluated the subcellular localization of C17orf37 in mouse embryonic fibroblasts (MEF) deficient in Rce1 and Icmt enzymes. Wild type MEF cells transiently transfected with GFP-tagged C17orf37 showed evenly distributed C17orf37 in the membrane and cytosol. However, in *Rce1*^{-/-} cells C17orf37 localization was abrogated and displayed increased nuclear and cytoplasmic accumulation (Fig. 2a). Surprisingly, in *Icmt*^{-/-} cells C17orf37 was found to be localized as dense punctuated spots, presumably in the vesicles, and also in the

Figure 2

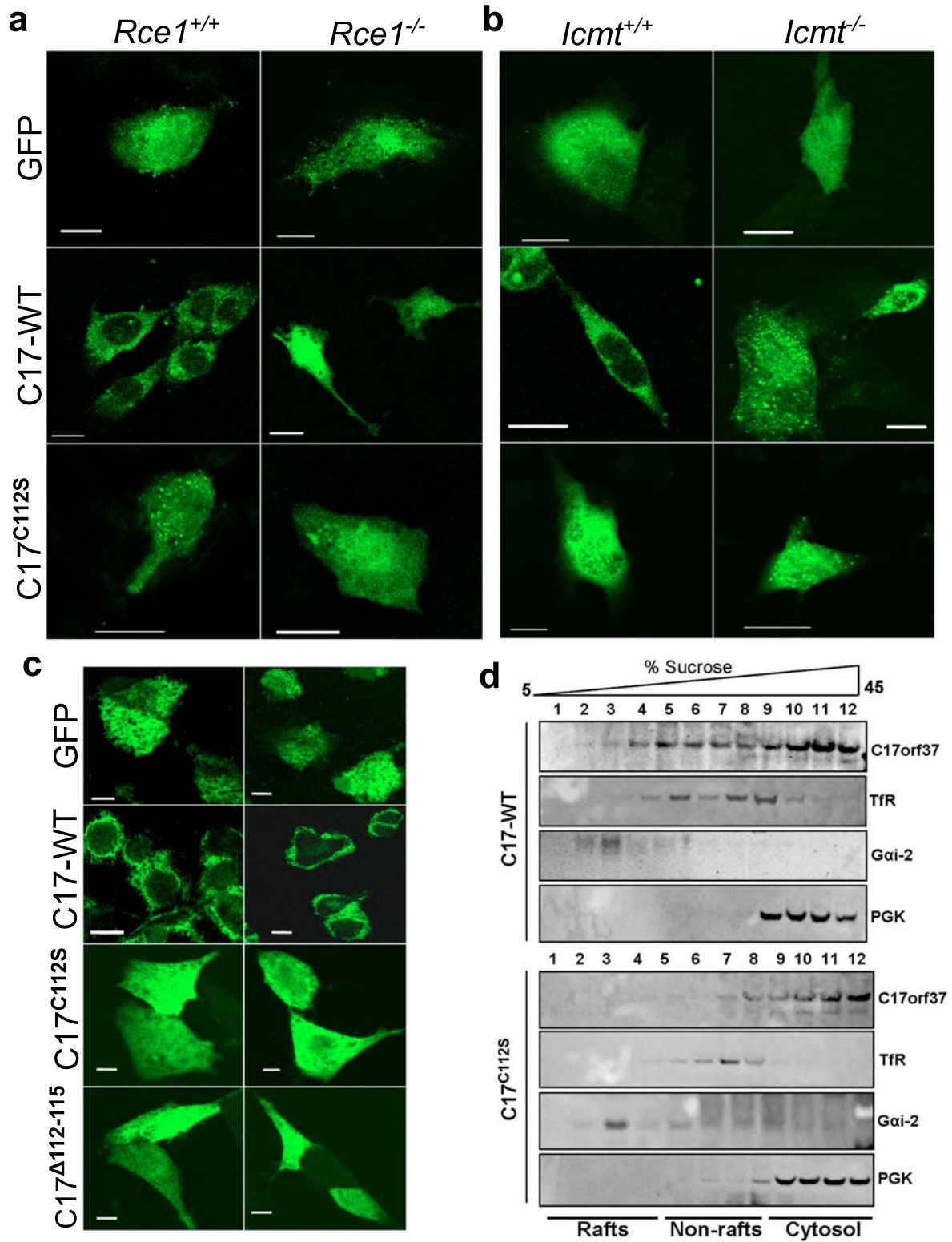


Figure 2. Post-translational modifications are necessary for membrane association of C17orf37 protein. (a) Rce1^{+/+} and Rce1^{-/-}, and (b) Icmt^{+/+}, and Icmt^{-/-} MEFS were transiently transfected with GFP fused expression constructs of blank vector only (GFP), wild type C17orf37 (C17-WT) and C17orf37-C112S mutant (C17^{C112S}) and confocal microscopy performed to visualize the localization of the tagged protein. (c) NIH3T3 cells were stably transfected with constructs mentioned above and polyclonal pools selected were visualized. (d) Immunoblotting of GFP tagged C17orf37 in NIH3T3 cells stably expressing either C17-WT or C17^{C112S} constructs fractionated on a 5-45% discontinuous sucrose gradient. Total 12 fractions were collected based on their density in sucrose gradient and numbered from the top. Galpha_{i-2} (Gα_{i-2}), transferrin receptor (Tfr) and phosphoglycerate kinase (PGK) were used as marker proteins to analyze raft, non-raft and cytosolic fractions respectively.

cytosol and nucleus (Fig. 2b). Absence of carboxyl-methylation probably mislocalized C17orf37 protein to the vesicles, which was rarely observed in wild type cells. We also generated a GFP-tagged C17orf37 mutant in which Cys 112 was mutated to Ser (C17^{C112S}), and transient transfection in wild type, *Rce1*^{-/-} or *Icmt*^{-/-} MEFs showed nuclear accumulation (Fig. 2a, b; bottom panels). Taken together, these findings provide evidence that C17orf37 is geranylgeranylated by GGTase-I enzyme, and membrane association of C17orf37 is also dependent on post-prenylation processing mediated by *Rce1* and *Icmt* enzymes. Next we generated stable polyclonal pooled populations of C17orf37-null NIH3T3 cells, expressing GFP-vector, GFP-C17orf37, or C17orf37 mutants- C17orf37^{C112S}, and C17orf37^{Δ112-115} in which the entire “CAAX” box was deleted (Supplementary Information, Fig. S3). As expected, C17orf37 mutants showed increased cytoplasmic and nuclear accumulation in NIH3T3 whereas the wild type C17orf37 (C17orf37^{WT}) efficiently localized to the membrane (Fig. 2c). Although, C17orf37^{Δ112-115} mutant behaved as expected, the stability of the protein recovered from NIH3T3 cells was low, suggesting deletion of entire ‘CAAX’ box affected protein integrity (Supplementary Information, Fig. S3). Plasma membrane is a vast dynamic structure composed of extremely complex set of 500 different lipid species with proteins embedded in it (Mayor and Rao, 2004). Most of the prenylated proteins have the ability to interact with the plasma membrane, although they maintain a substantial cytoplasmic soluble pool (Magee and Seabra, 2003). Studies have shown that farnesylated Ras protein has the ability to aggregate in cholesterol enriched membrane microdomains known as

'lipid rafts' present in the inner leaflet of the plasma membrane, and there is a dynamic relation between raft and non-raft associated proteins (Prior and Hancock, 2001). We determined the spatial and temporal distribution of prenylated C17orf37 in the membrane microdomains. Total protein recovered from NIH3T3 cells stably expressing either C17orf37^{WT} or C17orf37^{C112S} were subjected to differential centrifugation on a discontinuous sucrose gradient, and fractions collected based on their density on sucrose gradients were analyzed. The cholesterol-rich low density membrane fractions (fractions 2-4) were distributed at the interface between 5 and 45% sucrose, and contain an enrichment of raft marker Gal α _{i-2}; the heavier membrane fractions (fractions 5-9) showed a predominant expression of the non-raft marker transferrin receptor (Tfr), whereas most cellular protein were localized to the bottom of the gradient in fractions (fractions 9-12) (Fig. 2d, e). C17orf37^{WT} was distributed in two different pools - as soluble fraction in the cytosol (fractions 9-12), and in the membrane associated with the non-raft microdomains (fractions 5-7) and surprisingly, very less in the rafts (Fig. 2d). Even endogenous C17orf37 in DU-145 cells showed similar membrane distribution (Supplementary Information, Fig. S4). However, C17orf37^{C112S} was mostly localized to the soluble fractions comprising of cytosolic proteins (fractions 10-12), and very less in the membrane microdomains (Fig. 2e). Although the definition of membrane rafts is currently under extreme scrutiny, several revised definitions of membrane microdomains suggest the importance of understanding the lipid composition of 'non-raft' domains as well (Shaikh and Edidin, 2006). Our studies provide evidence that prenylated C17orf37

localizes to the membrane microdomains, particularly to the ‘non-raft’ domains, supporting previous report that geranylgeranylated proteins cluster in enriched microdomains outside lipid rafts (van Meer, 2002; Zacharias *et al.*, 2002).

Expression of prenylation-deficient C17orf37 mutant inhibits cell migration

We investigated whether functional role of C17orf37 dictates a dependence on the post-translational modifications at the ‘CVIL’ motif. Previously we have reported that ectopic overexpression of C17orf37 increases the migratory ability of cancer cells (Supplementary Information, Fig. S5) (Dasgupta *et al.*, 2009), and to identify the role of prenylation in C17orf37 mediated cell migration, we employed scratch-wound assays in NIH3T3 cells stably expressing GFP-vector, C17orf37^{WT}, or C17orf37^{C112S}. Scratch assays are commonly used to study the ability of cells to polarize and migrate into the wound with time (Magdalena *et al.*, 2003a; Magdalena *et al.*, 2003b). Cells expressing C17orf37^{WT} construct were able to migrate and cover nearly all of the wounded area within 18 hours (~2 fold increase in cell number), whereas GFP-vector or the C17orf37^{C112S} failed to do so (Fig. 3a, b). Even in transwell migration assay, C17orf37^{WT} construct led to a ~2.5 fold increase in migration compared to GFP-vector or C17orf37^{C112S} NIH3T3 cells (Fig. 3c), suggesting the role of C17orf37 in cell migration is dependent on its prenylation at the “CVIL” motif.

Figure 3

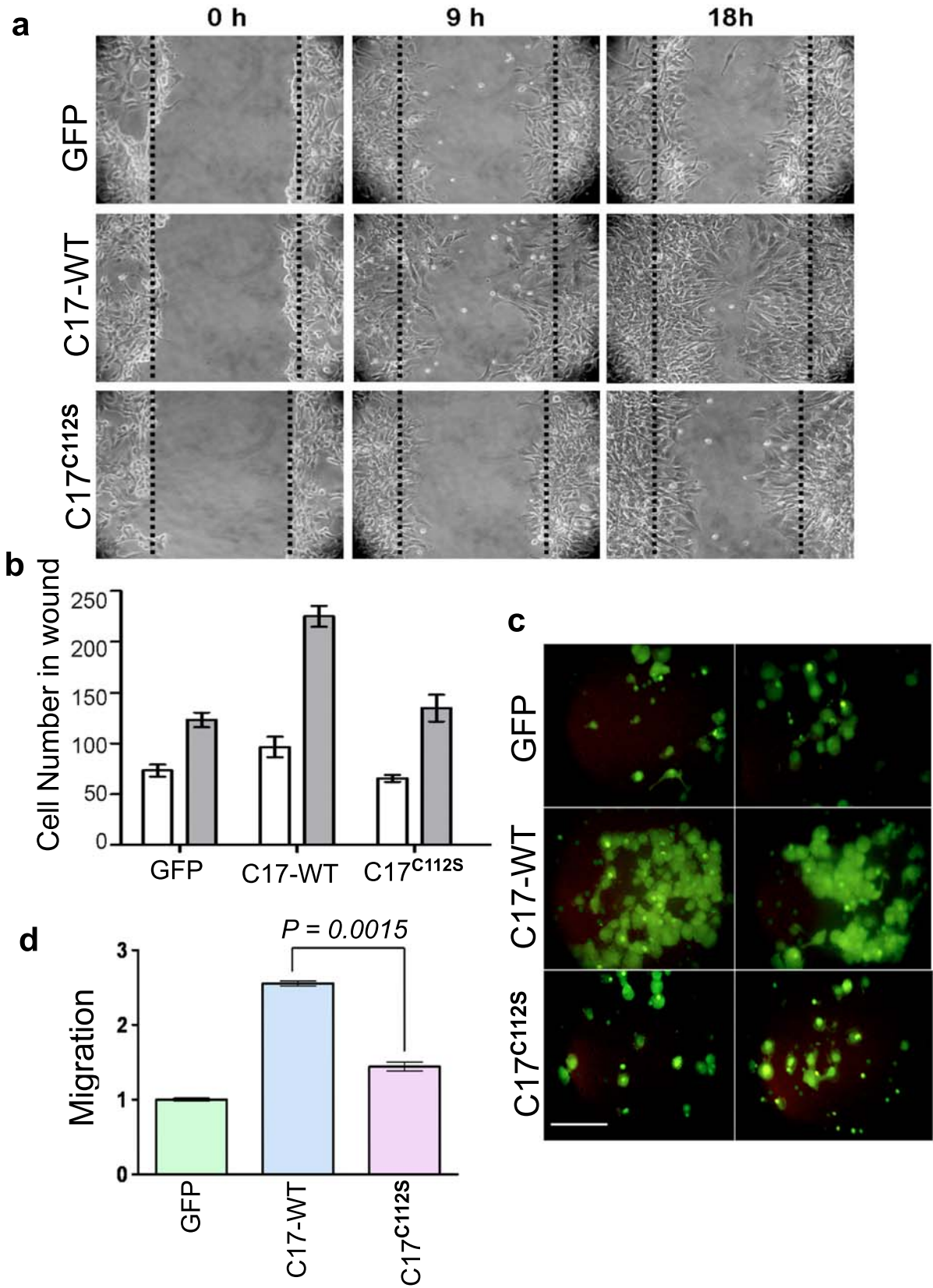


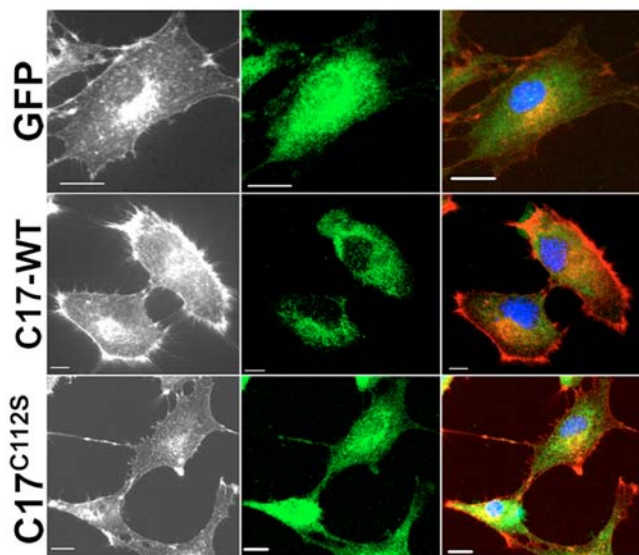
Figure 3. Expression of prenylation-deficient C17orf37 mutant inhibits cell migration. (a) Inhibition of wound closure in NIH3T3 cells stably expressing vector (GFP), GFP fused wild type C17orf37 (C17-WT) or GFP fused C17orf37-C112S mutant (C17^{C112S}). Confluent monolayers of cells were wounded and images taken at time 0 hour (left); 9 hours (middle); and 18 hours (right). (b) Migrated cells in the wound area at 9 hours (open bar) and 18 hours (grey bar) were counted from five different fields and expressed as mean \pm s.e.m of five independent experiments. (c, d) NIH3T3 cells expressing different constructs as mentioned in (a) were pre-labeled with Calcein AM fluorescent dye and transwell migration assay performed with 10% serum as a chemo attractant in the lower chamber. (c) After 24 hours, representative images of migrated cells from two different fields were obtained and fold change of migration was calculated normalized to parental NIH3T3 cells, and expressed as mean \pm s.e.m of three independent experiments (d).

C17orf37 prenylation by GGTase-I stimulates filopodia formation

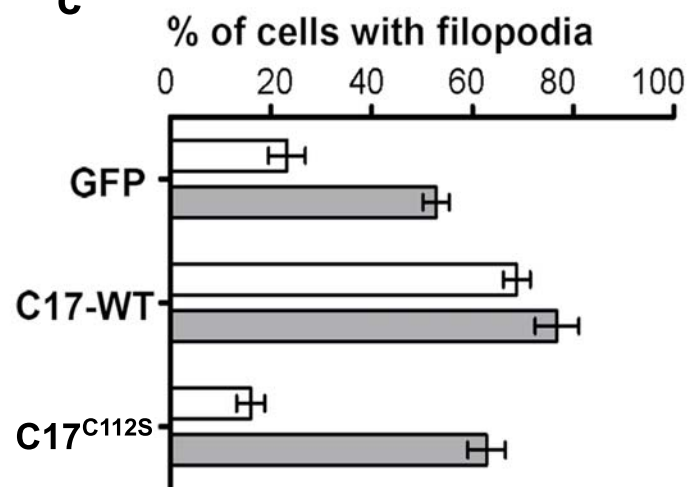
Cell migration depends on coordinated polymerization of actin filaments resulting in protrusive structures at the leading edge of motile cell called lamellipodia (Chhabra and Higgs, 2007). From the lamellipodia arise thin finger-like projections filled with parallel bundles of F-actin, known as filopodia (Mattila and Lappalainen, 2008). Surprisingly, ectopic expression of C17orf37^{WT} in NIH3T3 cells dramatically increased filopodia formation in more than 78% of the cells counted (Fig. 4a, c). However, in cells expressing GFP-vector or C17orf37^{C112S}, only 15-20% counted cells showed filopodia formation (Fig. 4a, c) and there was a ~4 fold decrease in the number of filopodia/cell compared to C17orf37^{WT} (Fig. 4d). Filopodia are often referred to as ‘tentacles’ used by the migrating cells to probe their microenvironment and known to facilitate directional movement (Mattila and Lappalainen, 2008). Inducing migration by wounding scratch in NIH3T3 cells, we observed increased actin polymerization and stress fiber formation in both wild type and mutant (Fig. 4b). Filopodia originating from the migratory cells were found to protrude towards to the wound supporting a directional migration (Fig. 4b), however number of filopodia radiating from C17orf37^{WT} cells was significantly higher than C17orf37^{C112S} cells (Fig. 4d), suggesting an involvement of prenylated C17orf37 in filopodia formation. We also observed global increase in filopodia formation particularly in cells surrounding the wound upon induction of migration (Fig. 4d), supporting the notion that filopodia formation is a well regulated process by the dynamic balance of actin polymerization (Mallavarapu and Mitchison, 1999). Nevertheless, our findings

Figure 4

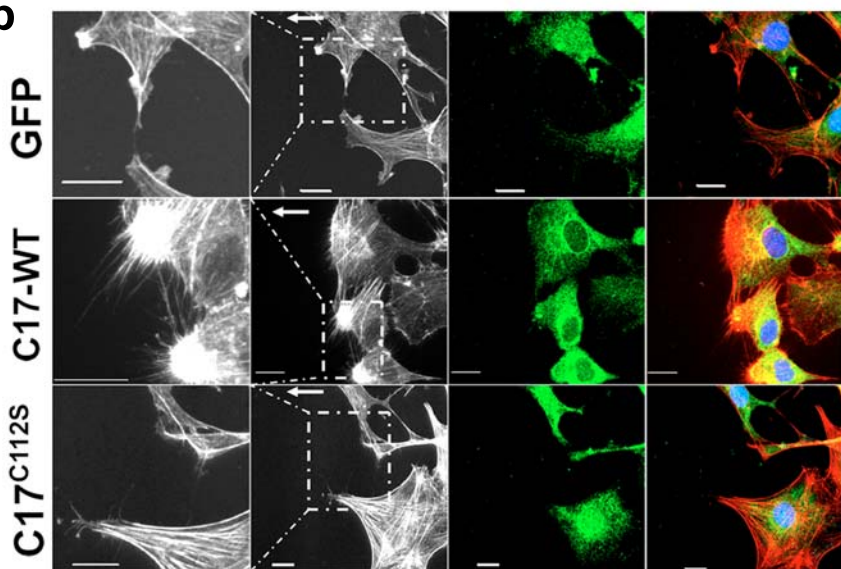
a



c



b



d

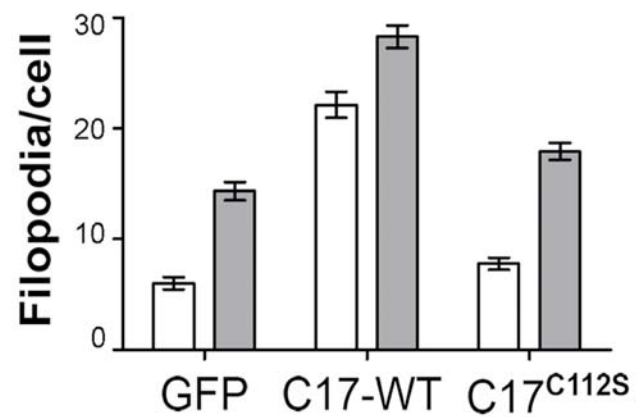


Figure 4. C17orf37 prenylation by GGTase-I stimulates filopodia formation. (a) NIH3T3 cells stably expressing vector (GFP), GFP fused C17orf37 (C17-WT), or GFP fused C17orf37-C112S mutant (C17^{C112S}) were plated on coverglass coated with fibronectin (5 μ g/mL), and then fixed and stained with rhodamine-phalloidin (left, image shown in monochrome). Middle: Localization of GFP fused proteins. Right: Overlay with phalloidin staining (red) of the same field. Scale bars, 10 μ m. (b) NIH3T3 cells expressing different constructs as mentioned in (a) were grown in a monolayer to confluency and then wounded. Six hours later cells were fixed and stained with rhodamine-phalloidin. Left: First two left panels shows the actin stained (monochrome) cells surrounding the wound. Extreme left image is magnified image of the boxed area. Arrow indicates direction of cell migration. Middle: Localization of GFP fused protein in the migrating cells (green), Right: Overlay of actin (red) and GFP (green). Scale bars 10 μ m. (c) NIH3T3 cells stably expressing constructs as mentioned in (a) and (b) stained with rhodamine-phalloidin were counted to determine percentage of cells with filopodia. In total 5 fields, with more than 80 cells per field were counted, and values represent: [(cells with at least 5 filopodia/cell)/(total number of cells selected)] X 100, and expressed as mean \pm s.e.m. of three independent experiments. (d) NIH3T3 cells stably expressing constructs as mentioned in (a) and (b) stained with rhodamine-phalloidin were counted to determine number of filopodia/cell. In total, 5 fields with more than 80 cells per field were counted, and expressed as mean \pm s.e.m. Open bars indicate non-migrating cells as mentioned in (a), and grey bars represent migrating cells as mentioned in (b).

strongly suggest a mechanism by which prenylated C17orf37 induces increased migratory behavior in cells.

Overexpression of C17orf37 promoted lung metastasis

Expression of C17orf37 positively correlates with grade and stage of breast cancer, and enhanced expression of protein was detected in patients with breast cancer to lungs and liver metastasis (Evans *et al.*, 2006). In prostate cancer, C17orf37 expression was also much higher in patients with advanced stage of the disease (Dasgupta *et al.*, 2009). To understand role of C17orf37 in tumor cell metastasis *in vivo*, we used the mouse tail vein injection model and determined the ability of tumor cells to form metastatic nodules within the lungs. DU-145 prostate cancer cells stably expressing GFP-vector only (Vector) or GFP-fused C17orf37 (C17orf37) (Supplementary Information, Fig. S6) were injected in athymic nude mice via tail vein injection. We observed mouse injected with vector had less colonization of cancer cells in the lungs, fewer lung nodules and micrometastasis 56 days post-injection compared to DU-145 overexpressing GFP-C17orf37, which showed enhanced lung colonization of tumor cells, increased number of metastatic lesions and ~4 fold increase in lung metastasis (Fig. 5a, b, c). Two mice injected with DU-145 expressing C17orf37 cells, died 50 days post-injection due to increased lung metastasis (animal 3 and 7) (Supplementary Information, Fig. S7). Microscopic examination of the lung sections showed abundant expression of GFP-C17orf37 overexpressing cells predominantly localized to the metastatic lesions, whereas very

few GFP expressing cells were observed in vector injected lung sections (Fig. 5b, middle panel). Although C17orf37 expression does not significantly alter cancer cell proliferation and growth in DU-145 cells *in vitro* (S.D. and J.K.V. unpublished observations), we observed a ~4 fold increased Ki-67 staining (Fig. 5d) in lung colonized tumor cells predominantly in the GFP-C17orf37 expressing cells, compared to minimal stain in the vector lung tissues (Fig. 5b bottom panel). This increased proliferation may be attributed to the tumorigenic ability of parental DU-145 cells, suggesting that ectopic expression of C17orf37 enhanced the migratory and metastatic ability of the cells to colonize to the lungs, whereas proliferation and increased Ki-67 staining is due to the inherent malignant phenotype of DU-145 cells. These studies reinforced our understanding that ectopic expression of C17orf37 affects invasion, migration and metastatic colonization.

The Cys112Ser mutation impairs C17orf37 function in vivo

To test whether C17orf37 mediated metastatic dissemination of tumor cells to the lungs is dependent on post-translational modification, we took advantage of NIH3T3 cells expressing GFP-vector, C17orf37^{WT}, or C17orf37^{C112S} (Supplementary Information, Fig. S6) and injected them into the tail veins of athymic nude mice. NIH3T3 is a non-transformed cell line and does not form tumors or lung metastasis when injected into nude mice (Bradley *et al.*, 1986). However, stable overexpression of different oncogenes has been known to induce oncogenic transformation of

Figure 5

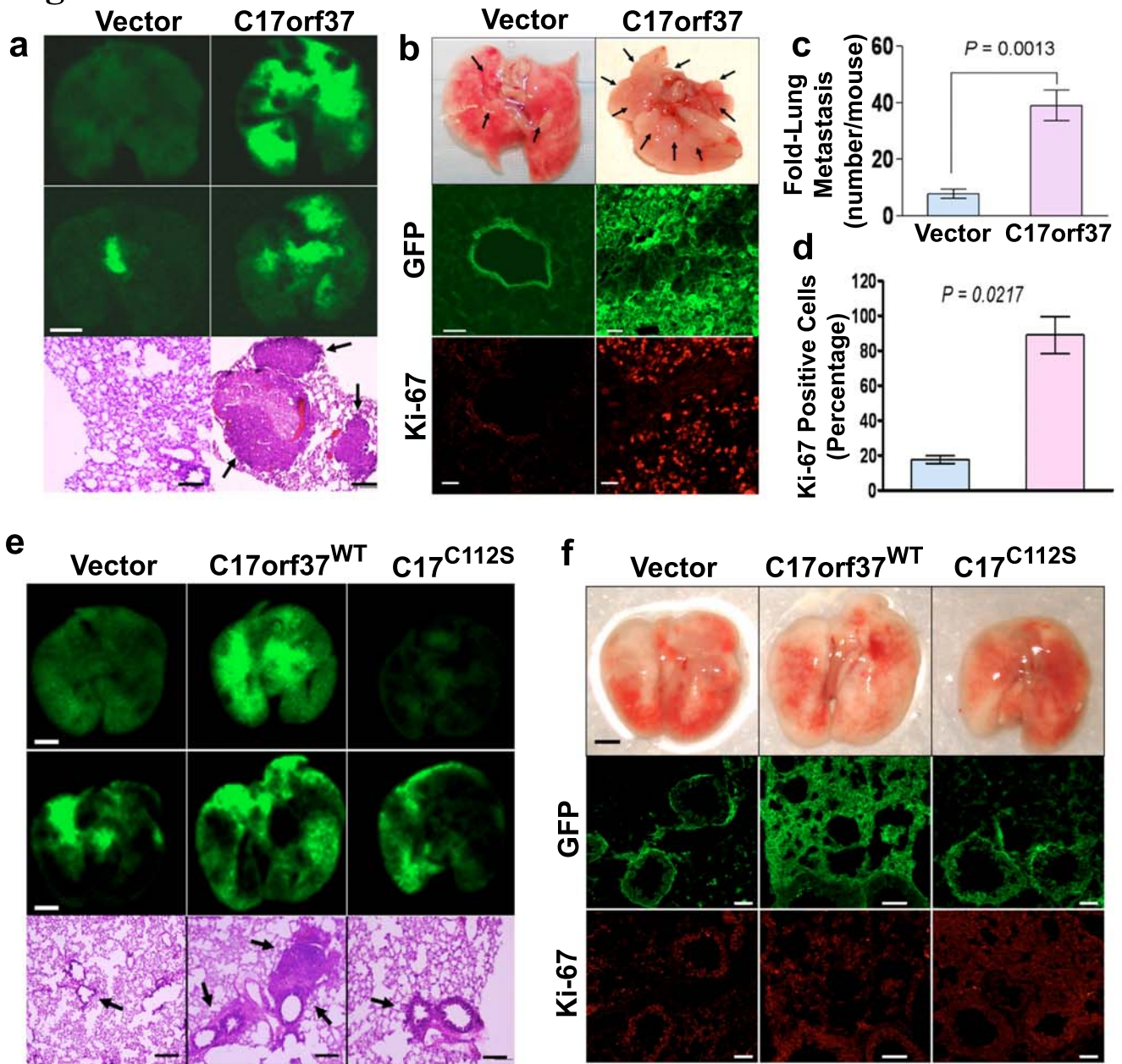


Figure 5. The Cys112Ser mutation impairs C17orf37 function *in vivo*. (a, b, c, d) DU-145 cells stably expressing GFP vector only (Vector) (n =5) or GFP tagged C17orf37 (C17orf37) (n =7) were injected into the tail vein of nude mice. Two mice from C17orf37 group died after 50 days, and experiment was terminated after 56 days. (a) Upper two panels: Representative images of murine lungs (maximum and minimum, fluorescence observed) to visualize GFP-labeled DU-145 cells 56 days after tail vein injection. Bottom panel: Hematoxylin & Eosin (H&E) stained sections of lungs shown in top panel. Arrows indicate metastatic foci. Scale bars, 1mm (white); 100 μ m (black). (b) Representative images of murine lungs injected with vector expressing (left) and C17orf37 expressing cells (right), and the corresponding GFP and Ki-67 immunostained sections shown in the upper panel. Scale bars, 100 μ m. (c) Quantification of metastatic nodules in the lungs and expressed as fold-lung metastasis, mean \pm s.e.m. (d) Ki-67 positive cells were counted, total 5 fields per section in vector (n = 5) and C17orf37 (n = 7), and expressed as mean \pm s.e.m. (e, f) NIH3T3 cells stably expressing GFP vector (Vector) - left, GFP fused C17orf37 (C17orf37^{WT}) - middle or GFP fused C17orf37-C112S (C17^{C112S}) - right, were injected into the tail vein of nude mice (n = 6). (e) Upper two panels: Representative images of murine lungs (maximum and minimum, fluorescence observed) to visualize GFP labeled NIH3T3 cells, 11 weeks after tail vein injection. Bottom panel: H&E stained sections of lungs shown in top panel. Arrows indicate colonized cells observed. Scale bars, 1mm (white); 100 μ m (black). (f) Murine lung images as

mentioned in (e) showing absence of visible tumor nodules (upper panel) and corresponding GFP and Ki-67 immunostained sections shown in bottom panels.

NIH3T3 cells (Bradley *et al.*, 1986). After 11 weeks of post-injection we did not observe any change in animal behavior and most of the animals looked healthy, and the isolated lungs were free of any visible external metastatic nodules. However, quite unexpectedly we observed increased colonization of C17orf37^{WT} cells in the lung parenchyma compared to GFP-vector or C17orf37^{C112S} injected animals (Fig. 5e). Most of the C17orf37^{WT} cells densely populate the lung parenchyma predominantly infiltrating from the blood vessels (Fig. 5e, bottom panel & Fig. 5f, middle panel), whereas minimal GFP stain was observed in GFP-vector or C17orf37^{C112S} lung sections (Fig. 5f, middle panel). Ki-67 staining of the lung sections was basal (Fig. 5f, bottom panel) and no significant differences were found between the groups (Supplementary Information, Fig. S7). This clearly suggests that ectopic expression of C17orf37 in cells significantly increases the migratory ability, and acquires aggressive trait required for dissemination and metastatic colonization. On the contrary, inhibiting prenylation of C17orf37 by genetically altering one amino acid from cys to ser (C112S), remarkably suppresses the effect. Taken together, our findings indicate overexpression of C17orf37 functionally predisposes cells to increased migratory and metastatic phenotype, and prenyl-modification at the 'CVIL' motif is critical for the C17orf37 mediated effect.

DISCUSSION

Implications of novel C17orf37 in cancer biology is still emerging. Based on the fact that the gene is located in an important amplicon of chromosome 17q12, previous studies have identified C17orf37 to be coamplified along with *ERBB2* in breast and colon cancer (Kauraniemi and Kallioniemi, 2006; Maqani *et al.*, 2006), and C17orf37 is postulated to play an important role in cancer. In this report, we demonstrate for the first time C17orf37 has a functional prenylation motif at the C-terminal end. We provide evidence that C17orf37 is geranylgeranylated by GGTase-I enzyme, and addition of this 20 carbon isoprenyl group to the cys residue of 'CVIL' motif translocates the protein to the inner leaflet of the plasma membrane. Proper subcellular localization of C17orf37 also depends on post-prenylation processes mediated by Rce1 and Icmt enzymes. Mutation of the cys to ser (C112S) fails to add the geranylgeranyl group catalyzed by GGTase-I and unprenylated protein is functionally inactive. Using both *in vitro* and *in vivo* studies, we find prenylated C17orf37 enhances the migratory and metastatic ability of tumor cells that generates increased colonization of tumor cells to distant organs, whereas prenyl-mutant C17orf37 fails to do so. Mechanistic studies reveal prenylated C17orf37 modulates increased filopodia formation and facilitates directional migration. Since it is known that membrane bound C17orf37 can act as a signaling molecule through the PI3K/Akt axis and activate NF- κ B downstream genes MMP-9, uPA and VEGF, it will be

important to understand whether C17orf37 induced filopodium formation is a direct effect, or is mediated by the Akt pathway.

Collectively, the findings of the present study have broadened our understanding regarding the importance of C17orf37 in metastatic progression of cancer and the implications of post-translational isoprenylation on the functional activity of the protein. Since metastasis of cancer cells to distant organs increases the mortality rate of human carcinomas, targeting C17orf37 may prove to be clinically useful to impede metastasis.

MATERIALS AND METHODS

Cloning, expression and purification of recombinant C17orf37

Full length human C17orf37 cDNA of 347 bp cloned into pGEX-4T-1 vector (GE Healthcare, Piscataway, NJ) in proper reading frame. Full length human C17orf37 cDNA was cloned into the *EcoRI* and *BamHI* restriction site of pEGFP-C1 vector and the resulting vector was named GFP-C17orf37 (Dasgupta *et al.*, 2009). The Cysteine residue in the 'CVIL' motif of C17orf37 (cloned in pGex-4T1 vector or pEGFP-C1 vector was mutated to serine, or the entire motif 'CVIL' motif of C17orf37 (cloned in pEGFP-C1 vector) was deleted using site directed mutagenesis using Quickchange site-directed mutagenesis kit (Stratagene). The primer pairs used are as follows:

C17orf37^{C112S}: 5'-CAGCCGTCCTCCCAGCGTCATCCTGTG-3'/ 5'-

GTCGGCAGGAGGGTCGCAGTAGGACAC-3'

C17orf37^{Δ112-115}: 5'- GCCGTCCTCCCTGAGTCATCCTGTGAC-3'/ 5'-

CGGCAGGAGGGACTCAGTAGGACACTG-3'

GST-C17orf37 fused protein was expressed in E.coli Bl-21 strain and purified using Glutathione Sepharose 4B column (GE Healthcare, Piscataway, NJ) according to manufacturer's instructions.

Cell lines, culture conditions, treatment and transfection procedures

DU-145, SKBR-3 and BT-474 cells were obtained from ATCC and maintained in RPMI1640 supplemented with 10% fetal bovine serum (FBS) and 1% penicillin-streptomycin (PS). NIH3T3 mouse fibroblast cells were maintained in DMEM supplemented with 10% FBS and 1% PS. Wild type MEF, *Icmt*^{-/-}, and *Rce1*^{-/-} were grown in DMEM supplemented with 15% Calf serum, 1% non-essential amino acid (NEAA), 1% PS and 3.6 uL beta-mercaptoethanol.

Cells were transfected using Lipofectamine 2000 (Invitrogen, Carlsbad, CA) with plasmid DNA for a period of 6 hours in OPTI-MEM (Invitrogen, Carlsbad, CA). After transfections, cells were grown in complete media overnight before mounting on slides using Vectashield (Vector Laboratories, Burlingame, CA) for confocal microscopy.

For generation of stable cells, NIH3T3 cells were transfected using Lipofectamine 2000, with GFP (empty-vector), GFP-C17orf37^{WT} or C17orf37^{C112S} plasmid DNA for 24hours. Stable transfected cell populations were challenged in complete medium supplemented with 500µg/ml G418 (Invitrogen, Carlsbad, CA) for about 3 weeks. For subsequent experiments, polyclonal pooled clones obtained from the transfected cells were used. DU-145 stable cells expressing C17orf37 or GFP was used as mentioned before (Dasgupta *et al.*, 2009).

GGTI-DU-40 and FTI-2148 inhibitors were dissolved in DMSO and added to DU-145 and SKBR-3 cells for a period of 24 hours at the indicated dose. Cells were either

fixed and stained with C17orf37 antibody for confocal microscopy or subjected to western immunoblot.

Antibodies and Reagents

Antibodies used for the study are as follows: mouse polyclonal C17orf37 (Abnova, Taiwan; 1:500), rabbit polyclonal anti-PGK, mouse monoclonal anti-Na,K-ATPase (Developmental studies hybridoma bank, Colorado), rabbit polyclonal anti-GFP (Cell signaling), mouse monoclonal anti-transferrin receptor (Zymed), mouse monoclonal anti-Ki-67 (DAKO) and rabbit polyclonal anti-G-alpha_{i-2} (Santa Cruz). FTI-2148 was purchased from Calbiochem.

Confocal microscopy

GFP-tagged cells were grown on coverslips and mounted on glass slides with Prolong Gold mounting media (Invitrogen). Confocal images were obtained using Zeiss confocal microscope LSM 510 under 40X, 1.2-numerical aperture water immersion objective at a 0.3µm Z-section as mentioned previously. Lungs sections were immunostained with GFP and Ki-67 antibody, and images were obtained under 20X objective.

Isolation of membrane microdomains on sucrose floatation gradients

Cells were fractionated and membrane microdomains were isolated by non-detergent method, according to the previously published protocols with few modifications

(Ostrom *et al.*, 2007). Briefly cells were grown to near confluence, transfected and treated in four 100 mm dishes. The cells were lysed in 500 mM Na₂CO₃, pH 11 with a cocktail of protease and phosphatase inhibitors, the lysate was homogenized with 20 strokes in a pre-chilled Dounce homogenizer followed by homogenization with a polytron homogenizer three times for 10 seconds with intervals of 10-15 seconds followed by sonication three times for 20 seconds with an interval of 60 seconds. 2 ml of the homogenized sample was mixed with 2 ml of 90% sucrose in MBS (25 mM 2-(N-Morpholino) ethanesulfonic acid, 150 mM NaCl, pH 6.0). A discontinuous sucrose gradient was generated by overlaying with 4 ml of 35 % sucrose in 1X MBS and 250 mM Na₂CO₃ followed by overlaying with 4 ml of 5% sucrose in 1X MBS and 250 mM Na₂CO₃. The gradient was centrifuged at 40,000 rpm in a SW40Ti rotor (Beckman). Twelve 1 ml fractions were collected from the top of the tube and the fractions were subjected to trichloroacetic acid (TCA) precipitation followed by SDS PAGE and western immunoblotting.

Scratch Wound Healing Migrating Assay

NIH3T3 and DU-145 cells were grown on coverslip coated with fibronectin (5µg/mL) in a monolayer and scratch was created using pipet tip. Floating cells were removed and incubated in serum free media, and imaged at indicated time points after wounded. For filopodia assay, cells were fixed, and stained with rhodamine-phalloidin (Molecular Probes) and subjected to confocal microscopy.

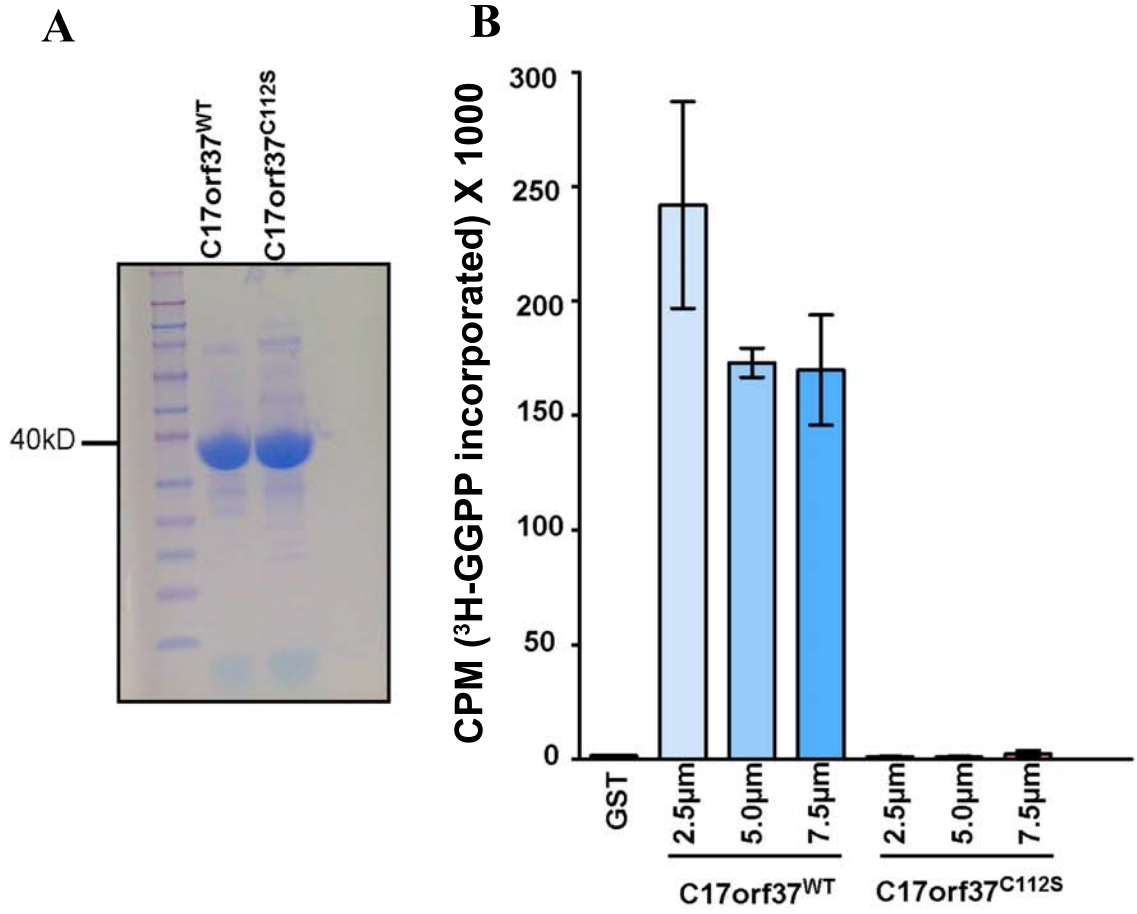
In vitro migration assay

Transwell migration assay performed using HTS FuoroBlok Multiwell Insert system (Falcon; 8µm pore size). Cells were pre-labeled with 4µg/ml of Calcein AM (Molecular Probes, Carlsbad, CA) and 2.5×10^4 cells/well suspended in DMEM media were added to the upper chamber whereas 10% FBS was added to the bottom chambers as chemoattractant. After incubation for 24 hours at 37°C, the nonmigratory cells were removed from the top chamber and the cells that successfully migrated to the lower side of the filter were imaged and counted.

Experimental Lung Metastasis

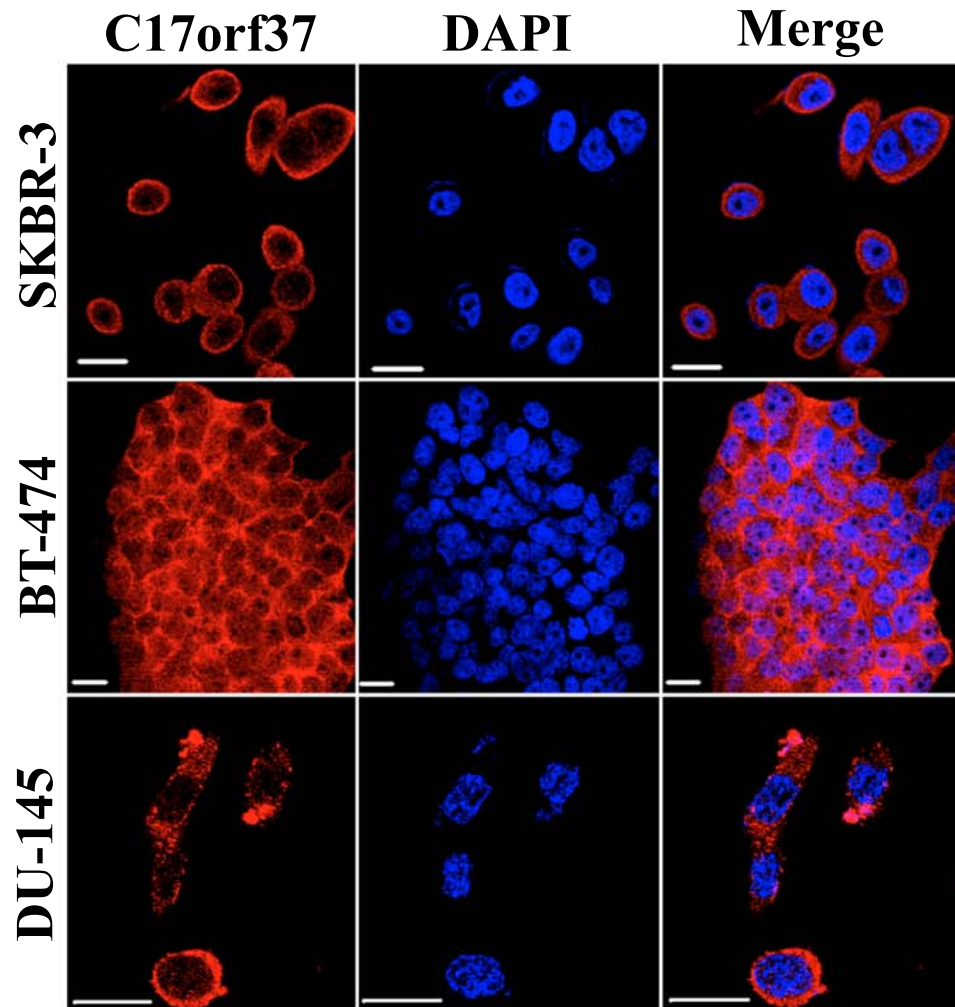
All animal experiments were performed in accordance with a protocol approved by the UNTHSC committee on animal health. Six to eight weeks old athymic nude mice were purchased from Harlan Laboratories. To perform lung metastasis, 5×10^5 cells (resuspended in PBS) were injected into the tail vein of mice, and after 56 days (for DU-145 cells) or 11 weeks (for NIH3T3 cells) animals were sacrificed. Isolated lungs were perfused and metastasis was quantified using Kodak Fluorescence Imager within 3 hours of specimen isolation according to the published report (Valastyan *et al.*, 2009).

Supplementary Figure 1



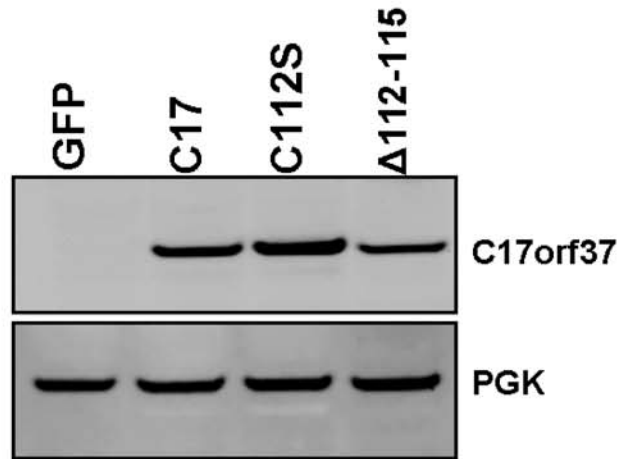
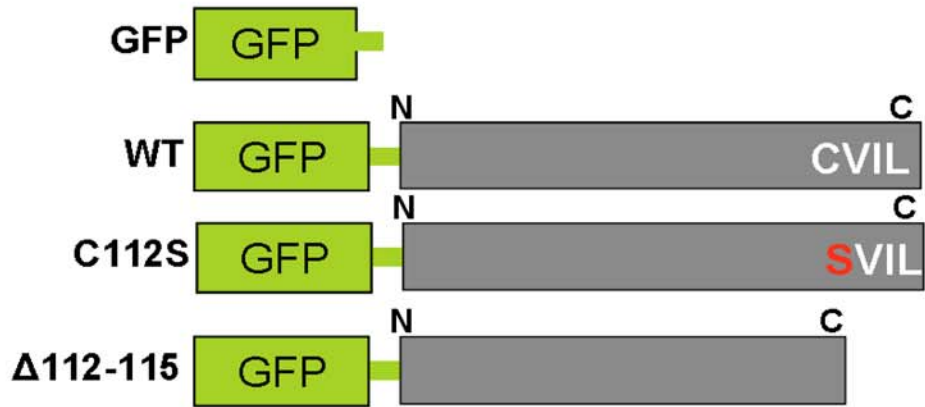
Supplementary Figure 1. Cys 112 to Ser mutation of C17orf37 impairs addition of geranylgeranyl group by GGTase-I enzyme. (a) Full length C17orf37 (C17orf37^{WT}) and site directed mutagenesis of Cys112 to Ser (C17orf37^{C112S}) cloned in pGEX-4T1 vector was expressed and purified from E. coli. Commassie stained SDS-PAGE gel showing the expression of the protein. (b) *In vitro* prenylation assay using 2.5, 5.0, and 7.5 μ m of C17orf37^{WT} and C17orf37^{C112S} in presence of GGTase-I enzyme and amount of ³H-GGPP (geranylgeranyl pyrophosphate) incorporated was counted by counts per minute (CPM) and expressed as mean \pm s.e.m.

Supplementary Figure 2



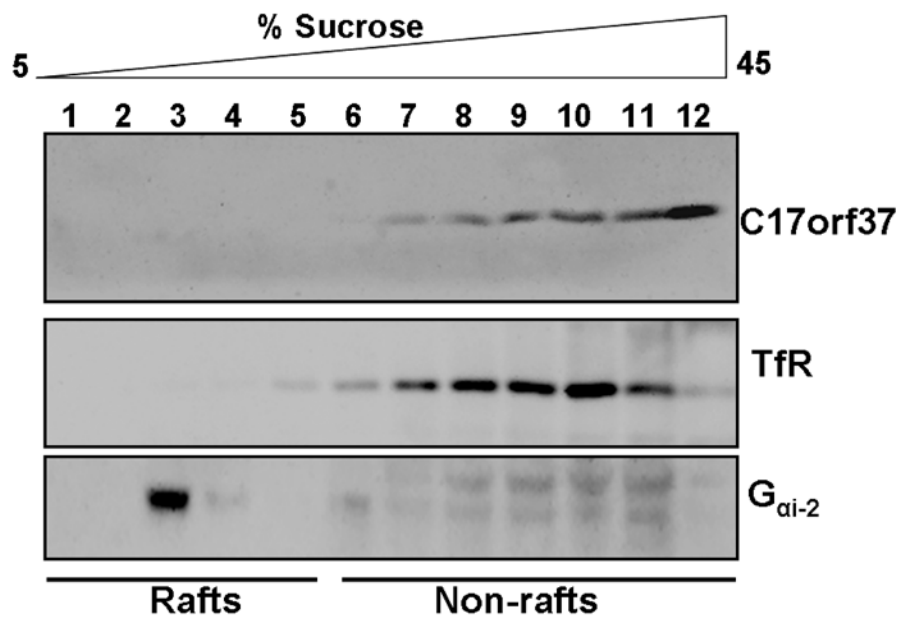
Supplementary Figure 2. Left: immunofluorescence staining of C17orf37 (red) in breast cancer cells SKBR-3 and BT-474, and DU-145 prostate cancer cells shows subcellular localization of C17orf37 protein. Middle: nuclear 4,6-diamidino-2-phenylindole (DAPI; blue) staining of the same field. Right: overlay of C17orf37 and DAPI staining. Scale bars, 20 μ m.

Supplementary Figure 3



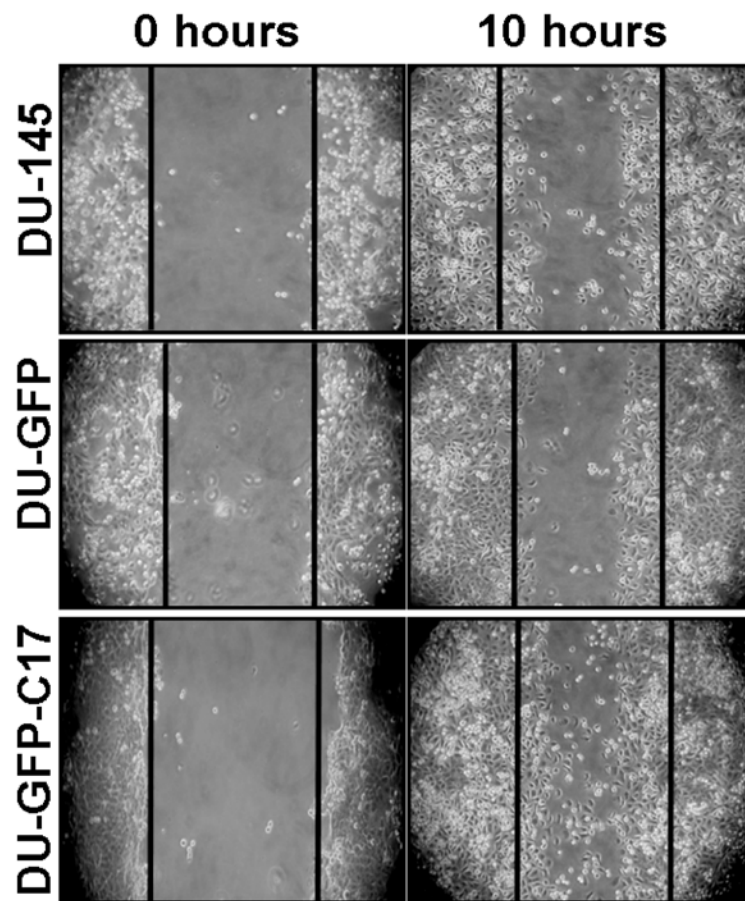
Supplementary Figure 3. Stable expression of GFP-tagged C17orf37 constructs in NIH3T3 cells. (a) schematic representation of GFP constructs: GFP vector only, GFP-C17orf37 (WT), GFP-C17orf37-C112S, and GFP-C17orf37- Δ 112-115. (b) NIH3T3 cells were transfected with these constructs, and selected in presence of 0.5 μ g/mL of G-418 for 3 weeks. Stable cells were then pooled and maintained as a polyclonal population. Immunoblot showing the expression of C17orf37 constructs expressed stably in NIH3T3 cells.

Supplementary Figure 4



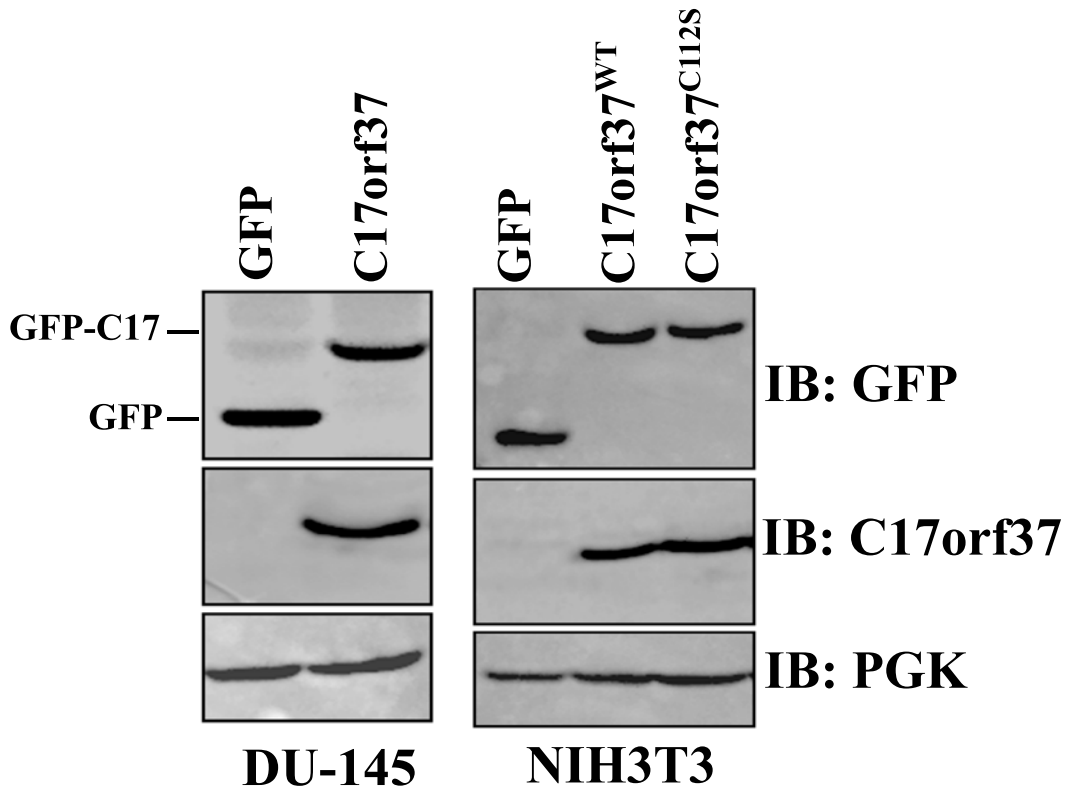
Supplementary Figure 4. C17orf37 is expressed in the non-raft microdomains of plasma membrane. Immunoblotting of endogenous C17orf37 in DU-145 cells fractionated on a 5-45% discontinuous sucrose gradient. Total 12 fractions were collected based on their density in sucrose gradient and numbered from the top. Galpha_{i-2} (Gα_{i-2}), and transferrin receptor (Tfr) were used as marker proteins to analyze raft, and non-raft fractions respectively.

Supplementary Figure 5



Supplementary Figure 5. Ectopic stable expression of C17orf37 increases migration of DU-145 cells. Parental DU-145 cells, GFP-vector expressing DU-145 (DU-GFP) and pooled clones expressing C17orf37 (DU-GFP-C17) was grown in a monolayer and wounded to create a scratch. Images were taken immediately after the scratch and after 10 hours, to observe the migratory potential of cells induced by C17orf37.

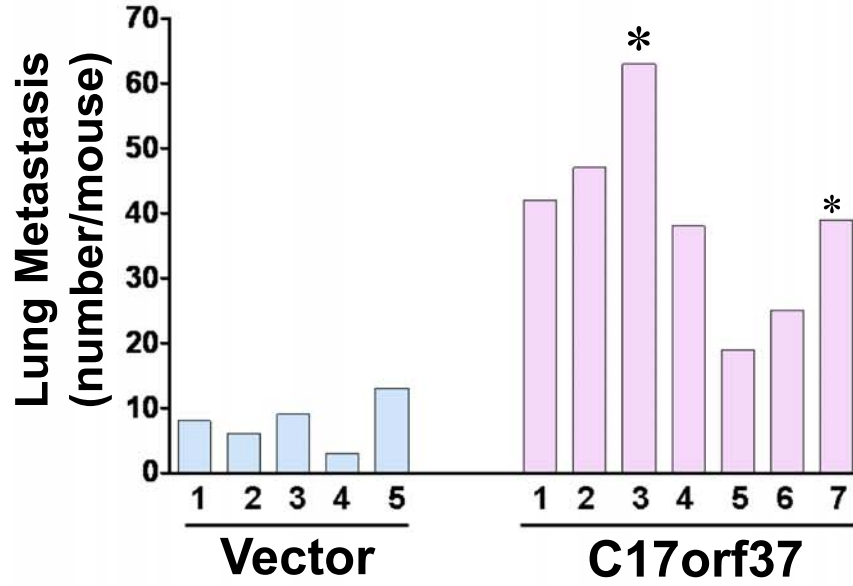
Supplementary Figure 6



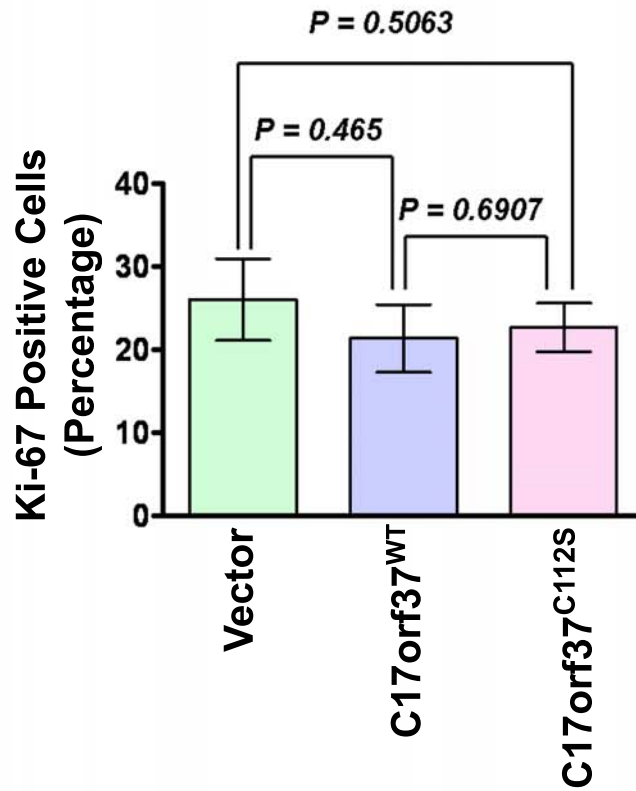
Supplementary Figure 6. Expression of GFP-fused constructs injected in the tail vein of the mouse. (a) Immunoblotting showing the expression of GFP vector only, or GFP-C17orf37 in DU-145 stable cells, and (b) expression of C17orf37 constructs, C17orf37^{WT}, C17orf37^{C112S} in NIH3T3 cells. PGK was used as a loading control.

Supplementary Figure 7

A



B



Supplementary Figure 7. (a) Graph showing the number of lung nodules in Vector (GFP-DU-145) and C17orf37 (DU-GFP-C17-WT) injected animals, 56 days post-injection. Asterisk denotes the animal died 50 days post-injection. (b) Ki-67 stained sections of animals injected with Vector (NIH3T3 cells expressing GFP vector only), C17orf37^{WT} (NIH3T3 cells expressing GFP-C17orf37) and C17orf37^{C112S} (NIH3T3 cells expressing C112S mutant C17orf37). Ki-67 positive cells were counted, total 5 fields per section in (n = 6), and expressed as mean \pm s.e.m.

REFERENCES

- Ashby MN. (1998). CaaX converting enzymes. *Curr Opin Lipidol* **9**: 99-102.
- Bergo MO, Leung GK, Ambroziak P, Otto JC, Casey PJ, Gomes AQ *et al.* (2001). Isoprenylcysteine carboxyl methyltransferase deficiency in mice. *J Biol Chem* **276**: 5841-5845.
- Bergo MO, Lieu HD, Gavino BJ, Ambroziak P, Otto JC, Casey PJ *et al.* (2004). On the physiological importance of endoproteolysis of CAAX proteins: Heart-specific RCE1 knockout mice develop a lethal cardiomyopathy. *J Biol Chem* **279**: 4729-4736.
- Bradley MO, Kraynak AR, Storer RD, Gibbs JB. (1986). Experimental metastasis in nude mice of NIH 3T3 cells containing various ras genes. *Proc Natl Acad Sci U S A* **83**: 5277-5281.
- Carrico D, Ohkanda J, Kendrick H, Yokoyama K, Blaskovich MA, Bucher CJ *et al.* (2004). In vitro and in vivo antimalarial activity of peptidomimetic protein farnesyltransferase inhibitors with improved membrane permeability. *Bioorg Med Chem* **12**: 6517-6526.

Casey PJ, Seabra MC. (1996). Protein prenyltransferases. *J Biol Chem* **271**: 5289-5292.

Chhabra ES, Higgs HN. (2007). The many faces of actin: Matching assembly factors with cellular structures. *Nat Cell Biol* **9**: 1110-1121.

Dasgupta S, Wasson LM, Rauniyar N, Prokai L, Borejdo J, Vishwanatha JK. (2009). Novel gene C17orf37 in 17q12 amplicon promotes migration and invasion of prostate cancer cells. *Oncogene* **28**: 2860-2872.

Der CJ, Cox AD. (1991). Isoprenoid modification and plasma membrane association: Critical factors for ras oncogenicity. *Cancer Cells* **3**: 331-340.

Evans EE, Henn AD, Jonason A, Paris MJ, Schiffhauer LM, et al. (2006). C35 (C17orf37) is a novel tumor biomarker abundantly expressed in breast cancer. *Mol Cancer Ther* **5**: 2919.

Glomset JA, Farnsworth CC. (1994). Role of protein modification reactions in programming interactions between ras-related GTPases and cell membranes. *Annu Rev Cell Biol* **10**: 181-205.

Kauraniemi P, Kallioniemi A. (2006). Activation of multiple cancer-associated genes at the ERBB2 amplicon in breast cancer. *Endocr Relat Cancer* **13**: 39.

Kauraniemi P, Kuukasjärvi T, Sauter G, Kallioniemi A. (2003). Amplification of a 280-kilobase core region at the ERBB2 locus leads to activation of two hypothetical proteins in breast cancer. *Am J Pathol* **163**: 1979.

Kim E, Ambroziak P, Otto JC, Taylor B, Ashby M, Shannon K *et al.* (1999). Disruption of the mouse Rce1 gene results in defective ras processing and mislocalization of ras within cells. *J Biol Chem* **274**: 8383-8390.

Lin X, Jung J, Kang D, Xu B, Zaret KS, Zoghbi H. (2002). Prenylcysteine carboxylmethyltransferase is essential for the earliest stages of liver development in mice. *Gastroenterology* **123**: 345-351.

Magdalena J, Millard TH, Etienne-Manneville S, Launay S, Warwick HK, Machesky LM. (2003a). Involvement of the Arp2/3 complex and Scar2 in golgi polarity in scratch wound models. *Mol Biol Cell* **14**: 670-684.

Magdalena J, Millard TH, Machesky LM. (2003b). Microtubule involvement in NIH 3T3 golgi and MTOC polarity establishment. *J Cell Sci* **116**: 743-756.

Magee AI, Seabra MC. (2003). Are prenyl groups on proteins sticky fingers or greasy handles? *Biochem J* **376**: e3-4.

Mallavarapu A, Mitchison T. (1999). Regulated actin cytoskeleton assembly at filopodium tips controls their extension and retraction. *J Cell Biol* **146**: 1097-1106.

Maqani N, Belkhiri A, Moskaluk C, Knuutila S, Dar AA, El-Rifai W. (2006). Molecular dissection of 17q12 amplicon in upper gastrointestinal adenocarcinomas. *Mol Cancer Res* **4**: 449-455.

Mattila PK, Lappalainen P. (2008). Filopodia: Molecular architecture and cellular functions. *Nat Rev Mol Cell Biol* **9**: 446-454.

Mayor S, Rao M. (2004). Rafts: Scale-dependent, active lipid organization at the cell surface. *Traffic* **5**: 231-240.

Peterson YK, Kelly P, Weinbaum CA, Casey PJ. (2006). A novel protein geranylgeranyltransferase-I inhibitor with high potency, selectivity, and cellular activity. *J Biol Chem* **281**: 12445.

Prior IA, Hancock JF. (2001). Compartmentalization of ras proteins. *J Cell Sci* **114**: 1603-1608.

Roberts PJ, Mitin N, Keller PJ, Chenette EJ, Madigan JP, Currin RO *et al.* (2008). Rho family GTPase modification and dependence on CAAX motif-signaled posttranslational modification. *J Biol Chem* **283**: 25150-25163.

Shaikh SR, Edidin MA. (2006). Membranes are not just rafts. *Chem Phys Lipids* **144**: 1-3.

van Meer G. (2002). Cell biology. the different hues of lipid rafts. *Science* **296**: 855-857.

Zacharias DA, Violin JD, Newton AC, Tsien RY. (2002). Partitioning of lipid-modified monomeric GFPs into membrane microdomains of live cells. *Science* **296**: 913-916.

Zhang FL, Casey PJ. (1996). Protein prenylation: Molecular mechanisms and functional consequences. *Annu Rev Biochem* **65**: 241-269.

CHAPTER IV

SUMMARY AND DISCUSSION

This study advances our knowledge about C17orf37 protein and its implication in cancer biology. C17orf37 is located in an important amplicon right next to ERBB2 in a tail to tail rearrangement and frequently amplified in breast and colon cancer (Dasgupta and Vishwanatha, 2009; Evans *et al.*, 2006). Expression of C17orf37 is basal in 29 human tissues examined so far, except for Leydig cells in testis which shows prominent expression of the protein. Our objectives of the present study were to characterize the expression of C17orf37 in prostate cancer cells and identify its functional role.

Our studies indicate expression of C17orf37 is enhanced in prostate cancer lines compared to minimal expression in normal prostate epithelial cells. C17orf37 expression was also higher in patients with advanced stage of the disease. Interestingly, we found C17orf37 expression in the PIN lesions of the prostate, suggesting C17orf37 expression persists from initial to late stages of the disease. It will be important to extend our study with increased patient population to determine if C17orf37 can be used as biomarker for early detection of the disease. This will be clinically very useful, as most men who are diagnosed with prostate cancer show signs of bone metastasis.

Following our understanding about the expression pattern of C17orf37 in prostate cancer patients, we sought to investigate its role in cancer biology. We utilized loss and gain of function experiments by silencing expression of C17orf37 using siRNA or ectopically overexpressing the protein in prostate cancer cells. We found that C17orf37 overexpression functionally enhances migratory and invasive behavior of prostate cancer cells. Migration and invasion is the hallmark of cancer cell dissemination and metastatic spread to distant organ coordinated by several proteins which regulate the process. We identified C17orf37 overexpression simultaneously increases expression of MMP-9, uPA and VEGF. These proteins are known to play crucial role in prostate cancer metastasis, and their expression is increased in patients with advanced disease (Sheng, 2001; Sliva, 2004). Interestingly, we identified that C17orf37 modulates phosphorylation of Akt, an upstream kinase which activates DNA binding activity of NF- κ B thereby transcriptionally upregulating MMP-9, uPA and VEGF. Cell fractionation and microscopic evaluation of cells revealed C17orf37 protein localization in the cytosol, predominantly in the plasma membrane and very less in the nucleus. However, C17orf37 protein sequence does not have any hydrophobic sequence responsible for its membrane association. We identified that C17orf37 has a prenylation motif at the C-terminal end. Prenylated proteins are class of proteins which are known to play crucial role in cellular physiology. Biochemical and genetic studies demonstrated that C17orf37 is prenylated by geranylgeranyl transferase-I enzyme, which specifically adds 20 carbon isoprenyl tail to the protein. We also showed that the cysteine residue of the 'CVIL'

motif is important for the enzyme catalysis, since mutation to serine abrogates the addition, and the protein fails to bind to the membrane. Based on this understanding we proposed a model that C17orf37 exists in two distinct states: one *prenylated* which is hydrophobic and has higher affinity for membrane lipids, and other one cytosolic *non-lipidated* (Dasgupta and Vishwanatha, 2009) (Fig. 1). A recent report also identified that C17orf37 has a selenocysteine residue, interacts with glutathione peroxidase and probably plays role in cell redox homeostasis (Dikiy *et al.*, 2007).

Membrane is a vast dynamic structure composed of different classes of lipids. Our studies indicate majority of the C17orf37 protein localize to the non-raft microdomains low in cholesterol composition (Mayor and Rao, 2004). This finding makes it difficult to understand its role in signal transduction events, since majority of signaling molecules cluster in the raft complex. Recently, there has been a great debate in the field to better understand the raft and non-raft lipid compositions and re-evaluate our understanding of the membrane microdomains (Shaikh and Edidin, 2006). Although, it is pretty clear that rafts are enriched in cholesterol and glycosphosphatidylinositol (GPI) (van Meer, 2002), the lipid composition of ‘non-cholesterol’ rich microdomains are in general categorized as ‘non-rafts’ (Shaikh and Edidin, 2006). Thus understanding the affinity of proteins to the so-called ‘non-raft’ region and their role in cell biology is vague. Some studies in prostate cancer cells have revealed that raft and non-raft associated proteins are regulated in different ways. Protein kinase B/Akt has been found to be associated in both raft and non-raft regions (Cinar *et al.*, 2007), however the downstream signaling mediated by raft or

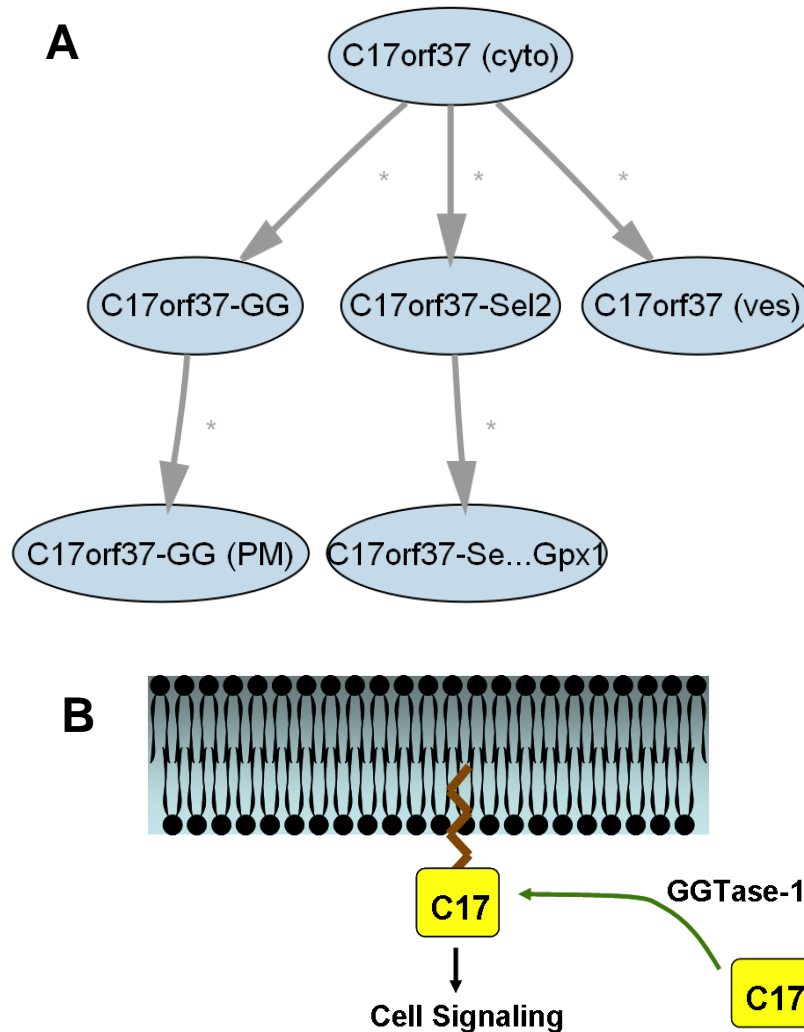


Figure 1: (a) Different states of C17orf37 protein. (b) Mechanism of C17orf37 prenylation and membrane association. ‘Cyto’: cytoplasm; ‘GG’: geranylgeranylated; ‘PM’: plasma membrane; ‘Sel2’: selenylation; ‘Gpx1’: glutathione peroxidase; and ‘Ves’: vesicular.

Adapted from: Dasgupta S, Vishwanatha JK. (2009). C17orf37. UCSD-Nature Molecule Page.

non-raft localized Akt is differentially regulated. Phospholipase A2 (PLA2) is an enzyme known to mediate the release of fatty acids and activate PI3K which further phosphorylates Akt. PLA2 has been shown to exclusively reside in the non-raft regions of the membrane (Shaikh and Edidin, 2006). Recent studies from our laboratory have identified C17orf37 as an interactor of PLA2 binding protein called annexin A2. Thus, it will be interesting to understand whether prenylated C17orf37 has an affinity for PLA2 and in turn mediates Akt phosphorylation.

In an approach to understand functional role of C17orf37 is dependent on post-translational modification by GGTase-I enzyme, we performed migration assays in cells ectopically expressing mutant form of C17orf37 protein. Our studies clearly show that mutant C17orf37 fails to potentiate migration of cells. We identified overexpression of C17orf37 induces increased filopodia formation which propel the cells forward favoring directional migration. Filopodia formation is a tightly regulated process mediated by cortical actin polymerization in response to stimuli. Several proteins have been identified to mediate the assembly and disassembly of actin, which includes small GTPases like Rho family of proteins, Rac1, and Arp. Interestingly, most of these proteins are isoprenylated which is important for protein-protein interaction and GTP loading. Although, C17orf37 protein does not have canonical GTP binding site, it will be important to identify how C17orf37 protein induce filopodia formation.

In nude mice C17orf37 overexpressed cancer cells showed increased lung colonization and metastasis, supporting the clinical finding that breast cancer patients

with liver and lung metastasis show increased C17orf37 expression. Non-transformed mouse fibroblasts stably expressing C17orf37 or prenyl-deficient C17orf37 failed to generate lung nodules, suggesting that C17orf37 expression cannot drive oncogenic transformation. Surprisingly, we found fibroblasts with increased C17orf37 expression were able to colonize in the lungs predominantly infiltrating into the lung parenchyma from the surrounding blood vessels, whereas prenyl-deficient C17orf37 mutant expressing cells were unable to do so. This might argue the fact that prenylated C17orf37 can drive the migratory and invasive potential of cancer cells facilitating metastasis to distant organs, but probably need other oncogenes to facilitate proliferation and tumorigenesis. Taken together, we proposed a model depicting the cellular mechanisms of C17orf37 that promote prostate cancer migration and invasion (Fig. 2). C17orf37 is prenylated at the C-terminal end by GGTase-I enzyme, which translocates the protein to the inner leaflet of the membrane. At the membrane interface, C17orf37 modulates Akt activation triggering downstream signals thereby transcriptionally upregulating NF- κ B downstream genes MMP-9, uPA, VEGF. These molecules are then secreted favoring invasion and migration. Prenyated C17orf37 at the membrane can also induce increased filopodia formation, by some yet unknown mechanism and potentiate migration. Thus, we propose overexpression of C17orf37 in cancer cells contribute to the migratory and invasive phenotype in prostate cancer cells.

Figure 2

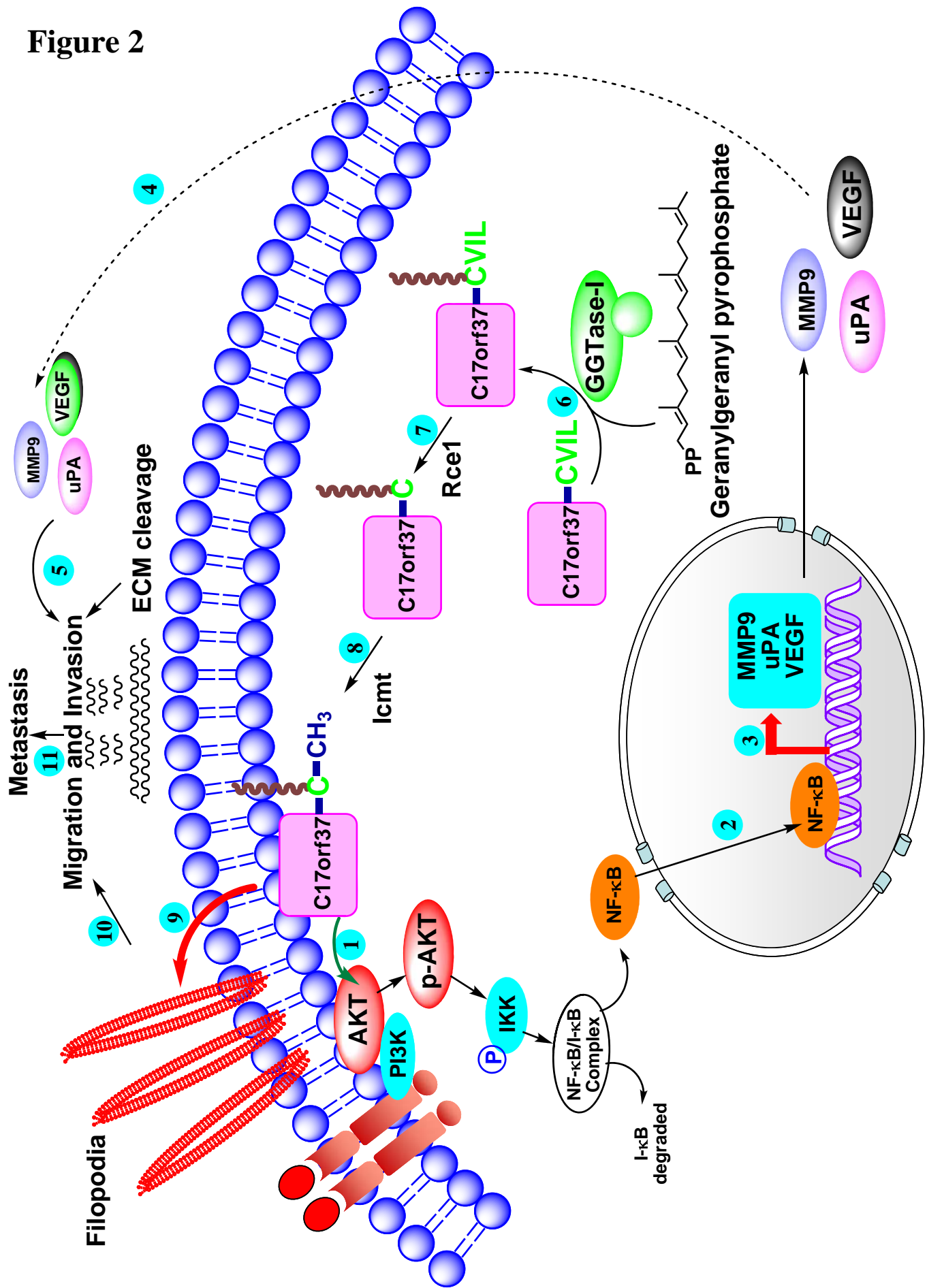


Figure 2. Role of C17orf37 in migration and invasion of cancer cells. (1) Membrane bound C17orf37 modulates the phosphorylation of Akt which triggers downstream signaling increasing the nuclear translocation and (2) DNA binding activity of NF- κ B. (3) NF- κ B upregulates downstream target genes MMP-9, uPA and VEGF, (4) which are then secreted out of the cells facilitating ECM cleavage and cancer cell invasion. (6) C17orf37 is prenylated by GGTase-I enzyme by the addition of geranylgeranyl group to the cysteine residue of the 'CVIL' motif. (7) Following addition of the isoprenyl group, 'CAAX'-protease Rce1 cleaves the last three amino acids 'VIL' and (8) Icmt enzyme methylates the free carboxyl group. (9) The post-translationally modified C17orf37 then binds to the plasma membrane and induces the formation of filopodial structures, which propels the cell forward. (10) Increased filopodia formation activates the migratory behavior of cancer cells, and allows it to glide through the ECM. (11) This increased migratory and invasiveness of cancer cells potentiated by C17orf37 facilitates the metastatic dissemination to the distant organs.

FUTURE STUDIES

In addition to prenylation motif, we have identified an immunoreceptor tyrosine based activation motif (ITAM) at the N-terminus of C17orf37 protein. ITAM proteins have two tyrosine residues which are cross phosphorylated by SH2-domain of receptor tyrosine kinases or other kinases, which then trigger down stream signal transduction events. Currently we are evaluating the importance of this domain with respect to C17orf37 mediated signaling events. It is important to detect probable kinases that can phosphorylate C17orf37 tyr 39 and tyr 50. Ongoing investigations are directed towards identifying some of the potential interactors of prenylated C17orf37, which will allow us to identify its role in the membrane interface. An interesting finding that C17orf37 expression is enhanced only in cancer cells might argue for specific transcriptional or post-transcriptional regulation of the gene. Several micro RNAs (miRNAs) downregulated in cancer have been identified by computational algorithms which specifically bind C17orf37 mRNA. It will be interesting to determine specific miRNA(s) targeting C17orf37 gene, which can be utilized to block C17orf37 in cancer cells. It is also important to identify transcription factors which have binding site at the C17orf37 promoter, to understand transcriptional regulation of the gene. These studies will further broaden our understanding about the implications of novel gene C17orf37 in cancer progression and metastasis, and validate it as a potential target for cancer therapy.

REFERENCES

Cinar B, Mukhopadhyay NK, Meng G, Freeman MR. (2007). Phosphoinositide 3-kinase-independent non-genomic signals transit from the androgen receptor to Akt1 in membrane raft microdomains. *J Biol Chem* **282**: 29584-29593.

Dasgupta S, Vishwanatha JK. (2009). C17orf37. *UCSD-Nature Molecule Pages*.

Dikiy A, Novoselov SV, Fomenko DE, Sengupta A, Carlson BA, Cerny RL *et al.* (2007). SelT, SelW, SelH, and Rdx12: Genomics and molecular insights into the functions of selenoproteins of a novel thioredoxin-like family. *Biochemistry* **46**: 6871-6882.

Evans EE, Henn AD, Jonason A, Paris MJ, Schiffhauer LM, *et al.* (2006). C35 (C17orf37) is a novel tumor biomarker abundantly expressed in breast cancer. *Mol Cancer Ther* **5**: 2919.

Mayor S, Rao M. (2004). Rafts: Scale-dependent, active lipid organization at the cell surface. *Traffic* **5**: 231-240.

Shaikh SR, Edidin MA. (2006). Membranes are not just rafts. *Chem Phys Lipids* **144**: 1-3.

Sheng S. (2001). The urokinase-type plasminogen activator system in prostate cancer metastasis. *Cancer Metastasis Rev* **20**: 287-296.

Sliva D. (2004). Signaling pathways responsible for cancer cell invasion as targets for cancer therapy. *Curr Cancer Drug Targets* **4**: 327.

van Meer G. (2002). Cell biology. the different hues of lipid rafts. *Science* **296**: 855-857.

APPENDIX

NATURE PUBLISHING GROUP LICENSE TERMS AND CONDITIONS

Apr 29, 2010

This is a License Agreement between Subhamoy Dasgupta ("You") and Nature Publishing Group ("Nature Publishing Group") provided by Copyright Clearance Center ("CCC"). The license consists of your order details, the terms and conditions provided by Nature Publishing Group, and the payment terms and conditions.

All payments must be made in full to CCC. For payment instructions, please see information listed at the bottom of this form.

License Number	2363961404565
License date	Feb 07, 2010
Licensed content publisher	Nature Publishing Group
Licensed content publication	Oncogene
Licensed content title	Novel gene C17orf37 in 17q12 amplicon promotes migration and invasion of prostate cancer cells
Licensed content author	S Dasgupta, L M Wasson, N Rauniyar, L Prokai, J Borejdo, J K Vishwanatha
Volume number	28
Issue number	32
Pages	
Year of publication	2009
Portion used	Full paper
Requestor type	Student
Type of Use	Thesis / Dissertation
Billing Type	Invoice
Company	Subhamoy Dasgupta
Billing Address	3500 Camp Bowie Blvd
	Fort Worth, TX 76107
	United States
Customer reference info	
Total	0.00 USD